Pontificia Universidad Católica de Chile
Instituto de Astrofísica

Outer Bulge RR Lyrae stars in the VVV Survey

by

Felipe Eduardo Gran Merino

Practice report presented to the Physics Faculty
of Pontificia Universidad Católica de Chile,
as one of the requirements for the
Master of Science degree in Astronomy.

Supervisor	:	Dr. Manuela Zoccali (PUC, Chile)
Co-supervisor	:	Dr. Dante Minniti (UNAB, Brazil)
Correctors	:	Dr. Márcio Catelan (PUC, Chile)
		Dr. Roberto Saito (UFS, Chile)
		Dr. A. Katherina Vivas (NOAO, Chile)

July, 2015 Santiago, Chile

Para todos los que hicieron esto posible,
en especial para Sofía

"One man's constant is another man's variable." – Alan Perlis

Contents

Abstract

The VISTA Variables in the Vía Láctea (VVV) is a near-IR time-domain survey of the Galactic bulge and southern plane. One of the main goals of this survey is to reveal the 3D structure of the Milky Way through their variable stars. This primary distance indicator are the RR Lyrae stars due to the high number density present in the bulge area and the tight period–luminosity (P–L) relation that they follow in near-IR bands.

Our goal in this project is to characterize the RR Lyrae population in the *outer bulge* ($-10^\circ \lesssim \ell \lesssim 10^\circ$ and $-10^\circ \lesssim b \lesssim -8^\circ$) in terms of their periods, amplitudes, Fourier coefficients, and distances, in order to evaluate the 3D structure of the bulge in this area. The distance distribution of RR Lyrae stars will be compared to the one of red clump stars that is known to trace a x-shaped structure in order to determine if these two different stellar populations share or not the same Galactic distribution.

A search for RR Lyrae stars was performed in more than $\sim$ 40 sq deg. In the procedure the χ^2 value and analysis of variance (AoV) statistic methods were used for determining the variability and periodic features of the light curves, respectively. On the other hand, the red clump stars of the same analyzed region were selected applying cuts in the color-magnitude diagram and restricting the maximum distance to $\sim$ 20 kpc to construct a similar catalog in terms of distances and covered area compared to the RR Lyrae stars.

As a result of this analysis, we report the detection of more than 880 RR Lyrae ab-type stars in the VVV Survey located in the outskirts of the Galactic bulge. Some of them possibly associated with the Sagittarius Dwarf Spheroidal Galaxy. We calculated colors, reddening, extinction, and distances of the detected RR Lyrae stars in order to determine the outer bulge 3D structure. Our main result is that, at the low galactic latitudes mapped here, the RR Lyrae stars trace a centrally concentrated spheroidal distribution. This is a noticeably different spatial distribution to the one traced by red clump stars known to follow a bar and x-shape structure.

Chapter 1

Introduction

Big astronomical surveys are changing the way we analyze and understand the processes in the Universe. In particular, the Milky Way galaxy is the best laboratory to comprehend these processes as it allow us to study in great detail as many stars as possible. In this context, massive photometric surveys have continuously been observing our Galaxy, providing us valuable information regarding the spatial distribution and structure of the Milky Way. Although these surveys have been crucial to understand our Galaxy as we know it, only recently the new-era of infrared variability surveys have been taking place, opening a new venue for studies of the inner and most obscured parts of the Galaxy through their variable star content.

IIn this framework, the VISTA Variables in the Vía Láctea (VVV) Survey aims to probe the internal structure of the Milky Way bulge and southern disk using near-IR filters (ZYJHKs) that break through the layer of dust and gas of the Galaxy. The accuracy and deep photometry obtained by the VVV survey greatly overcome other near-IR surveys, such as 2MASS. In order to reach its goals, the VVV Survey is using as main distance indicators the red-clump giants and pulsating variable stars, such as RR Lyrae stars, classical Cepheids, among others. RR Lyrae stars, as variable stars, have a distinctive periodic light curve, easy to identify in time series. In the VVV survey, RR Lyrae stars are extremely useful as they follow tight near-IR period–luminosity relations, leading to accurate distances, which allow us to reconstruct the 3D structure of the bulge traced by this old ($\simeq$ 10 Gyr) metal-poor stars. Through this report the steps perform to detect, classify, characterize, and analyze the RR Lyrae star population in the inner Galaxy will be presented. The area selected is a limited part of the region of the bulge observed by the VVV survey, located between

$-10^\circ \lesssim \ell \lesssim 10^\circ$ and $-10^\circ \lesssim b \lesssim -8^\circ$, hereafter referred as the outer bulge. This region was selected because it has a low stellar density that implies reduced crowding and a more accurate and deeper photometry than for the other fields in the VVV survey area which are closer to the Galactic center. The spatial distribution of RR Lyrae stars is compared to the one of the metal-rich red clump stars, which is known to trace a x-shaped structure. The possibility that RR Lyrae stars, as metal-poor horizontal branch stars, follow the same Galactic distribution as the red-clump stars is analyzed and discussed.

This thesis report presents the results of the first comprehensive variability search of RR Lyrae stars in the VVV survey. This report is divided in four chapters. Chapter 2 includes the first attempt of RR Lyrae identification and classification on the single VVV tile *b201*, explaining the observations and the detection method, comparing the RR Lyrae found with previously known ones, and finishing with the individual distance determination of these variable stars that lead to the estimation of the distance to the Galactic center. Chapter 3 extends the previous survey of RR Lyrae stars in the VVV scanning more than 40 sq deg located in an unexplored region in the outer bulge ($-10^\circ \lesssim \ell \lesssim 10^\circ$ and $-10^\circ \lesssim b \lesssim -8^\circ$). This more extended area is analyzed in order to obtain a general view of the RR Lyrae population across the Galaxy at this low Galactic latitude region. This chapter contains, besides the methods of identification and classification of the RR Lyrae stars found, the comparison and analyzed of the spatial distribution of RR Lyrae and red-clump stars in the outer bulge observed by the VVV survey, giving an unprecedented view of the stellar structure of the Milky Way bulge. Chapter 4 summarizes the completed work and presents new challenges and projects to be undertaken in the near future. Finally, Annex A contains reference/template-like light curves and the complete up to date catalog of RR Lyrae stars found in the tiles of the VVV survey studied.

Chapter 2

Bulge RR Lyrae stars in the VVV tile *b201*[*]

The structure and evolution of the Galactic bulge is far from completely explored. The high complexity of the Milky Way formation and the fact that we are embedded in the disk of the Galaxy, impede direct observations because of the extensive layer of dust and gas of the Galaxy in this line of sight. In the era of large-surveys, much effort have been made to reveal its structure, taking advantage of a wide variety of near-, mid- and far-IR filters to bypass the layer of dust that does not permit deeper observations in the optical bands (e.g., Freudenreich 1996; Skrutskie et al. 2006; Wright et al. 2010).

In this context, the VISTA Variables in the Vía Láctea (VVV) Survey aims to probe the internal structure of the Milky Way bulge through the near-IR ($ZYJHK_{\rm s}$) filters, using as its main distance indicators the red-clump giants and pulsating variable stars (Minniti et al. 2010), such as RR Lyrae stars (hereafter RR Lyr), classical Cepheids, anomalous Cepheids and Miras, and semiregular variables. In particular, RR Lyr stars have been useful probes of the bulge structure and evolution (Carney et al. 1995; Gratton & Carretta 1996; McWilliam & Zoccali 2010; Soszyński et al. 2011; Dékány et al. 2013). RR Lyr stars are old and low-mass stars ($\approx 0.7 M_{\odot}$, Smith 2004) that are in the horizontal branch (HB) stage (helium-burning phase) and have a very tight period–luminosity ($P-L$) relation in the near-IR bands (Longmore et al. 1990; Catelan et al. 2004). This relation is a powerful tool that has previously provided distances to Galactic globular clusters (Longmore et al. 1990; Del Principe

[*]Based on the article published by Gran et al. 2015, A&A, 575, 114.

et al. 2005, 2006; Sollima et al. 2006; Coppola et al. 2011), extragalactic globular clusters, dSph galaxies (Dall'Ora et al. 2004; Pietrzyński et al. 2008; Borissova et al. 2009), and the Galactic center (Carney et al. 1995; Groenewegen et al. 2008; Dékány et al. 2013). Dékány et al. (2013) searched for near-IR counterparts of the RR Lyr stars that were found by the OGLE III survey (Soszyński et al. 2011) in the Galactic bulge in an area limited by $2° \leq |b| \leq 7°$ and $|\ell| \leq 10°$. They derived the distance to the Galactic center and discovered that the RR Lyr trace a more spheroidal shape than the red-clump stars, which suggests that the Milky Way has a composite bulge.

In this work, we have selected a low density field to conduct a variability search. We find new RR Lyr stars in the VVV tile *b201*, which allows us to measure precise reddening and distances to the bulge in this direction. The tile *b201* samples the spatial distribution of RR Lyr in the older outer bulge, $b \gtrsim 4°$ away from the Galactic center region analyzed by Dékány et al. (2013). Our motivation also is to update the known RR Lyr stars present at these longitudes ($\ell \sim -10°$) that are covered by the VVV Survey area.

2.1 Observations

The VVV Survey is being carried out with the 4m Visible and Infrared Survey Telescope for Astronomy (VISTA) located at ESO's Cerro Paranal Observatory in Chile, using the wide-field VISTA InfraRed Camera (VIRCAM; Dalton et al. 2006; Emerson & Sutherland 2010). Photometric catalogs are based on the VISTA system, for which 2MASS (Cutri et al. 2003) coordinates are automatically produced by the Cambridge Astronomical Survey Unit (CASU)[1]. They are publicly available through the VISTA Science Archive (VSA)[2]. The pixel scale and field of view (FoV) are $0.34''$ pix^{-1} and 1.64 deg^2. This FoV represents one "tile"; the entire VVV observations comprise of 348 tiles (196 covering the bulge and 152 and the southern Galactic plane). The VVV observation schedule includes single-epoch near-IR photometry in $ZYJHK_{\rm s}$ bands and a variability campaign in $K_{\rm s}$ with up to a total of 100 epochs planned by the end of the scheduled observing time (1929 hours, Minniti et al. 2010; Catelan et al. 2011b). Technical details of the telescope and observation strategy can be found in Minniti et al. (2010) and Saito et al. (2012a).

In this study, we used observations of tile *b201* ($\ell, b \approx -9°, -9°$; Fig. 2.1). This

[1] http://casu.ast.cam.ac.uk/vistasp/
[2] http://horus.roe.ac.uk/vsa/

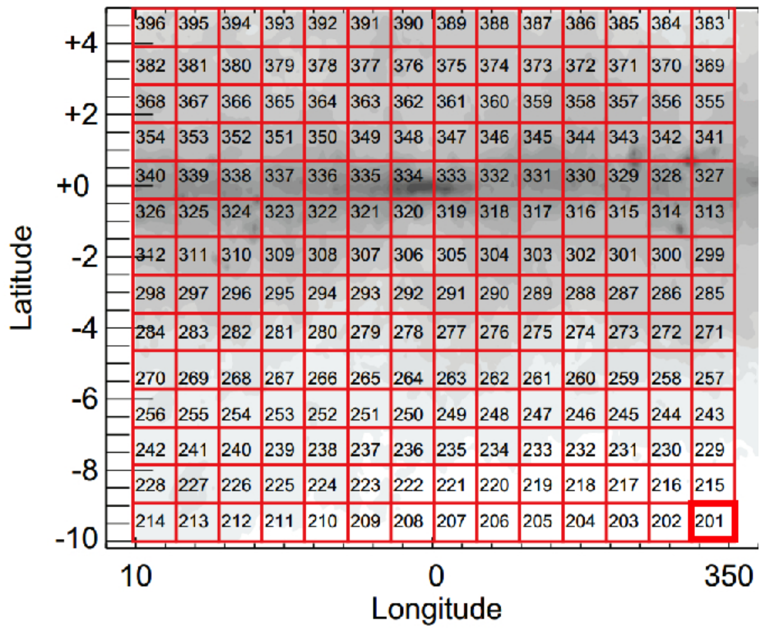

Figure 2.1: VVV Survey bulge region, shown in Galactic coordinates with its individual numbered tiles. Tile *b201* is highlighted in the bottom right corner. The Galactic center is contained in tile *b333*. Adapted from Catelan et al. (2011b).

tile is the bulge field most distant from the Galactic center observed by the VVV, and it has the lowest stellar density, as shown in Fig. 2 of Saito et al. (2012b). The VVV has observed this tile 36 times between April 2010 and July 2013. A total of 394 047 point sources with $K_{\rm s} \leq 17.0$ mag were detected, of which 353 935 have more than 25 epochs of observations, which is the number we require to include a source in this study.

The main reason to choose this tile was its stellar density, lower than other observed VVV bulge tiles. Specifically, for a cutoff of 25 points per light curve, there were 353 935 time series to be analyzed in this tile of the total 394 047 (~ 10 % excluded). This number is similar to that of the adjacent tile *b202* with 408 858 sources in $K_{\rm s}$ band. Another reason for analying this tile is its low extinction with values of $A_{K_{\rm s}} \lesssim 0.1$ mag in certain lines of sight, or equivalently, $A_{\rm V} \leq 0.35$ mag (Catelan et al. 2011b; Gonzalez et al. 2011, 2012), which allowed the previous detection of RR Lyr stars by Swope (1942), Ponsen (1954) and Kooreman (1966). Even though it is not completely free of selection biases, the low density implies reduced crowding and a more accurate and deeper photometry than for the other fields in the VVV survey area. Furthermore, the lower extinction in this area minimizes the reddening uncertainties.

Identifying and classifying variable sources

A semi-automated classification scheme was developed to select the variable stars. First we computed the standard deviation ($\sigma K_{\rm s}$) and χ^2 test for each time series. The cut-off for considering a non-variable star was determined by simulating a random noise χ^2 distribution, as described by Carpenter et al. (2001); this resulted in $\chi^2 = 2$. This constraint places a lower limit of $\mathrm{A}_{K_{\rm s}} \approx 0.03$ mag at $K_{\rm s} \lesssim 13$ mag on the amplitudes of the RR Lyr to be detected. We estimate, based in the ω Cen RRc stars $\mathrm{K_s}$-amplitude distribution (Navarrete et al. 2015), that at $\mathrm{K_s} \sim 15.2$ mag our search procedure has a variability detection efficiency of ∼90%, which drops to ∼50% at $\mathrm{K_s} \sim 16.5$ mag. These candidates were analyzed by the analysis of variance (AoV) statistis (Schwarzenberg-Czerny 1989) to determine their periods. Periods were restricted to the range in which RR Lyr are typically found: $0.2 \leq P(\text{days}) \leq 1.2$. After this step, the light curves of 167 candidates were visually inspected, and 42 objects were foundto be as RR Lyr. Of the remaining 125 light curves, 32 were clearly variables but without a clear variability class, and we classified the remaining 83 as eclipsing-binary candidates. Better phase coverage is needed to classify these variables. Finally, ten variable-star candidates as selected by the algorithm were determined to be non-variables that showed period-aliasing of ≈1 day and were therefore excluded from further analysis. Fig. 2.2 presents the magnitude–variability diagram of all sources with more than 25 epochs of observation, in which the RR Lyr stars are identified.

2.2 Results

Catalogue of RR Lyr stars

To characterize our sample of RR Lyr stars, Table 2.1 contains the number of each variable type found and the mean, longest and shortest periods of each population. These values define the Oosterhoff and Bailey type of the RR Lyr. Additionally, our RR Lyr candidates lie in the magnitude range between $13 \lesssim K_{\rm s}\,(\text{mag}) \lesssim 16.5$, resulting in a distance between $5.2 \lesssim d\,(\text{kpc}) \lesssim 13.6$.

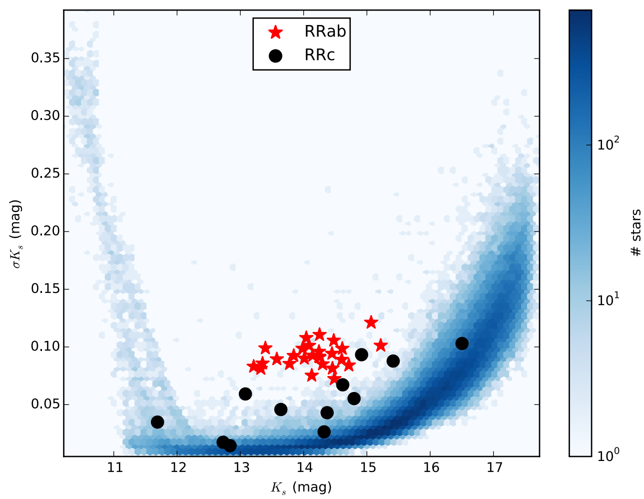

Figure 2.2: Magnitude-variability diagram for the sources detected in *b201* with more than 25 epochs (levels of blue). The contribution of saturated ($K_{\rm s} \lesssim 12.0$ mag) and faint ($K_{\rm s} \gtrsim 16.5$ mag) stars are clearly visible in the $\sigma K_{\rm s}$ value. RRab are shown as red stars and RRc stars as black circles.

Table 2.1: Summary of the periods (in days) of the RR Lyr found in *b201*.

Variability type	Quantity	$\langle P \rangle$ (days)	$P_{\rm min}$ (days)	$P_{\rm max}$ (days)
RRab	27	0.578	0.448	0.787
RRc	12	0.312	0.202	0.379

Bailey (1902) classified the RR Lyr (in that epoch called “cluster variables”) in three groups, the a-, b- and c-type by its period and light-curve shape (amplitude of variation). The first two groups were merged later into the ab-type known today. This relation of period and amplitude (today called the Bailey diagram) is shown in the upper panel of Fig. 2.3.

J and H photometry taken during 2010 and the $K_{\rm s}$-mean magnitudes are shown in Table 2.2. A brief discussion of the error introduced in the RR Lyr color $(J - K_{\rm s})$ and $(H - K_{\rm s})$ is presented in Sect. 2.2. The RR Lyr stars are shown on a Hess color–magnitude diagram of the whole tile in Fig. 3.2. The bulge red-giant branch (RGB) and the disk main-sequence (MS) stars are presented in the Hess diagram, with the label aligned in the direction of each branch. The superposition of a young population (the disk) hides the MS turn-off and part of the Galactic bulge HB, where

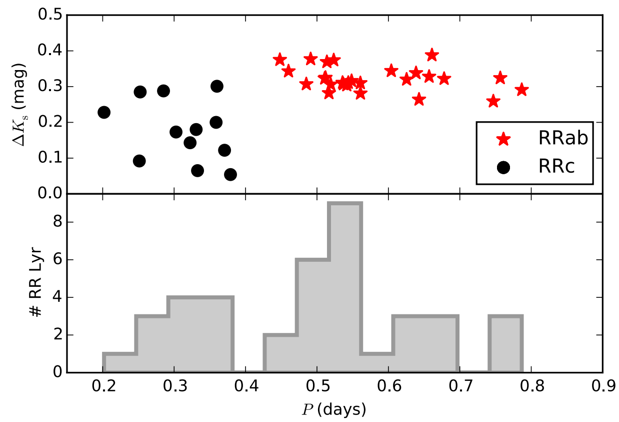

Figure 2.3: Top: Bailey diagram for the 39 RR Lyr variable stars. As expected, there is a clear separation between the amplitude and period among RRab (upper right) and RRc stars (lower left), following the same symbols as in Fig. 2.2. **Bottom**: Period histogram of the RR Lyr.

most of our RR Lyr belong. However, the bulge instability strip locus can be inferred over the disk MS in a color range between $0.1 \lesssim (J - K_s) \lesssim 0.6$, according to the position of the RR Lyr in the diagram.

Table 2.2: Color information of RRab and RRc stars found in tile *b201*. We list the VVV ID, right ascension (J2000), declination (J2000), magnitude-weighted mean from the Fourier fit $\langle K_s \rangle$, and $(J - K_s)$ and $(H - K_s)$ colors from the first K_s-band epoch. Typical $(J - H)$ and $(H - K_s)$ photometrical errors are ≈ 0.05 mag.

VVV ID (RRab)	RA(J2000)	DEC(J2000)	$\langle K_s \rangle$	$(J - K_s)$	$(H - K_s)$
VVV J2712426.16-421241.6	18:05:37.7	−42:12:41.6	14.59	0.54	0.22
VVV J2712711.57-421314.0	18:05:48.8	−42:13:14.0	14.23	0.65	0.29
VVV J2712912.05-420223.7	18:05:56.8	−42:02:23.7	14.23	0.44	0.17
VVV J2711512.06-415330.1	18:05:00.8	−41:53:30.1	14.00	0.51	0.22
VVV J2703434.23-413322.1	18:02:18.3	−41:33:22.1	13.35	0.57	0.24
VVV J2703536.01-412829.4	18:02:22.4	−41:28:29.4	13.97	0.42	0.20
VVV J2703343.00-412731.0	18:02:14.9	−41:27:31.0	14.45	0.60	0.25
VVV J2711523.24-413619.8	18:05:01.5	−41:36:19.8	13.78	0.64	0.27
VVV J2710804.03-413241.7	18:04:32.3	−41:32:41.7	14.51	0.50	0.21
VVV J2704944.51-412248.6	18:03:19.0	−41:22:48.6	13.36	0.34	0.16
VVV J2714215.15-414058.6	18:06:49.0	−41:40:58.6	14.29	0.64	0.25

Continued on next page...

Table 2.2 – Continued

VVV ID (RRab)	RA(J2000)	DEC(J2000)	$\langle K_s \rangle$	$(J - K_s)$	$(H - K_s)$
VVV J2710759.32-411700.5	18:04:31.9	−41:17:00.5	13.39	0.41	0.20
VVV J2714823.59-413121.7	18:07:13.6	−41:31:21.7	14.44	0.26	0.15
VVV J2711644.06-411744.6	18:05:06.9	−41:17:44.6	13.84	0.50	0.21
VVV J2710158.99-410727.3	18:04:07.9	−41:07:27.3	14.22	0.42	0.20
VVV J2704656.26-421805.3	18:03:07.7	−42:18:05.3	15.22	0.64	0.26
VVV J2701149.18-420358.3	18:00:47.3	−42:03:58.3	13.22	0.59	0.25
VVV J2705101.04-405300.9	18:03:24.1	−40:53:00.9	13.58	0.44	0.18
VVV J2711836.69-405946.8	18:05:14.4	−40:59:46.8	14.24	0.56	0.25
VVV J2705334.00-421303.7	18:03:34.3	−42:13:03.7	15.04	0.67	0.28
VVV J2702317.06-420003.9	18:01:33.1	−42:00:03.9	14.14	0.50	0.23
VVV J2705622.48-420853.7	18:03:45.5	−42:08:53.7	14.08	0.66	0.29
VVV J2711018.90-421253.4	18:04:41.2	−42:12:53.4	14.03	0.60	0.27
VVV J2712342.04-421647.8	18:05:34.8	−42:16:47.8	14.13	0.28	0.15
VVV J2712855.63-421832.3	18:05:55.7	−42:18:32.3	14.46	0.40	–[3]
VVV J2710638.97-420755.7	18:04:26.6	−42:07:55.7	14.59	0.43	0.19
VVV J2702400.61-415026.5	18:01:36.0	−41:50:26.5	14.72	0.34	0.18

VVV ID (RRc)	RA(J2000)	DEC(J2000)	$\langle K_s \rangle$	$(J - K_s)$	$(H - K_s)$
VVV J2711026.32-415037.7	18:04:41.7	−41:50:37.7	15.39	0.29	0.13
VVV J2702945.91-413239.9	18:01:59.0	−41:32:39.9	12.73	0.33	0.09
VVV J2710200.43-413446.0	18:04:08.0	−41:34:46.0	12.84	0.05	0.02
VVV J2705846.71-411723.2	18:03:55.1	−41:17:23.2	14.63	0.43	0.17
VVV J2705404.77-422910.0	18:03:36.3	−42:29:10.0	14.36	0.13	0.08
VVV J2713458.02-412608.5	18:06:19.9	−41:26:08.5	13.63	0.10	0.06
VVV J2711142.24-411611.0	18:04:46.8	−41:16:11.0	14.79	0.18	0.10
VVV J2714054.14-412637.6	18:06:43.6	−41:26:37.6	14.33	0.01	0.02
VVV J2711803.26-411635.8	18:05:12.2	−41:16:35.8	11.70	0.05	0.01
VVV J2710857.12-410712.8	18:04:35.8	−41:07:12.8	14.90	0.37	0.17
VVV J2702329.86-415953.8	18:01:34.0	−41:59:53.8	16.51	0.61	0.22
VVV J2704051.15-420503.6	18:02:43.4	−42:05:03.6	13.07	0.12	0.10

The period distribution of the RRab and RRc stars is divided by a gap in $P \sim 0.4$

[3] H-magnitude not available.

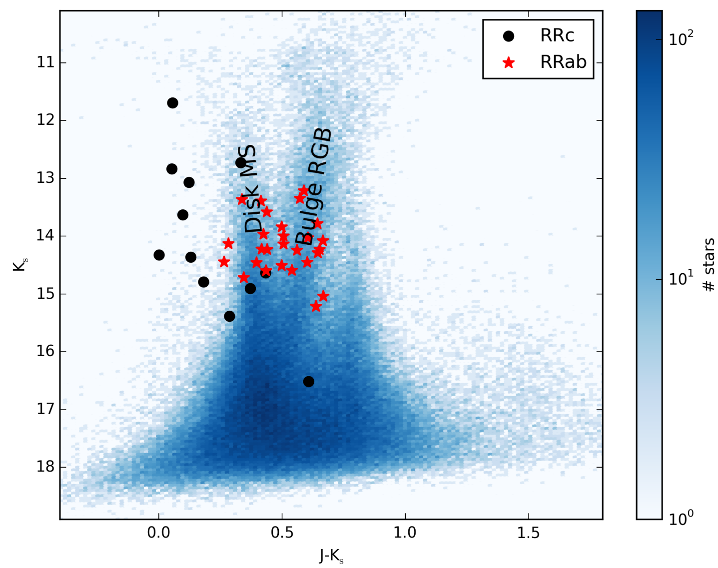

Figure 2.4: Hess diagram of the tile *b201*. The disk MS and bulge RGB are easily recognizable from this field and similar to the ones derived in Saito et al. (2012b). The symbols of the RR Lyr are the same as in Fig. 2.2.

days, as shown in the bottom panel of Fig. 2.3, which reflects the distribution derived by Kunder & Chaboyer (2009a) in V and R bands. These authors analyzed the Oosterhoff type of RR Lyr in the Galactic bulge. This near-IR diagram shows a different slope for the RRab in the optical wavelengths. It is more horizontal, similar to that reported by Gavrilchenko et al. (2014) and Navarrete et al. (2015) using mid- and near-IR data.

Previously known RR Lyr stars

As a test of consistency, we compared our RR Lyr positions and periods with those found in the literature. There are already ten variables in the International Variable Star Index[4] (VSX) catalog classified as RR Lyr in the analyzed area.

We recovered all ten previously known variables and correctly classified them as RR Lyr. These ten RR Lyr are listed in Table 2.3, along with their General Catalogue of Variable Stars (GCVS; Samus et al. 2009) designations, periods, and astrometric offsets. In three cases (MO CrA, V397 CrA and V467 CrA), periods different from

[4] `http://www.aavso.org/vsx`

Table 2.3: Results of the match with the VVV tile *b201* data and the VSX catalog.

VVV ID	GCVS	$P_{\rm VVV}$ (days)	$P_{\rm Lit.}$ (days)	d ($''$)
VVV J2705101.04-405300.9	MO CrA	0.657005	–	0.475
VVV J2712855.63-421832.3	V397 CrA	0.491175	0.3293815	0.771
VVV J2701149.18-420358.3	V463 CrA	0.604052	0.6040585	0.139
VVV J2702329.86-415953.8	V467 CrA	0.359989	0.4480160	1.931
VVV J2703434.23-413322.1	V469 CrA	0.678028	0.6780236	0.528
VVV J2705622.48-420853.7	V475 CrA	0.511933	0.5119430	17.41
VVV J2710759.32-411700.5	V482 CrA	0.541709	0.5417140	2.725
VVV J2712342.04-421647.8	V483 CrA	0.485059	0.4850490	0.105
VVV J2712711.57-421314.0	V486 CrA	0.460161	0.4601694	0.573
VVV J2714823.59-413121.7	V493 CrA	0.519262	0.5194291	31.26

those in the literature were identified. MO CrA was classified, without an assigned period, as a "cluster variable" by Swope (1942). V397 CrA and V467 CrA were previously observed by Ponsen (1954) and Kooreman (1966), respectively. Ponsen (1954) classified V397 CrA as an RRc, but with only 16 points in the light curve. Kooreman (1966) classified V467 CrA as an RRab, remarking that this star was very faint, with a large dispersion in magnitude in the 120 available plates. V475 CrA and V493 CrA do not have counterparts within our initial $2''$matching radius, but RR Lyr with near identical periods were identified at $17''$and $31''$, respectively, from their VSX positions. According to CASU, VVV astrometry is accurate to $\approx$50 mas and the similarity in periods make it very likely that V475 CrA and V493 CrA are counterparts to VVV J2705622.48-420853.7 and VVV J2714823.59-413121.7.

RR Lyr star with the shortest period in our catalog

We found that the RRc candidate VVV J2705846.71-411723.2 has a very short period of $P = 0.202$ days. In contrast, the RRc with the shortest period found in the OGLE III sample has $P = 0.237$ days (Soszyński et al. 2011). This variable warrants a more detailed study to confirm that it is an RRc instead of an eclipsing binary or a long-period SX Phe, as reported by Cohen & Sarajedini (2012).

Fourier coefficients

The complete catalog of light curves is shown in Figs. 2.5 and 2.6 for the RRab and RRc types. Following an approach similar to that of Dékány et al. (2013), the light curves of the RRab and RRc stars were fitted with Fourier series compound of sines, up to sixth order using the direct Fourier fitting (DFF) method of Kovács & Kupi (2007). This order was the highest possible calculated, but in some cases the returned order was lower to prevent over-fitting of the light-curve. This method allows us to recover the mean K_s-magnitude plus the Fourier coefficients (A_{21}, ϕ_{21}, ..., A_{61}, ϕ_{61}), which are shown in Table 2.4.

The photometric iron abundance of RR Lyr stars is typically found by analyzyng of V- and I-band light-curves (e.g., Jurcsik & Kovacs 1996; Smolec 2005). However, since there is no relationship between the Fourier parameters and iron content already established in the near-IR, it cannot be determined individually for our variables. Hence, we used the value of Pietrukowicz et al. (2012), who found that RR Lyr trace the distribution of the metallicity in the Galactic bulge with a sharply peaked distribution, centered on −1.02 dex with a dispersion of 0.25 dex. This metallicity complete agree with the spectroscopic value found by Walker & Terndrup (1991) of $\langle[Fe/H]\rangle = -1.0$ dex with a dispersion of 0.16 dex. They analyzed 59 RR Lyr in Baade's window. Taking a fixed metallicity does not significantly affect the distance estimation; it imparts a mean of 0.20 kpc ($\sim 3\%$ at 8 kpc) uncertainty to distances derived using the $P - L$ relation, taking into account the extreme values on the dispersion of [Fe/H].

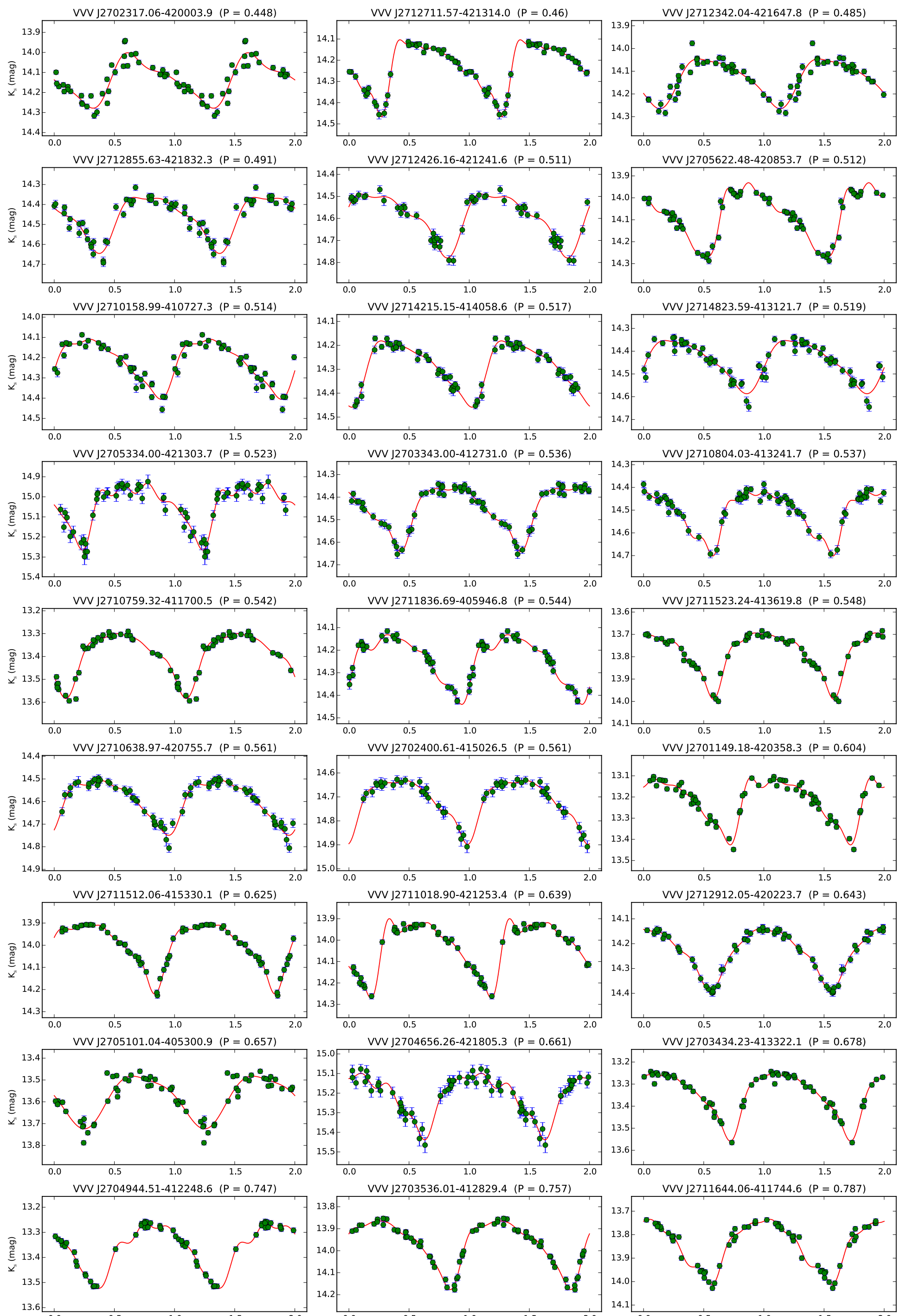

Figure 2.5: 30 RRab stars found in tile *b201*, sorted by increasing period. The solid line represents the Fourier decomposition of each RR Lyr using the DFF method. The internal name and period are indicated at the top of each light-curve. Error bars are plotted, but are generally smaller than the point sizes.

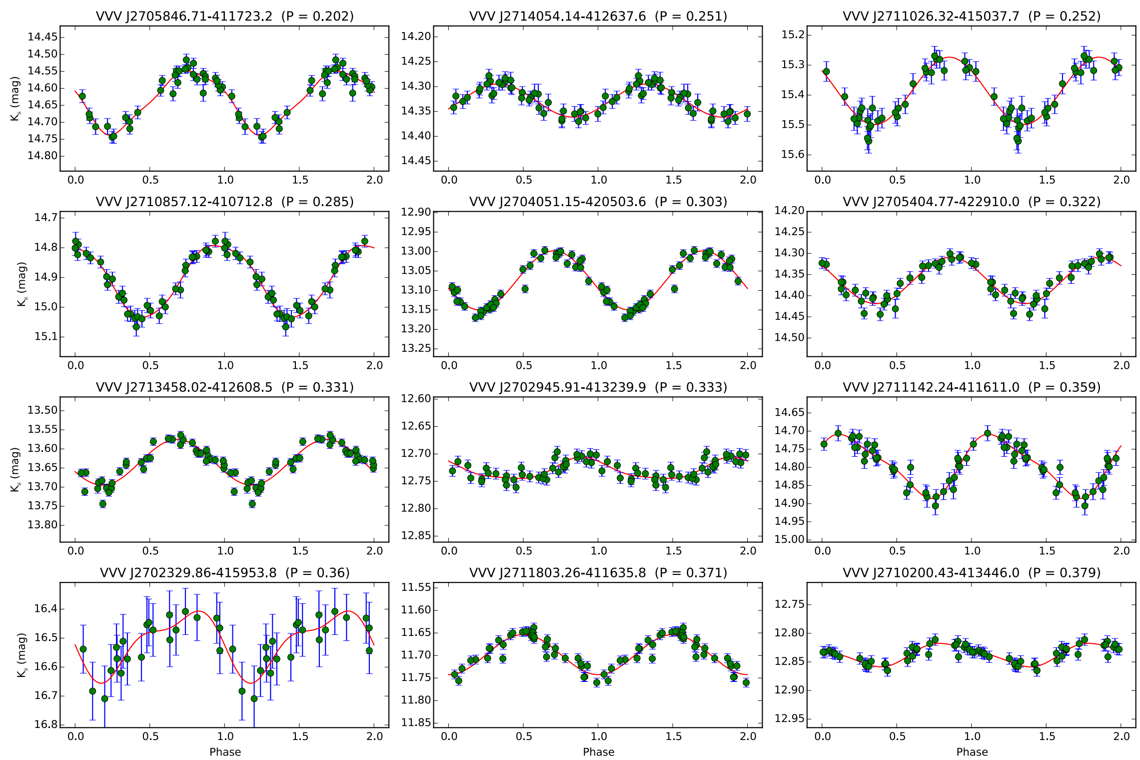

Figure 2.6: Same as Fig. 2.5, but for the RRc stars.

Table 2.4: Period and Fourier coefficients for the RR Lyr in tile *b201*.

VVV ID (RRab)	P (days)	A_1	ϕ_1	A_{21}	ϕ_{21}	A_{31}	ϕ_{31}	A_{41}	ϕ_{41}	A_{51}	ϕ_{51}	A_{61}	ϕ_{61}
VVV J2702317.06-420003.9	0.448043	0.108	0.146	0.442	3.361	0.156	0.038	–	–	–	–	–	–
VVV J2712711.57-421314.0	0.460161	0.127	0.595	0.454	3.768	0.336	1.103	0.179	−1.599	0.156	1.955	0.132	−0.353
VVV J2712342.04-421647.8	0.485059	0.098	1.042	0.336	3.942	0.109	1.388	–	–	–	–	–	–
VVV J2712855.63-421832.3	0.491175	0.122	5.804	0.376	−8.542	0.196	−17.03	–	–	–	–	–	–
VVV J2712426.16-421241.6	0.510823	0.120	3.069	0.403	−2.386	0.228	−4.592	–	–	–	–	–	–
VVV J2705622.48-420853.7	0.511933	0.137	5.191	0.413	−8.957	0.174	−11.045	0.123	−20.52	0.117	−23.676	0.099	−27.225
VVV J2710158.99-410727.3	0.513884	0.128	2.769	0.295	−2.487	0.157	−4.873	0.116	−7.579	–	−13.846	–	–
VVV J2714215.15-414058.6	0.516757	0.116	1.954	0.393	−2.456	0.183	−5.302	0.098	−1.648	–	−9.772	–	–
VVV J2714823.59-413121.7	0.519262	0.105	2.818	0.317	−2.442	0.118	−4.912	–	–	–	–	–	–
VVV J2705334.00-421303.7	0.523466	0.118	0.447	0.432	4.396	0.310	2.112	0.175	0.423	0.197	3.431	–	–
VVV J2703343.00-412731.0	0.535809	0.117	5.564	0.321	−8.513	0.258	−11.026	0.102	−19.275	0.072	−27.465	–	–
VVV J2710804.03-413241.7	0.536988	0.114	4.762	0.355	−8.314	0.159	−10.869	0.141	−13.575	0.131	−21.91	0.121	−24.132
VVV J2710759.32-411700.5	0.541709	0.113	1.205	0.378	−2.069	0.254	2.238	0.111	0.374	–	–	–	–
VVV J2711836.69-405946.8	0.543833	0.126	2.396	0.290	−1.936	0.173	−4.095	0.187	−7.041	0.125	−9.401	–	–
VVV J2711523.24-413619.8	0.548459	0.113	4.514	0.407	−8.315	0.185	−10.374	0.177	−12.632	0.123	−20.615	–	–
VVV J2710638.97-420755.7	0.560748	0.107	2.260	0.330	−2.067	0.159	−4.570	0.114	−7.347	–	–	–	–
VVV J2702400.61-415026.5	0.560889	0.108	2.005	0.325	−2.066	0.239	−4.529	0.131	−6.443	0.069	−8.248	–	–
VVV J2701149.18-420358.3	0.604052	0.122	3.905	0.387	−2.170	0.255	−11.105	0.235	−13.759	0.131	−16.498	–	–
VVV J2711512.06-415330.1	0.625496	0.122	2.897	0.375	−2.041	0.271	−4.298	0.130	−6.362	0.055	−14.464	0.055	−15.268
VVV J2711018.90-421253.4	0.638694	0.136	1.014	0.404	4.155	0.304	1.629	0.218	−1.227	0.172	−3.558	0.089	−0.497
VVV J2712912.05-420223.7	0.642877	0.109	4.470	0.266	−8.214	0.130	−9.892	0.091	−17.681	–	–	–	–
VVV J2705101.04-405300.9	0.657015	0.116	0.131	0.238	4.176	–	–	–	–	–	–	–	–
VVV J2704656.26-421805.3	0.660970	0.133	4.211	0.366	−8.292	0.152	−10.250	0.137	−13.372	0.144	−20.435	–	–
VVV J2703434.23-413322.1	0.678028	0.121	3.676	0.386	−2.160	0.234	−10.655	0.114	−12.769	0.074	−14.812	–	–
VVV J2704944.51-412248.6	0.746910	0.113	5.754	0.241	−7.914	0.126	−16.045	0.102	−18.418	0.104	−28.086	–	–
VVV J2703536.01-412829.4	0.756627	0.126	2.947	0.372	−2.210	0.214	−4.254	0.124	−6.989	0.063	−8.932	–	–
VVV J2711644.06-411744.6	0.786726	0.122	4.691	0.207	−8.180	0.119	−10.891	0.114	−13.366	0.110	−21.196	–	–

VVV ID (RRc)	P (days)	A_1	ϕ_1	A_{21}	ϕ_{21}	A_{31}	ϕ_{31}
VVV J2705846.71-411723.2	0.201895	0.089	6.168	0.109	−7.217	0.101	−14.489
VVV J2714054.14-412637.6	0.251285	0.033	2.613	–	–	–	–
VVV J2711026.32-415037.7	0.252489	0.113	5.647	–	–	–	–
VVV J2710857.12-410712.8	0.285146	0.124	4.937	0.066	−7.98	0.057	−13.387
VVV J2704051.15-420503.6	0.302654	0.076	0.275	–	–	–	–
VVV J2705404.77-422910.0	0.322360	0.055	5.595	–	–	–	–
VVV J2713458.02-412608.5	0.330849	0.060	0.422	–	–	–	–
VVV J2702945.91-413239.9	0.332772	0.019	5.313	0.236	−4.388	–	–
VVV J2711142.24-411611.0	0.358777	0.080	3.571	0.255	−2.865	–	–
VVV J2702329.86-415953.8	0.359989	0.105	0.209	0.409	5.568	–	–
VVV J2711803.26-411635.8	0.370611	0.044	1.560	–	–	–	–
VVV J2710200.43-413446.0	0.378936	0.019	5.662	0.220	−9.100	–	–

RR Lyr stars: reddening estimation

Generally, the reddening can be expressed as the difference of the measured and intrinsic color between two filters,

$$E(J-K_{\mathrm{s}}) = (J-K_{\mathrm{s}}) - (J-K_{\mathrm{s}})_0, \tag{2.1}$$

in this case for J and K_{s}. The first term of the equation is limited by the phase coverage and the number of points of each variable in multiple wavelengths. The VVV, as a variability survey, provides time-series exclusively in K_{s} band. For J and H band, only one observation has been taken during the first year of operation, which limits the precision of $(J-K_{\mathrm{s}})$ and $(H-K_{\mathrm{s}})$. The colors $(J-H)$ and $(H-K_{\mathrm{s}})$ were calculated using the faintest point of the light curve according to the Fourier fit, and taking into account the ratio of amplitudes between J, H and K_{s} described in Feast et al. (2008), as follows:

$$\Delta H = +0.11 + 1.65(\Delta K_{\mathrm{s}} - 0.18), \tag{2.2}$$

$$\Delta J = -0.02 + 3.60(\Delta K_{\mathrm{s}} - 0.18). \tag{2.3}$$

This approximation has a larger error for the shorter-period RRab (higher amplitudes) with a maximum of ± 0.2 mag and ± 0.1 mag for the J and H band, respectively. However, for Z and Y bands (also available in the VVV Survey), we are unable to conduct the same analysis because we lack detailed near-IR variability studies. This problem can be solved in the future with a database of well-defined near-IR template light-curves that the VVV Templates Project (Catelan et al. 2011a; Angeloni et al. 2014) is collecting. The next step was to calculate the intrinsic color of the sample, that is $(J-K_{\mathrm{s}})_0$, analogous to the difference in absolute magnitude of the two filters. This modifies the latter reddening equation into

$$E(J-K_{\mathrm{s}}) = (J-K_{\mathrm{s}}) - (J-K_{\mathrm{s}})_0 = (J-K_{\mathrm{s}}) - (M_{\mathrm{J}} - M_{\mathrm{K_s}}) \tag{2.4}$$

for J and K_{s} bands. The absolute magnitudes were calculated using the $P-L$ relation given in Alonso-García et al. (2015),

$$M_{\mathrm{J}} = -0.6365 - 2.347 \log P + 0.1747 \log Z, \tag{2.5}$$

$$M_{\mathrm{K_s}} = -0.6365 - 2.347 \log P + 0.1747 \log Z, \tag{2.6}$$

with $\sigma_{\mathrm{J}} = 0.17$ mag and $\sigma_{\mathrm{K_s}} = 0.13$ mag the systematic errors in J and K_{s} bands, respectively. The errors were calculated as the difference between the average magnitudes, published by Del Principe et al. (2005), and the theoretical values obtained using the $P-L$ relations listed above. The theoretical propagated error of $(J-K_{\mathrm{s}})_0$ is ~ 0.21 mag, which introduces a difference of 0.14 mag in the distance moduli. These relations are crucial for determining the distances to our RR Lyr stars, because it is a very accurate solution to calculate the reddening corrected colors, especially in the near-IR (Catelan et al. 2004). We used the same approach as Pietrukowicz et al. (2012) to calculate the $\log Z = [Fe/H] - 1.765$, based on a solar metallicity of $Z_{\odot} = 0.017$ (Catelan et al. 2004). This relation was established for fundamental-mode pulsators, therefore we must exclude the RRc stars of future analyses. Finally, these colors give us an estimate of the individual reddening of the RRab stars, which is shown in Table 2.6. We compared these reddening values with those obtained by Kunder et al. (2008) in the same Galactic latitude as our values ($\ell, b \sim -5°, -9°$) from the Galactic bulge fields of the MACHO survey. The mean converted value of $E(J-K_{\mathrm{s}})$ at that latitude is ~ 0.20 mag, with a dispersion of 0.04 mag, which is consistent with our measurements within the errors. In some cases, our estimates are slightly higher than those of Kunder et al. (2008), which may be due to larger distances or larger errors in the determination of the color $(J-K_{\mathrm{s}})$ in our light curves.

Distance to the RR Lyrae stars

We calculated the individual distances to the RRab stars using the $P-L$ relations for the K_{s} band. This distance can be expressed in terms of the absolute and the extinction-corrected K_{s}-band magnitudes,

$$\log R = 1 + 0.2(K_{\mathrm{s},0} - M_{\mathrm{K_s}}), \tag{2.7}$$

with R the individual distance in pc to our RRab stars and converting the color excess into extinction using the law of Cardelli et al. (1989),

$$A_{K\mathrm{s}} = 0.73E(J - K_{\mathrm{s}}). \tag{2.8}$$

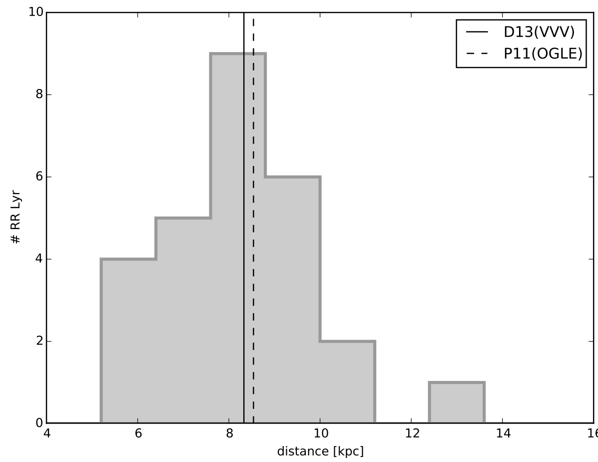

Figure 2.7: Distance to the sample of RR Lyr stars in tile *b201* in a 1.2 kpc binning size. The solid (D13) and dashed lines (P11) represent the values of the Galactic center distance given in Dékány et al. (2013) and Pietrukowicz et al. (2012).

Figure 3.6 shows the histogram of the distances calculated for the individual RR Lyr. A strong agreement with previous results is recovered even at this high latitude ($\ell \sim -10°$) with more than the 50% of the variables in the central kiloparsec according to a Gaussian fit with $d_{\rm mean} = 8.14$ kpc and a dispersion of $\sigma_d = 1.56$ kpc. Adopting the reddening law of Nishiyama et al. (2009) does not significantly change the distance distribution of our RRab stars; it adds 0.4 kpc to the mean, but keeps the dispersion unchanged.

The results of this analysis, including reddening, extinction, and distances with their error are shown in Table 2.6. The uncertainties consider the error propagation on the color, reddening, extinction, and distance of each individual RRab star. Another visualization of the derived distances, assuming a constant ℓ and b coordinate, is shown in Fig 3.7 as a cone view. This approach is useful in identifying groups or streams of variable stars in our FoV, which is not possible with their spatial distribution (ℓ, b) alone, as also shown in Fig. 3.7. Although there may be a group of RR ab stars at $d \sim 7$ kpc, these stars do not cluster in any other parameters, for example, in the period-amplitude diagram or spatially, and hence we are hesitant to consider them as a group.

An interesting topic of the RR Lyr studied in large areas is the possibility that they can trace an old stream-like structure (Sesar et al. 2013) in addition to the

Table 2.6: Reddening, extinction and distances computed for the RR Lyr found in tile *b201*.

VVV ID (RRab)	$E(J-K_s)$ (mag)	A_{Ks} (mag)	Distance (kpc)
VVV J2712426.16-421241.6	0.33 ± 0.13	0.23 ± 0.09	9.14 ± 0.31
VVV J2712711.57-421314.0	0.47 ± 0.11	0.32 ± 0.08	7.05 ± 0.21
VVV J2712912.05-420223.7	0.18 ± 0.16	0.12 ± 0.11	9.05 ± 0.40
VVV J2711512.06-415330.1	0.25 ± 0.13	0.17 ± 0.09	7.85 ± 0.26
VVV J2703434.23-413322.1	0.30 ± 0.13	0.21 ± 0.09	5.95 ± 0.19
VVV J2703536.01-412829.4	0.13 ± 0.13	0.09 ± 0.09	8.79 ± 0.28
VVV J2703343.00-412731.0	0.38 ± 0.13	0.26 ± 0.09	8.61 ± 0.31
VVV J2711523.24-413619.8	0.42 ± 0.13	0.29 ± 0.09	6.34 ± 0.22
VVV J2710804.03-413241.7	0.28 ± 0.14	0.19 ± 0.09	9.16 ± 0.33
VVV J2704944.51-412248.6	0.04 ± 0.16	0.03 ± 0.11	6.80 ± 0.30
VVV J2714215.15-414058.6	0.43 ± 0.15	0.30 ± 0.10	7.74 ± 0.32
VVV J2710759.32-411700.5	0.19 ± 0.14	0.13 ± 0.09	5.64 ± 0.21
VVV J2714823.59-413121.7	0.05 ± 0.14	0.04 ± 0.09	9.40 ± 0.35
VVV J2711644.06-411744.6	0.19 ± 0.14	0.13 ± 0.10	8.27 ± 0.31
VVV J2710158.99-410727.3	0.21 ± 0.10	0.14 ± 0.07	8.05 ± 0.20
VVV J2704656.26-421805.3	0.37 ± 0.09	0.25 ± 0.06	13.58 ± 0.28
VVV J2701149.18-420358.3	0.34 ± 0.11	0.23 ± 0.08	5.23 ± 0.15
VVV J2705101.04-405300.9	0.17 ± 0.12	0.12 ± 0.08	6.79 ± 0.21
VVV J2711836.69-405946.8	0.34 ± 0.13	0.23 ± 0.09	8.00 ± 0.28
VVV J2705334.00-421303.7	0.45 ± 0.10	0.31 ± 0.07	10.93 ± 0.26
VVV J2702317.06-420003.9	0.33 ± 0.10	0.22 ± 0.07	6.98 ± 0.17
VVV J2705622.48-420853.7	0.45 ± 0.12	0.31 ± 0.09	6.94 ± 0.23
VVV J2711018.90-421253.4	0.34 ± 0.12	0.24 ± 0.08	7.79 ± 0.23
VVV J2712342.04-421647.8	0.08 ± 0.14	0.06 ± 0.09	7.80 ± 0.29
VVV J2712855.63-421832.3	0.20 ± 0.09	0.13 ± 0.07	8.81 ± 0.21
VVV J2710638.97-420755.7	0.20 ± 0.13	0.14 ± 0.09	9.95 ± 0.35
VVV J2702400.61-415026.5	0.11 ± 0.15	0.08 ± 0.10	10.83 ± 0.45

spheroidal shape described by Dékány et al. (2013). Unfortunately, the small number of variables in this single tile prevent us from making any strong statements about the presence of streams in this direction.

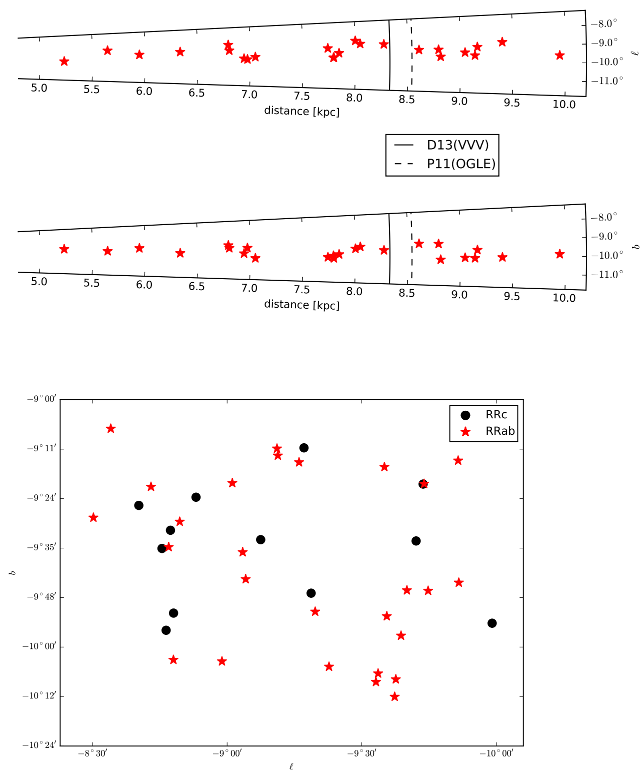

Figure 2.8: Left: Distance to the sample of RR Lyr stars, between 5 and 10 kpc, in a cone view. We did not find any apparent cluster or group in the RRab due to streams, except for the variables in the Galactic center. The solid and dashed lines have the same meaning as in Fig. 3.6. **Right:** Spatial distribution in Galactic coordinates of the 39 RR Lyr found in tile *b201*.

2.3 Summary

A search for RR Lyr stars was performed in the VVV tile *b201*, one of the outermost bulge regions covered by the VVV Survey. A total of 39 RR Lyr were found, of which 27 and 12 belong to the ab- and c-type, respectively. For the total sample, coordinates, periods, amplitudes, and near-IR colors were presented. Using the International Variable Star Index, we found counterparts of the ten previously known RR Lyr in the field, in agreement with past measurements. We found differences in only three of them, for which we suggested a revised period. From the analysis of the RRab sample, individual reddening, extinction, and distance were obtained, based on line-of-sight extinction values given by Cardelli et al. (1989) and the $P-L$ relation of Alonso-García et al. (2015). The distribution of these variables on the Milky Way follows a central distribution around $\sim$ 8.1 and $\sim$ 8.5 kpc. using the Cardelli or Nishiyama extinction law, respectively. This value is consistent with the results of Dékány et al. (2013), placing the center of the distribution at $\sim$8.3 kpc. An analysis of a larger area around $\ell \sim -10^{\circ}$ will be conducted to complement the studies of the inner Galactic bulge that are already published.

Chapter 3

Mapping the outer bulge with RRab stars from the VVV survey

Big astronomical surveys are changing the way we understand the formation, structure and evolution of our Galaxy. Among those, only a few have been able to access the inner regions of the Milky Way because of the effects of severe crowding and high interstellar extinction of these dense Galactic regions. Near- and mid-IR surveys such as 2MASS, GLIMPSE, and UKIDSS-GPS (Skrutskie et al. 2006; Benjamin et al. 2005; Lucas et al. 2008) have helped to overcome the extinction problem covering the innermost regions of the Galaxy, but the lack of multiple-epoch observations within those surveys prevents us from using them to study and characterize the large number of variable sources in the bulge. Optical time-domain surveys such as OGLE, MACHO, and EROS (Udalski et al. 2015; Alcock et al. 1996; Aubourg et al. 1993) have partially solved this problem but unfortunately the high extinction found towards the bulge line-of-sight restricts them from accurately map the innermost regions.

In response to these limitations, the VISTA Variables in the Vía Láctea (VVV) ESO public survey (Minniti et al. 2010) provides a near-IR, multi-epoch photometric coverage of the inner Galaxy ($-10° < \ell < 10°$, $-10° < \mathrm{b} < 5°$). The large near-IR coverage of the VVV survey, high spatial resolution, and depth of the survey enables the capacity to perform studies globally across the entire inner Galaxy, reaching larger distances than it has ever been possible before. The first stage of the VVV Survey provided full-coverage, multi-color photometry of the inner 520 sq. deg. of the Galaxy. These data was used for the construction of 2-D and 3-D extinction maps (Gonzalez et al. 2011, 2012; Schultheis et al. 2014), metallicity gradient maps (Gonzalez et al. 2013) of the Galactic bulge.

One of the main scientific goals of the VVV Survey is to build a global 3D map of the Milky Way using well known primary distance indicators. In this context, the first epoch of VVV observations has been used to investigate the shape of the bulge using the observed magnitude of red-clump giant stars as distance indicators. Bulge studies using red-clump stars have help unveiling the global shape of the stellar bar, confirming that the Milky Way hosts a peanut or x-shape bulge (Wegg & Gerhard 2013; Saito et al. 2012b).

On the other hand, the ongoing variability campaign of the VVV survey now allows us to investigate the shape of the inner Galaxy using variable stars as distance estimators. Variable star searches are expected to yield many more candidates in the near future (Catelan et al. 2013a,b), allowing us to measure the extinctions and distances along the line of sight, providing another 3D view of the inner Milky Way (Dékány et al. 2013, 2015). RR Lyrae stars are particularly interesting in this context as they allow us to trace, unequivocally, the oldest stellar component of the Galaxy (Dékány et al. 2013; Catelan & Smith 2015). Interestingly, the distance distribution of RR lyrae stars found by Dékány et al. (2013) follows a different shape than the one traced by red-clump stars. While the distances obtained from red-clump stars trace tightly the position angle of the bar, as well as the distance split along the minor axis due to the far and near arms of the x-shaped bulge, distances to the RR Lyrae population from Dékány et al. (2013) appear to follow a spheroidal distribution instead of the stellar bar traced by RC stars.

With this aim, in this present study we perform the search of RR Lyrae stars using VVV data continuing the analysis which was started by Gran et al. (2015), extending the work to 28 more VVV tiles (*b201-b228*), covering more than ~ 40 sq deg through Galactic latitudes between $-8^{\circ} \lesssim b \lesssim -10^{\circ}$. These regions have been not been covered by the OGLE survey yet, therefore the RR Lyrae presented here are particularly important in this context as this is where the x-shape bulge becomes most prominent making it the ideal location to investigate how different are the structures traced by these two populations. We calculate their distances and compare their spatial distribution with respect to those derived from red-clump stars.

3.1 Observations

The VVV Survey is a public ESO near-IR survey that is mapping the inner Milky Way, including the inner halo, the bulge and an adjacent section of the disk with the VISTA 4m telescope at ESO Paranal Observatory (Minniti et al. 2010). The survey covers an area of 562 sq deg in total, and the VVV database now contains $ZYJHK_\mathrm{s}$ photometry of about one billion sources on the VISTA system for which 2MASS coordinates have been used to construct the coordinate system, and a variability campaign in the K_s-band (Saito et al. 2012a; Hempel et al. 2014). See Gran et al. (2015) for more details of the instrument and their spatial configuration on the Galactic bulge and disk.

In this analysis we used data covering more than ~ 40 sq deg in the outer bulge, around $-10^\circ \lesssim \ell \lesssim 10^\circ$ and $-10^\circ \lesssim b \lesssim -8^\circ$. This area corresponds to the VVV tiles *b201* through *b228*, obtained between April 2010 and August 2014 with 60-62 epochs in all the selected tiles. We use aperture photometry applied to the stacked images (e.g. "tiles"), provided by the Cambridge Astronomical Survey Unit (CASU)[1] and setting the minimum number of epochs per star analyzed to 30 in order to achieve a better frequency analysis and avoid gaps in the light curves.

Detection and classification of RR Lyrae stars

We select variable candidates analyzing the χ^2 value for all the available time series; a similar analysis was presented in Carpenter et al. (2001). If this value exceeds the imposed cutoff of $\chi^2 = 2$ (see Gran et al. 2015), the time-series periodicities are tested by the analysis of variance (AoV) statistic (Schwarzenberg-Czerny 1989) in the RR Lyrae stars period range ($0.2 \leq P$ (days) ≤ 1.2). After this process the light curves were visually classified and 915 RRab stars candidates were added to the respective tile catalog of RRab stars with their VVV ID, coordinates, mean magnitudes, and periods.

We repeat the classification process over the 28 analyzed tiles (*b201-b228*) and check if there were duplicates in our catalogs. The tiling pattern produces about 7% of overlapping areas between the tiles (Saito et al. 2012b), thus we cleaned up duplicated RR Lyrae stars in the overlapping regions from our sample by combining their data, in a total of 32 stars. For those the number of data points roughly

[1] `http://casu.ast.cam.ac.uk/vistasp/`

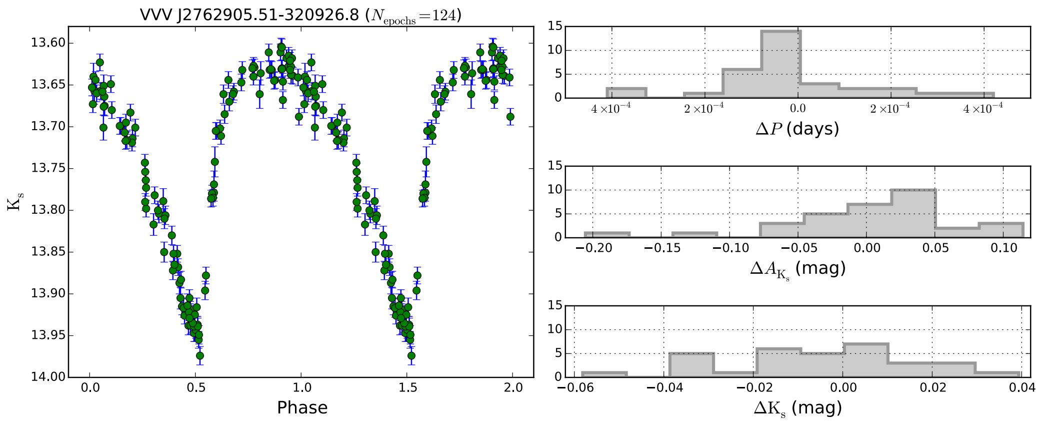

Figure 3.1: Left: RR Lyrae star in the overlap of two adjacent tiles (*b208* and *b222*). The light curve has the maximum number of epochs in our sample ($62 \times 2 = 124$). **Right:** Comparison of light curve features (peridod, amplitude and mean magnitude) for the 32 duplicated RR Lyrae stars.

doubles, with up to 124 epochs per target. RR Lyrae stars in the intersection areas are also important in order to check the parameters derived from two independent light-curves. Fig. 3.1 shows a RRab star with the maximum number of epochs in the intersection of the VVV tiles *b208* and *b222*, and a comparison of the derived periods (upper right), amplitudes (middle right) and mean magnitudes (lower right), for the overlapping RRab stars. As expected for the analysis of the same variable star, the independent three features differences (ΔP, ΔA_{K_s}, and ΔK_s) show a peak around 0, that confirms our derived values.

In this process we only assign a label to the RRab stars due to their characteristic light curve shape, high near-IR amplitude ($0.2 \lesssim A_{K_s}$ (mag) $\lesssim 0.5$) and narrow period range. As reported by Alonso-García et al. (2015), in near-IR bands the quantity of features to classify different variable types are fewer than in the optical regime. In the near future, we will also produce a catalog of VVV variable sources classified using automated procedures (see Catelan et al. 2013b; Angeloni et al. 2014, for more details).

One of the 28 tiles explored is obliterated by the presence of a very bright star, resulting in fewer RR Lyrae discovered. Tile *b205* contains the star η Sgr (HD 167600) which is very bright in the near-IR with $K_s \sim -1.55$ mag. Such a bright star not only saturates the detector, but also causes reflections that affect the flat fields, and the resulting mosaic of this tile contains regions that are not suitable for variability searches. This is the reason why tile *b205* contains fewer RRab stars ($N_{\mathrm{RRab}} = 28$) than the rest of the tiles ($N_{\mathrm{RRab}} \sim 32$ on average).

3.2 Results

After filtering the duplicates, the final catalog includes 883 RRab stars from 28 VVV tiles. Some of the lighcurves are shown in the Figs. A.1 and A.2. In the first step we characterized this sample in terms of its calculated the magnitude-weighted $\langle K_{\mathrm{s}} \rangle$, $\langle J \rangle - \langle K_{\mathrm{s}} \rangle$ color, periods, amplitudes, light-curve shapes, and, coordinates. Fig. 3.2 shows the $J \times K_{\mathrm{s}}$ color-magnitude diagram (CMD) for the complete RR Lyrae catalog with tile *b201* as a comparison field. Circles and stars represent the overlapping and single detection stars of the RRab sample, respectively. The RR Lyrae stars lie in a wide range of mean-K_{s} magnitudes due to their distance distribution in the Galaxy, but the $J - K_{\mathrm{s}}$ color is limited between ~ 0.0 and 0.6, similar values to those reported by Gran et al. (2015).

Besides the locus on the CMD, the RR Lyrae stars can be identified by their position on the Bailey diagram (Bailey 1902), which relates the period and amplitude of the RR Lyrae stars, and the period distribution of the entire sample. From the Bailey diagram (Fig. 3.3), we can select the high-amplitude short-period (HASP) RRab stars with the same criteria adopted by Fiorentino et al. (2015), for periods below $\log P$ (days) $\lesssim 0.35$. The fraction of HASP stars over the total number of RRab stars in our sample results in $N_{\mathrm{HASP}}/N_{\mathrm{RRab}} \approx 6\%$, far from the fraction derived for the Galactic bulge (17%) and closer to the values calculated for the Galactic halo ($6 - 8\%$).

In addition to the period and amplitude, another characteristic feature of the RRab stars is the light-curve shape, that can be described by a Fourier series. A sine decomposition up to sixth order was performed with the Direct Fourier Fitting (DFF) routine given by Kovács & Kupi (2007). Fig. 3.4 shows the R_{21}, ϕ_{21}, R_{31} and ϕ_{31} coefficients as function of the determined period. All the Fourier components tend to be clustered in a limited region in this space. There were some outliers in the distributions (e.g.: RRab with $R_{21} > 0.6$ or $\phi_{21} > 2$) which were visually inspected, finding some gaps in the light-curve that impact in the final value.

The spatial distribution in Galactic coordinates of the catalog is shown in Fig. 3.5. The observations span only 2° in b but more than 20° in ℓ, resulting in the very elongated figure shape. Although there are no globular clusters in the analyzed area

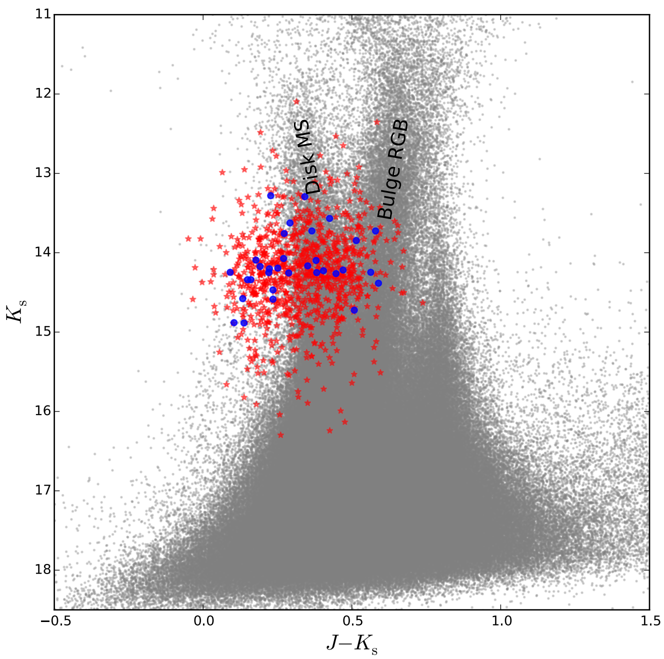

Figure 3.2: $J \times K_s$ CMD of the complete catalog of RR Lyrae stars and the tile *b201* as background. The CMD shows two prominent features, the disk main sequence (MS) and the bulge red giant branch (RGB), that are identified in the figure. Circles and stars represents the overlapping and single detection RR Lyrae stars, respectively.

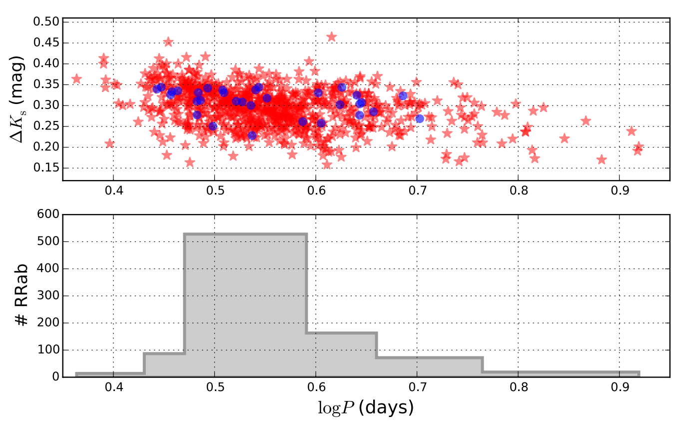

Figure 3.3: Upper: Bailey diagram of the complete RRab catalog. **Lower** Period histogram of the 883 RRab stars with bins adapted by the Bayesian Block algorithm (Scargle et al. 2013) through the `astroML` implementation (Vanderplas et al. 2012).

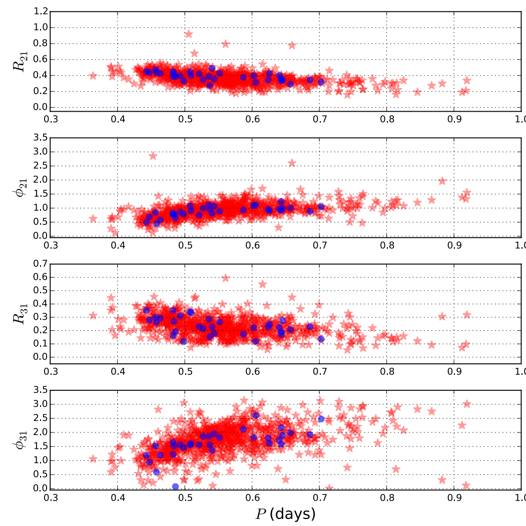

Figure 3.4: Top to Bottom: R_{21}, ϕ_{21}, R_{31} and ϕ_{31} coefficients of a Fourier series (sine based) using the DFF routine.

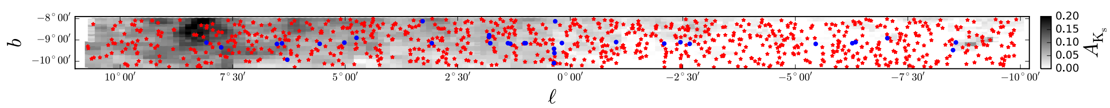

Figure 3.5: Spatial distribution in Galactic coordinates (ℓ, b) of the RRab stars found plotted over the extinction (A_{K_s}) map given by the BEAM Calculator (Gonzalez et al. 2011, 2012). The values of A_{K_s} were truncated at 0.2 for better visualization.

according to the Francis & Anderson (2014) catalog, their presence in nearby regions could bias the number of RR Lyrae stars found. This possible effect in our catalog was investigated on the three closest globular clusters to our sample of RRab stars. NGC 6656 is the only cluster that have associated RR Lyrae stars according to (Clement et al. 2001, ; online catalog[2], 2015 edition), but the closest variable is $10'$ further from the cluster tidal radius ($r_t \approx 30'$) given by the 2010 version of the Harris (1996) Catalog. NGC 6624 and 6637 are considered metal-rich clusters with [Fe/H] values of -0.63 and -0.77, respectively (Valenti et al. 2004, 2005). Both clusters develop a very red horizontal branch, which is the reason why they are not known to have associated RR Lyrae stars.

[2]http://www.astro.utoronto.ca/~cclement/read.html

Distances and the 3D view of the outer bulge

One of the main goals of the VVV Survey is to trace the Galactic structure using variable stars in order to make the most complete 3D view of the central regions ofour Galaxy (Minniti et al. 2010). The primary distance indicators are the RR Lyrae stars due to the high number density present in the bulge area (Soszyński et al. 2014) and the tight period–luminosity (P–L) relation that they follow in near-IR bands (Longmore et al. 1990; Catelan et al. 2004). To obtain the distance values, in first place we must calculate the reddening and extinction values to the individual variables. The former quantity can be obtained through the difference between the mean-apparent and absolute magnitudes of our RRab stars, given by,

$$E(J-K_{\rm s}) = (J-K_{\rm s}) - (J-K_{\rm s})_0 = (J-K_{\rm s}) - (M_J - M_{K_{\rm s}}),$$

where $(J-K_{\rm s})_0$ is the intrinsic color of our RRab star and M_X the absolute magnitude in the X-band. In our analysis we adopt the P–L relations derived by Alonso-García et al. (2015) to recover the absolute magnitudes of the RR Lyrae stars in the J- and $K_{\rm s}$-bands. To calculate the J-band mean magnitudes for the stars in our catalog we performed a linear regression between the J- and $K_{\rm s}$-band mean magnitudes of the RRab stars of ω Centauri studied by Navarrete et al. (2015, in preparation). This analysis is needed because the VVV Survey only provides one observation in the $ZYJH$-bands. The resulting fit is given by $\langle J\rangle = 0.98 \times \langle K_{\rm s}\rangle + 0.55$. As expected, the residuals are centered in 0 with a dispersion of 0.03 mag. These allows us to derive the reddening on a star-by-star basis, and additionally the extinction of each RRab star, by adopting an extinction law (e.g., Cardelli et al. 1989).

At this point we calculate the distances given by,

$$\log R = 1 + 0.2(K_{{\rm s},0} - M_{K_{\rm s}}),$$

with R the individual distance in pc to our RRab stars. Fig. 3.6 shows the distribution of distances of the RRab stars in our catalog. The complete catalog is also available in the Table A.1 with all the features derived until the distance. The vertical line corresponds to the Galactic center distance derived in Dékány et al. (2013) with a value of $R_0 \approx 8.33$ kpc. Our distances have a maximum frequency around R_0 where the center of the distribution is, and an asymmetric shape towards the far side of the bulge because the volume observed is bigger due to the cone effect.

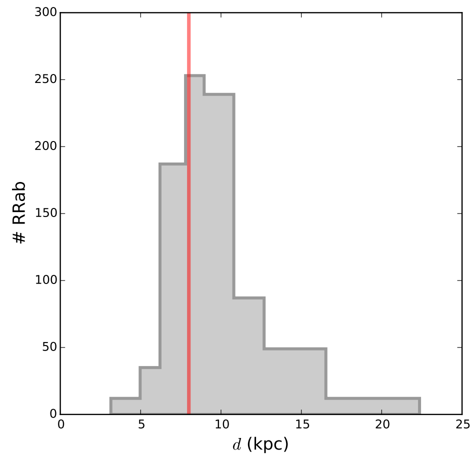

Figure 3.6: Distribution of distances of the RR Lyrae found. The vertical line represents the Galactic center derived by Dékány et al. (2013) with OGLE-III RR Lyrae stars of $R_0 \approx 8.33$ kpc.

According to their distances, there are some RR Lyrae stars which seem to belong to the Sagittarius dwarf spheroidal (Sgr dSph) galaxy (e.g., distances around ~ 20 kpc, in Fig. 3.7 stars with $\ell \gtrsim 6°$, and the left panel of Fig. 3.8). Kunder & Chaboyer (2009b) place the core of the Sgr dSph galaxy $\sim 22 - 27$ kpc from the Sun but $\sim 4°$ away from our analyzed region. Nevertheless, some RR Lyrae stars have been associated to the dwarf galaxy by MACHO (Alard 1996; Alcock et al. 1997) and OGLE (Soszyński et al. 2014), therefore we cannot rule out such an origin for this group. A posible explanation to the locus of these RR Lyrae stars could be the interaction Sgr dSph–Milky Way that places those remnants in the middle of both galaxies. Further analysis is required to make a decision on this elongated structure traced by the RR Lyrae stars.

The elongated shape of the analyzed area allow us to approximate the observation volume by a 2D cone, projecting the b coordinate. Fig. 3.7 shows distances and Galactic longitude in this line-of-sight cone projection. The RR Lyrae stars tend to stay near the projected Galactic center distance ($d \approx 8$ kpc) and the previously mentioned Sgr dSph RR Lyrae candidates are clearly visible in the $16 \leq d$ (kpc) ≤ 22 and $\ell \geq 6°$ zone. In contrast to Pietrukowicz et al. (2012) our data do not show any elongation along a particular direction.

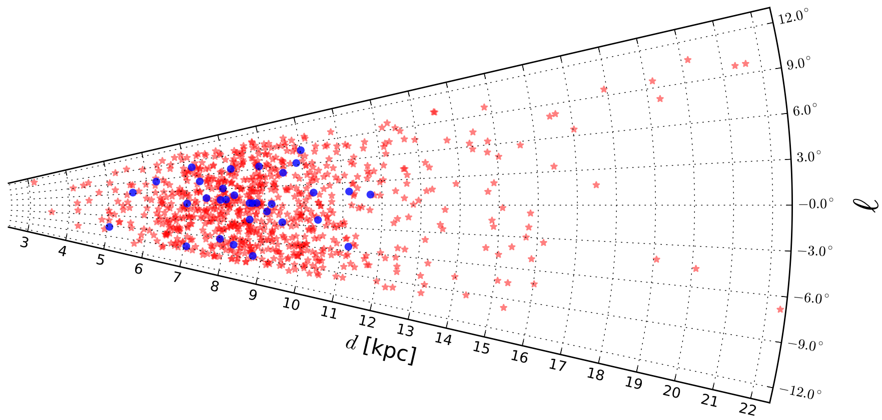

Figure 3.7: Cone-view (d, ℓ) of the analyzed area in the Galactic bulge. Just like previous Figures, stars and circles shows the single- and double-tile detections, respectively. The sample is concentrated around the projection of the Galactic center.

Trace or not to trace: the x-shape problem

Many efforts have been made to study the 3D structure of the Milky Way through its stellar content. One important distant indicator are the pulsating variable stars (e.g., RR Lyrae and Cepheids, among others), but besides this method, the red clump (RC) stars were also used in near-IR single epoch studies to derive accurate distances to the Milky Way edge (Minniti et al. 2011), bulge (Alves 2000) or the Large Magellanic Cloud (Alves et al. 2002). This feature of the RC stars has been used recently to discover the x-shape structure of the Milky Way (McWilliam & Zoccali 2010; Saito et al. 2011; Wegg & Gerhard 2013) that contains a bar in its central parts (Rattenbury et al. 2007; Gonzalez et al. 2011). It is clear and well studied that the RC stars follow this barred Galactic feature, but in the RR Lyrae case there is no clear evidence for the same trend. In one hand Pietrukowicz et al. (2012) with OGLE-III RR Lyrae stars claim the existence of the barred structure rotated about 30° with respect to the line of sight between the Sun and the Galactic center. On the other hand Dékány et al. (2013) completely rule out this possibility using the same dataset, but (crucially) including the near-IR results of the VVV Survey.

We have used our catalogue to compare the distribution of RR Lyrae at low

Galactic latitude with the distribution of RC stars in the same analyzed tiles. Both catalogues were divided in three longitude bins: $-10° < \ell < -3.5°$; $-3.5° < \ell < 3.5°$ and $3.5° < \ell < 10°$. The RC stars were selected with the same technique described in Minniti et al. (2011) with magnitudes $K_\mathrm{s} < 15$, effectively limiting our study to RC stars at distances lower than ~ 20 kpc. Assuming an intrinsic RC absolute magnitude $M_{K_\mathrm{s}} = -1.55$ and an intrinsic RC color $(J - K_\mathrm{s})_0 = 0.68$, as given by Gonzalez et al. (2011) for Baade's window RC stars, the distance equation yields:

$$\mu = -5 + 5 \log d \text{ (pc)} = K_\mathrm{s} - 0.73(J - K_\mathrm{s}) + 2.05,$$

where the Cardelli et al. (1989) extinction law was assumed.

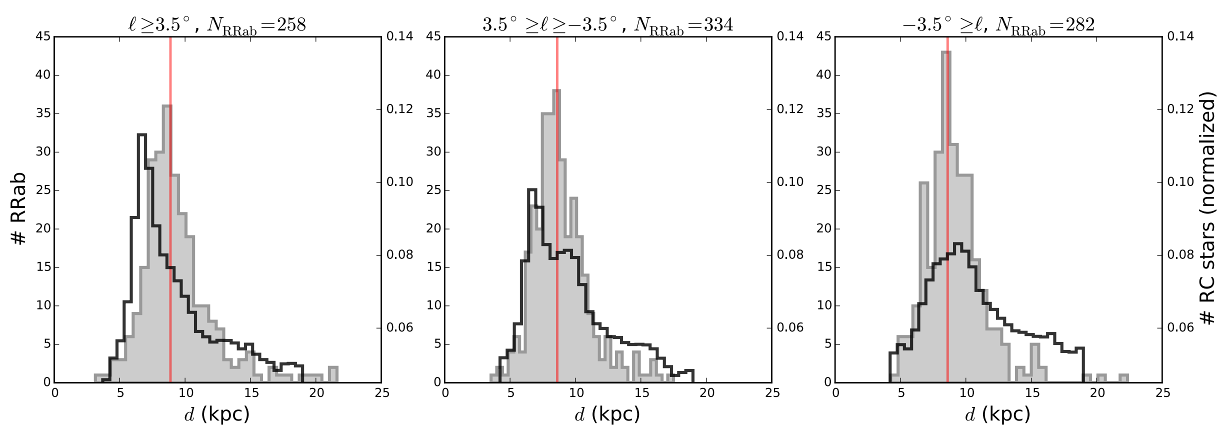

Figure 3.8: Histogram of distances of RR Lyrae (gray filled) and RC stars (black steps) as function of Galactic latitude (ℓ). Since the total number of RC stars in the same areas overwhelms the number of RR Lyrae, the histogram showing their distribution in distance was normalized for visualization purposes. The vertical line represents the RR Lyrae median distance of each region.

Fig. 3.8 shows the result of the comparison between the distance distribution of RC and RR Lyrae stars. The red vertical line shows the median distance of RR Lyrae in each longitude bin, namely $d_\mathrm{RRL} \sim 8.88$, 8.60, and 8.81 kpc, from positive to negative longitudes, respectively. Clearly, the variation in the median distance across the longitude direction is negligible for RR Lyrae. RC stars, on the contrary, show a single peak at $d_\mathrm{RC} \sim 6.8$ kpc at positive longitudes, two peaks at $d_\mathrm{RC} \sim 6.8$ and 9.5, kpc across the minor axis, and a single peak at $d_\mathrm{RC} \sim 9.4$ kpc at negative longitudes. In all three cases, a two-sample Kolmogorov-Smirnov test reveals that the distributions of RC and RR Lyrae stars are indeed different, with higher than

99.7% probability. This strongly suggests that the RC stars (but not the RR Lyrae) follow the main Galactic bar, flaring up into a peanut (x-shape) far away from the Galactic plane. The marked difference in the distance distribution of RR Lyrae variables and RC stars confirms, at low latitudes, the conclusion by Dékány et al. (2013), that RR Lyrae and RC stars trace two difference components in the bulge.

Chapter 4

Summary and future work

Divided in two separate projects a search for RR Lyrae stars was performed in more than ~ 40 sq deg in the outer parts of the Galactic bulge observed by the VVV Survey. In total, more than 880 fundamental mode RR Lyrae stars were found in this area using the χ^2 value and the analysis of variance statistic for testing the variability and periodicity, respectively. We have analyzed the periods, amplitudes, light curve shapes, and 3D positions of the RR Lyrae stars within the Galaxy. This sample allow us to compare the distribution along the Galactic longitude of RR Lyrae with a previously known distribution of RC stars (x-shape), resulting in a very significant difference of more than 1.5 kpc between the peaks of both distributions across all the mapped region. These differences prevail along the Galactic latitudes observed by the VVV Survey that shows an unchanged RR Lyrae distance distribution and a moving RC distribution tracing the Milky Way bar. This result fully supports the hypothesis which postulates a spheroidal or central distribution of the RR Lyrae stars in the Galactic bulge, not tracing the strong bar of the RC stars.

A complete scenario of the RR Lyrae stars over the entire Galactic bulge will be unveiled when fully automatic searches in the VVV Survey begin. As a preparation and support for this process this work is valuable source of a huge quantity of template-like light curves to feed machine learning algorithms. Moreover, this work lays the foundation for completing the density map of RR Lyrae stars in the 3D model of the Galaxy, only which so far it has only achieved in the area of observation of the OGLE survey. This model of RR Lyrae in the Galaxy could make clear the existence of streams or clusters that have been hidden by the layer of dust and gas of our Galaxy. Finally, an interesting branch that emerges from this work and is subject of study in the future is the distribution of RR Lyrae stars at the distances of the Sgr dSph Galaxy ($d \gtrsim 20$ kpc found in this work), and how they could trace and constrain dynamical models of the history of encounters with our Galaxy.

Annex A

RR Lyrae: figures and catalog

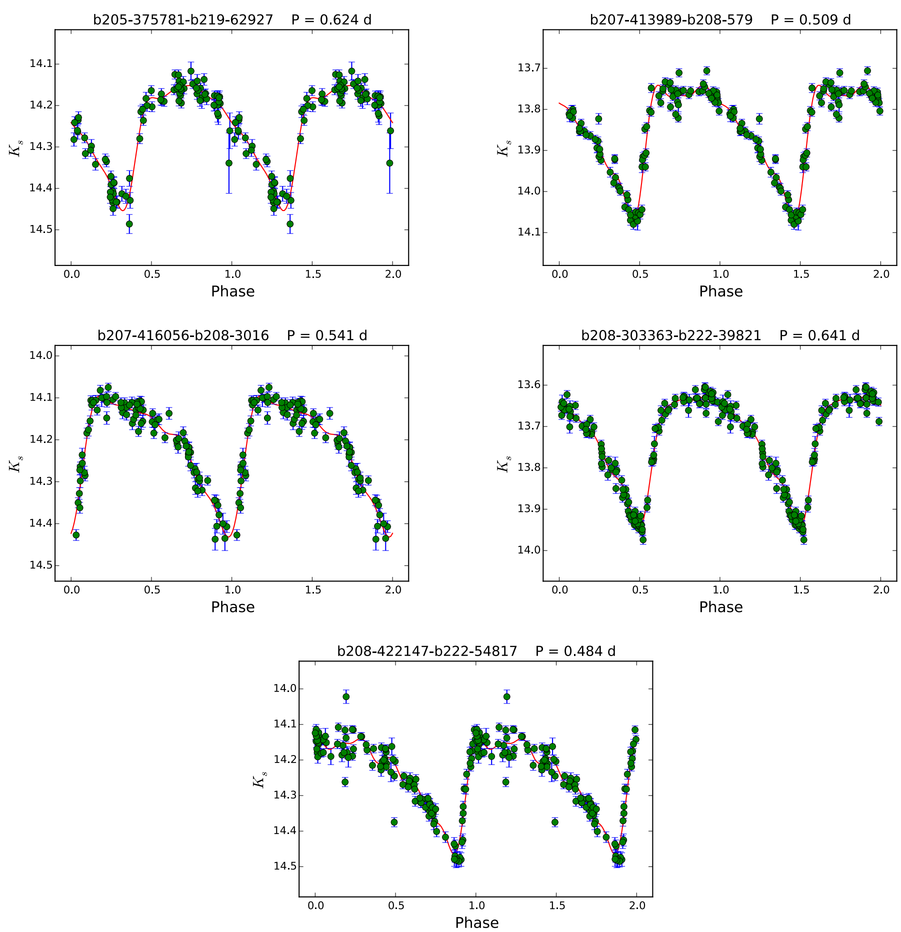

Figure A.1: Selected (overlapping) RR Lyrae stars lightcurves in the outer bulge region.

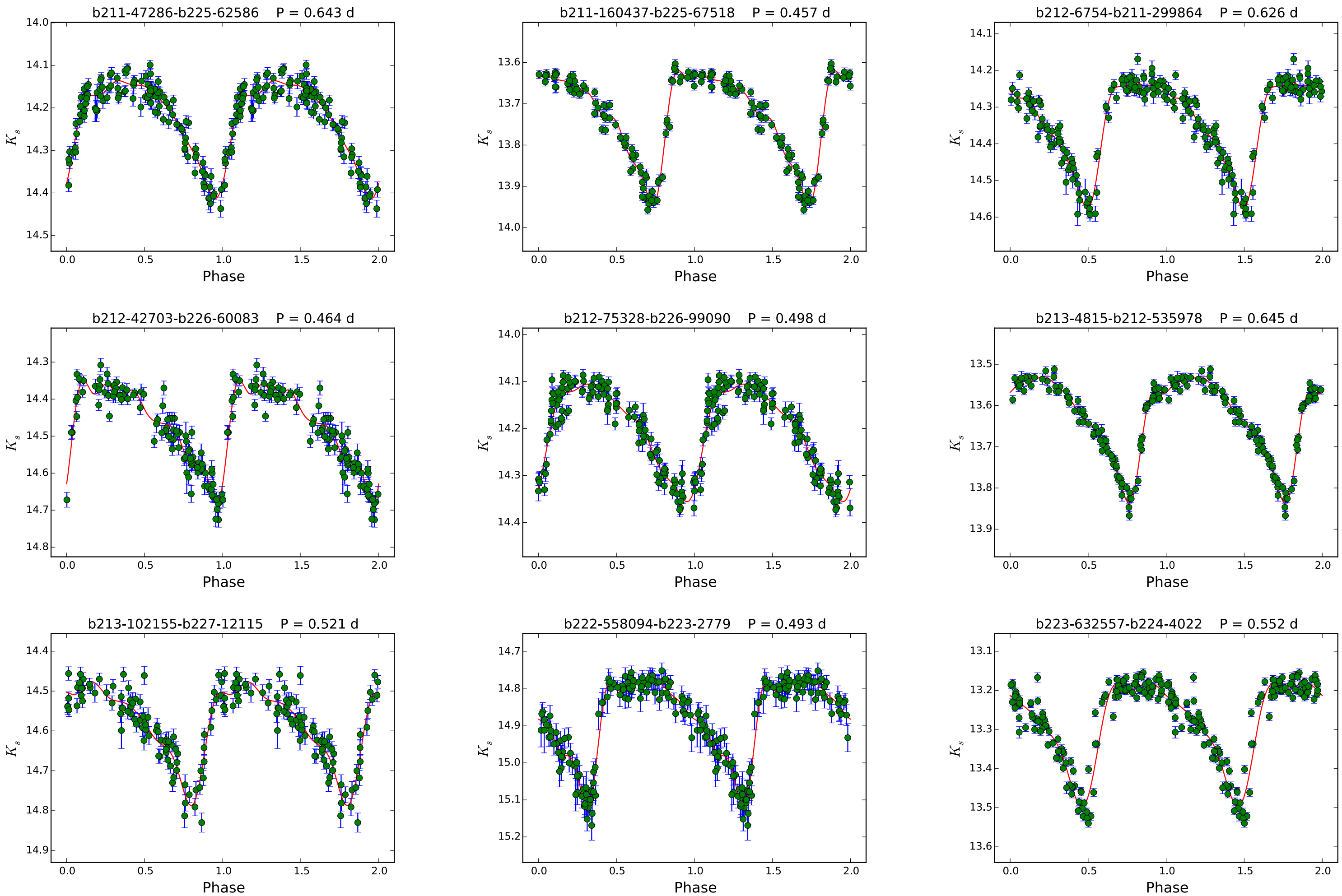

Figure A.2: Selected (overlapping) RR Lyrae stars lightcurves in the outer bulge region.

Table A.1: Complete parameters derived for the RR Lyrae stars in the VVV outer bulge.

RA(J2000) deg	Dec(J2000) deg	ℓ deg	b deg	X kpc	Y kpc	Z kpc	J mag	K_s mag	P days	A_{K_s} mag	d kpc
270.78228	-42.30151	-9.86052	-9.73939	6.59	-2.59	-2.62	15.632	15.222	0.660982	0.37	15.34
270.19694	-42.06621	-9.85798	-9.24595	-2.72	-0.97	-0.91	13.726	13.219	0.604051	0.28	5.74
270.89278	-42.21770	-9.74650	-9.77232	3.78	-2.08	-2.13	15.360	15.045	0.523470	0.34	12.45
270.38805	-42.00109	-9.73164	-9.33999	-0.99	-1.25	-1.22	14.363	14.146	0.448021	0.32	7.52
270.93957	-42.14826	-9.66776	-9.77044	-0.70	-1.30	-1.33	14.198	14.076	0.511941	0.33	7.83
271.17191	-42.21485	-9.64591	-9.95378	0.08	-1.43	-1.49	14.157	14.031	0.638696	0.36	8.64
271.39502	-42.27997	-9.62652	-10.13027	-0.73	-1.28	-1.37	14.297	14.132	0.485058	0.23	7.80
271.48213	-42.30899	-9.62234	-10.20082	0.58	-1.51	-1.62	14.632	14.460	0.491162	0.37	9.15
271.11082	-42.13214	-9.59306	-9.87516	1.88	-1.72	-1.80	14.843	14.598	0.560774	0.26	10.49
270.40015	-41.84070	-9.58420	-9.27192	2.54	-1.83	-1.80	15.021	14.728	0.560897	0.31	11.15
271.40727	-42.21158	-9.56070	-10.10661	1.31	-1.62	-1.74	14.926	14.584	0.510837	0.29	9.91
271.45322	-42.22059	-9.55278	-10.14094	-0.59	-1.30	-1.40	14.475	14.232	0.460162	0.35	7.95
271.48669	-42.03992	-9.37847	-10.07923	0.93	-1.53	-1.67	14.458	14.230	0.642893	0.25	9.51
271.25335	-41.89169	-9.32704	-9.85673	-0.12	-1.34	-1.44	14.174	14.000	0.625493	0.29	8.42
270.57617	-41.55613	-9.26718	-9.25294	-1.99	-1.03	-1.03	13.836	13.345	0.678049	0.24	6.48
271.34581	-41.84182	-9.24970	-9.89446	5.63	-2.27	-2.48	15.398	15.224	0.582245	0.33	14.33
270.59332	-41.47484	-9.18846	-9.22581	0.66	-1.45	-1.48	14.319	13.970	0.756624	0.31	9.20
270.56193	-41.45862	-9.18526	-9.19741	1.02	-1.51	-1.53	15.032	14.455	0.535828	0.27	9.57
271.25645	-41.60550	-9.06901	-9.72536	-1.40	-1.10	-1.19	13.998	13.785	0.548456	0.29	7.09
270.82903	-41.38015	-9.01935	-9.33692	-1.62	-1.06	-1.11	13.904	13.357	0.746910	0.24	6.86
271.70422	-41.68294	-8.98092	-10.05766	0.17	-1.34	-1.52	14.414	14.295	0.516761	0.30	8.71
270.80932	-41.18407	-8.85120	-9.23145	4.61	-2.01	-2.14	15.527	15.214	0.507123	0.32	13.24
271.13314	-41.28346	-8.82409	-9.49311	-2.59	-0.89	-0.96	13.521	13.393	0.541703	0.30	5.87
271.90279	-41.56047	-8.80099	-10.13286	-1.72	-1.02	-1.18	13.863	13.537	0.622886	0.19	6.77
271.27891	-41.29572	-8.78314	-9.59565	0.32	-1.33	-1.48	14.161	13.842	0.786720	0.28	8.85
271.03305	-41.12424	-8.71737	-9.35192	-0.10	-1.26	-1.37	14.581	14.227	0.513896	0.31	8.41
271.03130	-40.84768	-8.47064	-9.22077	0.98	-1.38	-1.53	14.604	14.442	0.534985	0.32	9.51
271.67788	-41.06448	-8.43374	-9.75379	0.79	-1.35	-1.58	14.758	14.264	0.602442	0.23	9.33
272.16050	-41.18800	-8.37466	-10.13330	-2.16	-0.90	-1.10	13.756	13.506	0.562019	0.27	6.31
271.83595	-41.05370	-8.36802	-9.85443	-1.19	-1.05	-1.25	13.697	13.387	0.816446	0.17	7.30
271.12254	-40.73189	-8.33421	-9.22731	-0.75	-1.11	-1.24	14.502	14.112	0.485555	0.35	7.73
272.13556	-40.95502	-8.17327	-10.00955	-0.43	-1.13	-1.40	14.035	13.929	0.616637	0.33	8.08

Continued on next page...

Table A.1 – Continued

RA(J2000) deg	Dec(J2000) deg	ℓ deg	b deg	X kpc	Y kpc	Z kpc	J mag	K_s mag	P days	A_{K_s} mag	d kpc
272.15406	-40.92303	-8.13790	-10.00724	2.55	-1.55	-1.94	14.623	14.410	0.736323	0.36	11.13
272.28431	-40.96613	-8.13090	-10.11443	-0.31	-1.14	-1.44	14.338	14.238	0.485446	0.28	8.20
272.55521	-40.93545	-8.00811	-10.28235	2.80	-1.56	-2.04	15.238	14.903	0.503069	0.33	11.40
271.91750	-40.59414	-7.92563	-9.69654	4.49	-1.78	-2.22	15.276	14.811	0.704642	0.30	13.11
272.33992	-40.73039	-7.89854	-10.04371	1.88	-1.41	-1.83	14.487	14.400	0.660589	0.30	10.45
272.59399	-40.79058	-7.86350	-10.24238	0.17	-1.17	-1.55	14.896	14.432	0.457733	0.30	8.70
271.44868	-40.33210	-7.85870	-9.25890	3.91	-1.69	-2.02	15.080	14.865	0.615358	0.19	12.49
272.07854	-40.55456	-7.83266	-9.78673	-0.29	-1.10	-1.40	13.906	13.742	0.746960	0.27	8.21
272.28236	-40.53839	-7.74571	-9.91677	1.93	-1.39	-1.81	15.273	15.100	0.363689	0.36	10.49
271.84035	-40.24469	-7.63921	-9.48252	0.28	-1.15	-1.45	14.367	14.370	0.491681	0.28	8.78
272.77774	-40.58778	-7.61553	-10.27404	2.71	-1.47	-2.02	14.766	14.685	0.596531	0.30	11.29
272.74344	-40.50066	-7.54876	-10.21117	1.36	-1.28	-1.76	14.421	14.172	0.728470	0.17	9.90
272.22972	-40.28055	-7.53208	-9.76254	1.30	-1.27	-1.67	14.922	14.424	0.577731	0.23	9.83
272.75172	-40.48301	-7.52988	-10.20874	1.39	-1.28	-1.77	14.698	14.518	0.543845	0.39	9.94
271.63075	-40.01912	-7.51248	-9.23568	3.15	-1.51	-1.89	15.344	15.042	0.468733	0.31	11.71
272.43755	-40.30619	-7.48123	-9.91510	-2.55	-0.75	-1.01	13.530	13.280	0.600875	0.22	5.89
272.35223	-40.24650	-7.45775	-9.82987	0.50	-1.15	-1.54	14.452	14.258	0.568469	0.28	9.02
271.98029	-40.09825	-7.45739	-9.50933	6.70	-1.96	-2.56	15.529	15.367	0.583989	0.29	15.35
271.82583	-40.01233	-7.43586	-9.36473	1.41	-1.27	-1.62	14.635	14.176	0.729320	0.18	9.93
272.67743	-40.34375	-7.43016	-10.09490	-0.49	-1.02	-1.40	14.221	14.071	0.535613	0.36	8.00
271.69265	-39.77910	-7.27498	-9.16567	0.90	-1.18	-1.50	14.009	13.800	0.912051	0.24	9.40
272.58642	-40.11410	-7.25502	-9.92812	0.92	-1.17	-1.63	14.851	14.434	0.531426	0.32	9.44
272.76404	-40.17996	-7.25150	-10.07899	7.34	-1.99	-2.83	16.117	15.713	0.468878	0.36	16.02
272.19306	-39.92486	-7.22506	-9.57360	3.90	-1.55	-2.09	15.453	15.188	0.464755	0.31	12.48
272.15396	-39.86263	-7.18316	-9.51824	0.86	-1.16	-1.55	15.019	14.540	0.478270	0.32	9.37
272.80518	-40.04974	-7.11922	-10.04760	-3.48	-0.60	-0.85	13.115	12.921	0.590514	0.25	4.93
272.82570	-40.04273	-7.10562	-10.05838	-2.24	-0.76	-1.08	14.079	13.756	0.438847	0.29	6.20
273.02902	-40.08187	-7.06912	-10.21477	0.64	-1.11	-1.63	14.852	14.324	0.552385	0.23	9.15
272.99769	-40.00546	-7.01102	-10.15869	1.48	-1.20	-1.77	14.546	14.421	0.599790	0.23	10.01
272.69763	-39.86503	-6.99062	-9.88989	1.47	-1.20	-1.72	14.669	14.327	0.648496	0.33	10.00
272.56702	-39.70214	-6.89036	-9.72605	1.86	-1.23	-1.76	14.989	14.677	0.514340	0.29	10.39
272.24403	-39.54471	-6.86487	-9.43271	13.58	-2.64	-3.71	16.553	16.293	0.526432	0.36	22.35
271.88074	-39.39405	-6.86151	-9.11437	0.21	-1.02	-1.38	14.472	14.278	0.521222	0.27	8.68

Continued on next page...

Table A.1 – Continued

RA(J2000) deg	Dec(J2000) deg	ℓ deg	b deg	X kpc	Y kpc	Z kpc	J mag	K_s mag	P days	A_{K_s} mag	d kpc
273.12844	-39.88997	-6.86024	-10.19558	-0.07	-0.99	-1.49	14.295	13.954	0.652405	0.33	8.43
272.00277	-39.42792	-6.84745	-9.21358	-0.41	-0.95	-1.29	14.486	14.165	0.499715	0.32	8.05
272.89236	-39.75132	-6.81856	-9.97104	0.39	-1.04	-1.54	14.571	14.188	0.588228	0.21	8.89
272.20679	-39.47545	-6.81610	-9.37520	2.03	-1.24	-1.72	14.497	14.274	0.749614	0.32	10.55
273.06643	-39.80841	-6.80836	-10.11614	2.23	-1.26	-1.90	15.222	14.806	0.492764	0.31	10.78
272.65286	-39.61572	-6.78169	-9.74512	3.07	-1.35	-1.98	15.247	14.743	0.598695	0.24	11.63
272.64275	-39.60972	-6.77990	-9.73545	0.33	-1.03	-1.49	14.498	14.194	0.576725	0.18	8.82
272.33992	-39.40541	-6.70497	-9.43400	2.61	-1.28	-1.84	14.811	14.482	0.693621	0.31	11.15
272.46532	-39.43123	-6.68291	-9.53187	1.77	-1.18	-1.71	14.806	14.648	0.518374	0.18	10.29
272.08710	-39.18264	-6.59671	-9.15742	-1.92	-0.74	-1.03	13.636	13.229	0.756601	0.28	6.51
272.88910	-39.46047	-6.55702	-9.83608	-1.95	-0.73	-1.10	13.737	13.522	0.583897	0.25	6.49
272.93777	-39.47170	-6.54974	-9.87464	1.63	-1.14	-1.75	14.682	14.513	0.567688	0.27	10.15
273.21292	-39.51707	-6.49269	-10.08436	2.64	-1.25	-1.97	14.420	14.166	0.917979	0.19	11.19
272.34529	-39.15771	-6.48036	-9.32325	-1.90	-0.73	-1.05	13.550	13.159	0.809363	0.25	6.54
272.36067	-39.15892	-6.47587	-9.33439	-0.58	-0.88	-1.28	14.343	14.269	0.439199	0.35	7.88
273.08312	-39.36872	-6.40475	-9.92766	3.59	-1.34	-2.11	15.209	14.883	0.576166	0.21	12.16
273.45785	-39.49206	-6.38313	-10.24156	-0.04	-0.92	-1.50	14.180	14.052	0.601830	0.25	8.45
272.75147	-39.20955	-6.38007	-9.62661	2.46	-1.20	-1.85	15.198	14.900	0.471125	0.25	10.99
272.93980	-39.18411	-6.28936	-9.74473	1.48	-1.08	-1.70	14.991	14.579	0.520855	0.22	9.99
273.02506	-39.20551	-6.27807	-9.81329	1.17	-1.04	-1.65	14.554	14.420	0.563517	0.28	9.68
272.72208	-38.98442	-6.18784	-9.50304	3.87	-1.32	-2.06	15.151	15.023	0.531237	0.34	12.42
273.19893	-39.09561	-6.11644	-9.88327	-1.90	-0.69	-1.12	14.032	13.646	0.531912	0.32	6.54
273.62300	-39.29196	-6.14314	-10.26522	1.28	-1.03	-1.75	14.603	14.380	0.596969	0.28	9.80
272.91941	-38.98362	-6.11581	-9.63898	-2.34	-0.64	-1.01	13.760	13.583	0.491210	0.23	6.08
272.54905	-38.80140	-6.08597	-9.29924	0.50	-0.94	-1.45	14.487	14.166	0.610139	0.20	8.97
272.76455	-38.84846	-6.05000	-9.46994	-0.58	-0.82	-1.29	14.272	13.990	0.557296	0.29	7.87
273.39786	-39.04919	-6.00326	-9.99980	1.49	-1.03	-1.74	14.671	14.505	0.556632	0.31	10.00
272.51111	-38.64249	-5.95700	-9.19963	-2.79	-0.57	-0.89	13.458	13.338	0.522999	0.25	5.61
272.67885	-38.70181	-5.94913	-9.34319	-0.18	-0.85	-1.34	14.074	13.997	0.608332	0.30	8.28
273.46115	-39.01043	-5.94556	-10.02608	1.39	-1.01	-1.73	14.659	14.557	0.522463	0.28	9.90
272.90556	-38.76821	-5.92660	-9.53077	1.26	-0.99	-1.62	14.365	14.119	0.741625	0.17	9.76
273.77419	-39.08009	-5.89726	-10.27448	0.13	-0.87	-1.54	14.519	14.016	0.644749	0.32	8.62
273.00941	-38.73233	-5.85666	-9.58636	1.56	-1.01	-1.68	15.040	14.512	0.558931	0.29	10.06

Continued on next page...

Table A.1 – Continued

RA(J2000) deg	Dec(J2000) deg	ℓ deg	b deg	X kpc	Y kpc	Z kpc	J mag	K_s mag	P days	A_{K_s} mag	d kpc
272.94888	-38.68747	-5.83813	-9.52383	3.49	-1.21	-2.00	14.850	14.679	0.672948	0.24	12.02
272.62972	-38.55113	-5.83155	-9.23970	0.76	-0.93	-1.49	14.679	14.284	0.580869	0.30	9.23
273.21431	-38.77493	-5.82113	-9.74797	1.53	-1.00	-1.70	14.609	14.369	0.629426	0.23	10.03
273.62405	-38.73472	-5.63760	-10.01448	1.38	-0.96	-1.72	14.532	14.049	0.807422	0.24	9.89
273.21604	-38.55255	-5.61968	-9.64784	0.64	-0.88	-1.53	14.428	13.940	0.764368	0.23	9.12
273.21895	-38.54508	-5.61189	-9.64646	0.59	-0.87	-1.52	14.725	14.293	0.557476	0.28	9.07
273.55099	-38.67156	-5.60660	-9.93506	1.62	-0.97	-1.75	14.261	13.996	0.882535	0.17	10.12
272.88075	-38.39596	-5.60031	-9.34278	1.62	-0.97	-1.65	14.791	14.302	0.675566	0.28	10.10
273.85665	-38.75927	-5.57678	-10.18747	-1.59	-0.66	-1.21	14.081	13.583	0.612329	0.22	6.85
273.84596	-38.48057	-5.32781	-10.05453	-1.72	-0.61	-1.17	13.812	13.821	0.480247	0.31	6.71
273.79307	-38.39191	-5.26642	-9.97757	0.85	-0.84	-1.62	14.963	14.586	0.456704	0.37	9.33
273.31802	-38.16637	-5.23413	-9.54292	0.48	-0.80	-1.48	14.570	14.121	0.630728	0.27	8.95
272.98779	-37.92991	-5.14167	-9.20348	2.39	-0.96	-1.75	15.004	14.714	0.543210	0.27	10.88
273.51356	-38.06549	-5.07201	-9.63397	-1.57	-0.60	-1.14	13.630	13.499	0.659326	0.35	6.86
273.19095	-37.92829	-5.06577	-9.34515	3.93	-1.08	-2.03	15.096	14.875	0.606211	0.25	12.45
273.12691	-37.87193	-5.03845	-9.27442	2.81	-0.98	-1.83	14.712	14.674	0.603464	0.34	11.31
273.25583	-37.86385	-4.98396	-9.36120	-1.84	-0.56	-1.06	14.191	13.671	0.526518	0.24	6.58
273.62166	-38.00404	-4.97726	-9.68192	7.29	-1.36	-2.70	15.791	15.484	0.562430	0.26	15.88
273.57691	-37.95615	-4.95022	-9.62875	0.14	-0.73	-1.44	14.512	14.210	0.542868	0.32	8.60
273.69814	-37.79699	-4.76231	-9.64178	-3.11	-0.43	-0.88	13.638	13.129	0.561060	0.28	5.29
274.22037	-37.95776	-4.71919	-10.08218	-2.83	-0.45	-0.97	13.669	13.407	0.488081	0.34	5.58
273.28019	-37.58041	-4.71962	-9.24868	1.03	-0.77	-1.53	14.952	14.496	0.509359	0.21	9.49
274.32532	-37.97018	-4.69280	-10.16172	0.69	-0.74	-1.62	14.470	14.277	0.577264	0.33	9.17
273.27688	-37.54405	-4.68809	-9.22971	-1.37	-0.57	-1.13	13.962	13.808	0.532229	0.28	7.05
273.38115	-37.54681	-4.65227	-9.30449	1.93	-0.83	-1.69	14.586	14.344	0.687673	0.24	10.40
273.97656	-37.78292	-4.64859	-9.83164	-0.09	-0.67	-1.43	14.432	14.085	0.573895	0.26	8.36
273.68490	-37.63927	-4.62459	-9.56087	1.36	-0.78	-1.64	15.099	14.652	0.474841	0.39	9.83
274.26896	-37.85668	-4.60997	-10.07110	1.56	-0.80	-1.76	14.809	14.652	0.494868	0.26	10.05
273.48657	-37.53852	-4.60613	-9.37508	-3.09	-0.42	-0.85	13.243	12.964	0.650030	0.30	5.30
274.51092	-37.77220	-4.44631	-10.20422	-0.47	-0.61	-1.41	14.232	14.031	0.552614	0.29	7.99
273.50923	-37.36507	-4.44138	-9.31198	-0.57	-0.60	-1.27	14.569	14.236	0.449275	0.30	7.86
274.60674	-37.78133	-4.42028	-10.27608	-3.37	-0.38	-0.89	13.559	13.132	0.509510	0.31	5.02
273.93390	-37.46850	-4.37946	-9.65945	-3.54	-0.36	-0.80	13.092	12.953	0.555133	0.27	4.84

Continued on next page...

Table A.1 – Continued

RA(J2000) deg	Dec(J2000) deg	ℓ deg	b deg	X kpc	Y kpc	Z kpc	J mag	K_s mag	P days	A_{K_s} mag	d kpc
274.54227	-37.61873	-4.29556	-10.15786	2.01	-0.77	-1.86	14.900	14.581	0.571327	0.31	10.51
273.52085	-37.18681	-4.27638	-9.23887	-0.59	-0.58	-1.26	14.255	14.079	0.512049	0.36	7.84
274.30561	-37.42483	-4.20491	-9.90319	0.15	-0.62	-1.48	14.346	14.074	0.611086	0.16	8.60
274.55371	-37.49423	-4.17830	-10.11034	10.42	-1.37	-3.38	16.243	15.892	0.554961	0.34	19.08
274.46730	-37.38100	-4.10663	-9.99831	-0.38	-0.57	-1.40	14.408	14.290	0.450187	0.27	8.07
274.35046	-37.25585	-4.03541	-9.85912	2.85	-0.79	-1.95	14.909	14.776	0.556967	0.29	11.36
274.34911	-37.24009	-4.02161	-9.85108	0.54	-0.62	-1.54	14.760	14.357	0.520143	0.32	9.00
273.83323	-36.90079	-3.90331	-9.33056	-1.90	-0.44	-1.05	13.772	13.821	0.452614	0.38	6.50
274.89412	-37.32053	-3.89785	-10.27496	-0.30	-0.55	-1.45	14.084	13.895	0.645403	0.24	8.15
274.07329	-36.94070	-3.85114	-9.51971	-1.28	-0.47	-1.18	13.980	13.631	0.634192	0.26	7.14
273.78318	-36.72325	-3.76157	-9.21411	-0.07	-0.54	-1.34	14.646	14.142	0.546263	0.27	8.36
274.94957	-37.15324	-3.72562	-10.24015	0.43	-0.57	-1.58	14.741	14.417	0.483823	0.29	8.90
274.29857	-36.84376	-3.68092	-9.63669	1.78	-0.65	-1.72	15.065	14.782	0.458781	0.37	10.25
274.82569	-36.90117	-3.54109	-10.03935	0.14	-0.52	-1.50	14.778	14.325	0.490595	0.30	8.59
274.14187	-36.48369	-3.41281	-9.36188	7.61	-0.95	-2.65	15.958	15.820	0.434575	0.29	16.16
274.52359	-36.63622	-3.41060	-9.70433	1.79	-0.60	-1.73	14.699	14.522	0.574538	0.27	10.26
274.58308	-36.65143	-3.40263	-9.75381	-2.10	-0.37	-1.06	13.853	13.326	0.656439	0.25	6.31
274.60840	-36.64001	-3.38303	-9.76684	-1.83	-0.38	-1.11	13.897	13.506	0.607478	0.20	6.58
274.58461	-36.62257	-3.37591	-9.74195	-0.13	-0.48	-1.41	14.292	13.853	0.693900	0.25	8.31
274.83103	-36.57481	-3.24265	-9.89744	0.16	-0.48	-1.48	14.800	14.314	0.496934	0.34	8.61
275.29099	-36.70156	-3.19119	-10.28438	0.55	-0.49	-1.61	14.786	14.289	0.552859	0.33	9.01
274.35854	-36.22001	-3.09446	-9.39826	-0.56	-0.42	-1.28	14.225	13.709	0.707879	0.31	7.86
274.57144	-36.29857	-3.08712	-9.58692	1.77	-0.54	-1.71	14.865	14.724	0.480716	0.33	10.23
274.53258	-36.23319	-3.04220	-9.52952	-1.95	-0.34	-1.06	13.993	13.803	0.452860	0.38	6.45
274.82402	-36.27981	-2.97743	-9.76044	-1.73	-0.34	-1.13	13.773	13.537	0.607648	0.33	6.68
274.46207	-36.06598	-2.91689	-9.40334	2.42	-0.55	-1.79	15.343	15.054	0.405131	0.30	10.88
275.34216	-36.35052	-2.85288	-10.16574	0.04	-0.42	-1.50	14.241	13.839	0.729884	0.23	8.49
274.26696	-35.91078	-2.84895	-9.19235	2.13	-0.52	-1.70	14.907	14.660	0.540368	0.30	10.58
275.18125	-36.21915	-2.79184	-9.99118	0.04	-0.41	-1.47	14.523	14.353	0.467854	0.37	8.48
275.02073	-35.96925	-2.62348	-9.76366	1.11	-0.43	-1.63	14.840	14.456	0.534345	0.33	9.56
274.52641	-37.05188	-3.78651	-9.89290	-1.31	-0.46	-1.22	13.907	13.694	0.596986	0.27	7.12
274.60291	-36.62028	-3.36715	-9.75405	-0.21	-0.48	-1.39	14.438	13.962	0.619276	0.34	8.22
274.46903	-35.69202	-2.57618	-9.23950	5.07	-0.60	-2.19	15.785	15.398	0.452464	0.40	13.57

Continued on next page...

Table A.1 – Continued

RA(J2000) deg	Dec(J2000) deg	ℓ deg	b deg	X kpc	Y kpc	Z kpc	J mag	K_s mag	P days	A_{K_s} mag	d kpc
274.89463	-35.86641	-2.57653	-9.62632	-1.00	-0.33	-1.24	14.294	13.798	0.589247	0.25	7.42
274.81908	-35.81539	-2.55814	-9.54870	2.57	-0.49	-1.84	15.147	14.723	0.553814	0.38	11.04
275.05010	-35.81041	-2.46851	-9.71397	-3.35	-0.21	-0.84	13.482	13.057	0.545292	0.29	5.03
275.58797	-36.01921	-2.46182	-10.19699	-1.34	-0.30	-1.25	14.313	13.976	0.463379	0.32	7.08
275.68847	-36.05885	-2.46150	-10.28741	-0.71	-0.33	-1.38	14.420	14.111	0.484856	0.27	7.72
275.22176	-35.85998	-2.45053	-9.86063	-0.74	-0.32	-1.31	14.418	13.992	0.531898	0.22	7.68
274.53829	-35.49585	-2.37311	-9.20109	1.31	-0.40	-1.56	14.776	14.424	0.569671	0.31	9.75
274.80472	-35.59598	-2.36470	-9.43974	-1.22	-0.29	-1.17	14.292	13.762	0.572931	0.27	7.18
275.01172	-35.55095	-2.24730	-9.57001	2.56	-0.43	-1.84	15.030	14.753	0.538297	0.29	11.03
275.07296	-35.45613	-2.13868	-9.57213	-0.90	-0.28	-1.25	14.008	13.821	0.591975	0.33	7.52
275.18571	-35.48867	-2.12656	-9.66881	3.82	-0.45	-2.08	15.182	15.066	0.503593	0.27	12.31
274.91953	-35.37037	-2.11780	-9.42190	6.35	-0.54	-2.45	15.662	15.299	0.583611	0.23	14.86
275.32956	-35.53465	-2.11533	-9.79412	-1.70	-0.24	-1.14	13.641	13.307	0.746993	0.18	6.71
275.87942	-35.73140	-2.09348	-10.28194	1.45	-0.36	-1.78	14.381	14.172	0.730818	0.29	9.92
275.60749	-35.61928	-2.09039	-10.03424	1.22	-0.35	-1.69	14.566	14.354	0.597054	0.28	9.68
274.76509	-35.24047	-2.05767	-9.25091	7.24	-0.56	-2.56	15.362	15.040	0.813829	0.19	15.77
274.86229	-34.89093	-1.70524	-9.16443	-1.95	-0.19	-1.02	13.786	13.469	0.601848	0.27	6.43
275.51765	-35.14126	-1.68857	-9.75644	-0.56	-0.23	-1.33	14.507	13.981	0.560444	0.25	7.86
275.12754	-34.96772	-1.67571	-9.39321	2.14	-0.31	-1.74	14.823	14.540	0.600759	0.26	10.60
275.61526	-35.08263	-1.59926	-9.80191	1.86	-0.28	-1.76	14.774	14.495	0.595086	0.20	10.32
275.36752	-34.93700	-1.55864	-9.55538	0.19	-0.23	-1.43	14.623	14.280	0.512818	0.30	8.62
275.70139	-35.06604	-1.55242	-9.85771	-3.37	-0.13	-0.85	13.403	13.100	0.520327	0.30	5.01
274.95195	-34.74562	-1.54024	-9.16471	2.16	-0.28	-1.70	15.215	14.813	0.475213	0.29	10.60
275.03187	-34.76622	-1.52896	-9.23261	1.79	-0.27	-1.65	14.816	14.702	0.489582	0.34	10.23
275.07130	-34.74277	-1.49299	-9.25101	0.61	-0.23	-1.45	14.631	14.220	0.589237	0.27	9.03
275.34850	-34.84181	-1.47935	-9.49890	1.48	-0.25	-1.64	14.960	14.457	0.571765	0.29	9.92
275.47595	-34.86555	-1.45356	-9.60309	0.35	-0.22	-1.47	14.420	14.256	0.542029	0.24	8.78
275.55144	-34.63966	-1.22045	-9.55792	-0.38	-0.17	-1.33	14.242	13.982	0.583505	0.38	8.04
275.37111	-34.54184	-1.19892	-9.38142	-0.90	-0.15	-1.22	14.158	13.922	0.541501	0.22	7.51
275.23304	-34.45807	-1.17469	-9.24216	2.05	-0.21	-1.69	14.657	14.522	0.599481	0.31	10.50
275.35968	-34.47652	-1.14399	-9.34376	-0.12	-0.16	-1.35	14.298	14.107	0.554911	0.28	8.29
275.77214	-34.55081	-1.05776	-9.68110	2.28	-0.20	-1.81	14.595	14.444	0.669004	0.30	10.74
275.47403	-34.40297	-1.03457	-9.39522	-1.17	-0.13	-1.18	14.087	13.788	0.567302	0.25	7.23

Continued on next page. . .

Table A.1 – Continued

RA(J2000) deg	Dec(J2000) deg	ℓ deg	b deg	X kpc	Y kpc	Z kpc	J mag	K_s mag	P days	A_{K_s} mag	d kpc
276.23489	-34.69955	-1.02228	-10.08841	-1.58	-0.12	-1.19	14.061	13.732	0.535269	0.32	6.83
275.77247	-34.45366	-0.96935	-9.63818	-0.52	-0.13	-1.32	14.252	13.988	0.561041	0.26	7.89
275.64506	-34.34421	-0.91740	-9.49533	-0.08	-0.13	-1.38	14.416	14.045	0.591048	0.25	8.34
276.07680	-34.51537	-0.91269	-9.89041	1.73	-0.16	-1.75	14.699	14.527	0.564528	0.27	10.18
276.17015	-34.47422	-0.84072	-9.94127	0.77	-0.13	-1.59	14.845	14.342	0.550343	0.29	9.21
275.43732	-34.16134	-0.82931	-9.26002	-1.40	-0.10	-1.12	14.423	13.922	0.474940	0.34	6.99
276.02155	-34.36358	-0.79497	-9.78241	-0.67	-0.11	-1.31	14.412	13.999	0.537014	0.26	7.75
275.80735	-34.27154	-0.79091	-9.58303	-1.31	-0.10	-1.18	14.240	13.680	0.601341	0.35	7.10
275.46469	-34.09849	-0.76209	-9.25214	0.13	-0.11	-1.37	14.824	14.432	0.443005	0.36	8.55
276.32819	-34.44095	-0.75210	-10.04359	7.25	-0.20	-2.78	15.619	15.437	0.580120	0.24	15.80
275.78574	-34.19387	-0.72842	-9.53248	-2.40	-0.08	-0.98	13.406	13.189	0.670084	0.26	5.98
275.53807	-34.07800	-0.71597	-9.29733	0.65	-0.11	-1.47	14.560	14.331	0.540690	0.30	9.08
276.59183	-34.49511	-0.70461	-10.26266	-1.13	-0.09	-1.30	14.146	14.005	0.477439	0.34	7.29
276.10188	-34.28266	-0.69155	-9.80611	0.38	-0.10	-1.50	14.770	14.303	0.524002	0.29	8.81
275.91214	-34.19667	-0.68385	-9.62739	-1.83	-0.08	-1.09	13.998	13.433	0.645082	0.23	6.57
276.43027	-34.21536	-0.50871	-10.02005	-0.82	-0.07	-1.32	14.128	13.826	0.602439	0.24	7.61
275.50528	-33.81045	-0.48591	-9.15326	5.13	-0.11	-2.18	15.540	15.140	0.569133	0.21	13.62
275.95886	-33.94426	-0.43704	-9.54999	-0.32	-0.06	-1.34	14.666	14.241	0.473344	0.25	8.10
276.43312	-34.00286	-0.31390	-9.92865	-0.32	-0.04	-1.40	14.561	14.146	0.514020	0.33	8.10
276.75001	-34.07152	-0.25947	-10.19474	6.54	-0.07	-2.69	15.666	15.319	0.589598	0.30	15.09
275.83373	-33.59271	-0.16485	-9.30039	0.13	-0.02	-1.38	14.182	13.903	0.699433	0.36	8.55
275.76795	-33.48787	-0.09458	-9.20453	1.98	-0.02	-1.67	14.783	14.246	0.750604	0.26	10.42
276.53776	-33.79810	-0.08844	-9.91651	1.01	-0.01	-1.63	14.531	14.122	0.697725	0.31	9.45
276.87461	-33.86308	-0.02310	-10.19648	-0.71	-0.00	-1.36	14.020	13.743	0.664991	0.25	7.72
276.07191	-33.50959	0.00014	-9.44114	-1.21	0.00	-1.18	14.037	13.783	0.563393	0.31	7.19
276.36615	-33.55170	0.07207	-9.67968	0.44	0.01	-1.49	14.355	14.019	0.678785	0.25	8.88
276.86824	-33.74559	0.08189	-10.14032	4.30	0.02	-2.27	15.567	15.173	0.493632	0.36	12.80
276.49440	-33.59108	0.08407	-9.79295	0.31	0.01	-1.49	14.500	14.256	0.537678	0.29	8.74
276.34403	-33.51325	0.09878	-9.64614	-0.38	0.01	-1.35	14.213	14.073	0.539255	0.33	8.04
276.29226	-33.42988	0.15524	-9.57052	0.36	0.02	-1.46	14.747	14.308	0.519095	0.29	8.79
276.90804	-33.60126	0.22844	-10.10694	-2.00	0.03	-1.12	13.833	13.448	0.607024	0.20	6.40
276.95312	-33.53047	0.30979	-10.10974	-0.24	0.04	-1.44	14.484	14.147	0.524216	0.38	8.19
276.92508	-33.50888	0.31912	-10.07928	-1.80	0.04	-1.15	14.350	13.757	0.492363	0.25	6.60

Continued on next page...

Table A.1 – Continued

RA(J2000) deg	Dec(J2000) deg	ℓ deg	b deg	X kpc	Y kpc	Z kpc	J mag	K_s mag	P days	A_{K_s} mag	d kpc
276.61607	-33.35686	0.34282	-9.78084	0.46	0.05	-1.51	14.888	14.611	0.409182	0.30	8.90
276.28198	-33.20003	0.36031	-9.46098	1.92	0.06	-1.71	14.942	14.397	0.652371	0.25	10.36
276.85954	-33.42221	0.37391	-9.99216	-0.62	0.05	-1.35	14.132	13.836	0.626060	0.27	7.80
277.06240	-33.49716	0.38069	-10.17713	-2.06	0.04	-1.11	13.808	13.459	0.590455	0.22	6.34
276.01203	-33.05374	0.39124	-9.19344	1.94	0.07	-1.66	14.577	14.490	0.603573	0.30	10.38
276.82493	-33.33179	0.44354	-9.92652	0.49	0.07	-1.54	14.543	14.355	0.513735	0.32	8.93
276.43723	-33.11427	0.49664	-9.53952	0.42	0.08	-1.47	14.761	14.359	0.502833	0.27	8.84
276.04419	-32.90058	0.54230	-9.14930	1.43	0.09	-1.57	14.954	14.440	0.573694	0.26	9.86
276.06855	-32.90746	0.54529	-9.17068	-1.14	0.07	-1.15	14.176	13.982	0.483269	0.30	7.26
276.88807	-33.18250	0.60324	-9.90844	-0.43	0.08	-1.37	14.527	14.177	0.487500	0.32	7.99
276.19755	-32.83585	0.65912	-9.23580	-0.71	0.09	-1.23	14.557	13.987	0.535326	0.34	7.69
276.73133	-32.97890	0.73021	-9.70096	-4.16	0.05	-0.69	13.393	12.981	0.416512	0.30	4.20
277.11971	-33.08880	0.77504	-10.04176	-0.93	0.10	-1.30	14.316	13.838	0.580134	0.32	7.49
277.22424	-32.88109	1.00368	-10.02980	0.22	0.15	-1.51	14.429	14.172	0.567524	0.30	8.65
276.61413	-32.41661	1.19759	-9.36414	3.49	0.25	-1.96	14.964	14.754	0.624672	0.30	11.96
277.21815	-32.65453	1.20828	-9.92610	0.18	0.18	-1.49	14.450	14.247	0.527629	0.27	8.62
276.88798	-32.47926	1.24408	-9.59915	-0.21	0.18	-1.37	14.315	14.077	0.558541	0.30	8.21
276.52242	-32.32770	1.24358	-9.25531	3.35	0.25	-1.91	14.958	14.798	0.587475	0.31	11.81
276.53972	-32.28267	1.29103	-9.24844	1.70	0.23	-1.64	15.036	14.581	0.534625	0.35	10.14
277.38192	-32.44894	1.45728	-9.96034	-0.92	0.19	-1.29	14.238	13.985	0.511444	0.31	7.50
277.68887	-32.37716	1.63761	-10.16227	1.72	0.29	-1.80	15.278	14.691	0.490333	0.34	10.19
277.05887	-32.08854	1.66436	-9.55679	1.45	0.28	-1.65	14.515	14.244	0.683667	0.33	9.90
277.03625	-32.05543	1.68594	-9.52500	3.87	0.36	-2.06	15.051	14.796	0.639672	0.29	12.35
276.88030	-31.98231	1.69333	-9.37409	8.94	0.51	-2.88	15.830	15.542	0.639337	0.22	17.49
277.76809	-32.29159	1.74546	-10.18535	4.77	0.40	-2.37	15.477	15.298	0.474944	0.39	13.29
277.00693	-33.18845	0.64208	-10.00045	-0.38	0.09	-1.40	14.371	14.042	0.554896	0.31	8.05
276.17427	-32.75686	0.72196	-9.18312	-0.07	0.10	-1.33	14.346	14.176	0.527961	0.33	8.34
276.34302	-32.46763	1.04841	-9.18173	-3.13	0.09	-0.83	13.473	13.245	0.498788	0.24	5.24
277.00915	-32.57475	1.20270	-9.73291	-0.84	0.16	-1.28	13.928	13.588	0.734446	0.26	7.58
277.16343	-32.39677	1.42292	-9.77169	-0.58	0.19	-1.33	14.483	14.087	0.509315	0.26	7.84
277.41348	-31.63771	2.20929	-9.62921	2.90	0.43	-1.91	14.949	14.765	0.564487	0.36	11.38
277.80252	-31.74480	2.25841	-9.97375	5.38	0.54	-2.43	15.093	14.875	0.743810	0.28	13.91
276.93751	-31.36706	2.27425	-9.14564	-0.43	0.31	-1.27	14.748	14.277	0.446076	0.28	7.98

Continued on next page. . .

Table A.1 – Continued

RA(J2000)	Dec(J2000)	ℓ	b	X	Y	Z	J	K_s	P	A_{K_s}	d
deg	deg	deg	deg	kpc	kpc	kpc	mag	mag	days	mag	kpc
277.79953	-31.68728	2.30985	-9.94639	1.14	0.38	-1.66	14.609	14.263	0.635292	0.29	9.60
277.19469	-31.37772	2.36285	-9.34734	0.42	0.36	-1.44	14.468	14.176	0.589018	0.24	8.85
277.22221	-31.36421	2.38564	-9.36248	0.25	0.36	-1.41	14.644	14.449	0.449386	0.34	8.68
277.45140	-31.40740	2.43356	-9.55719	-1.39	0.29	-1.16	13.758	13.232	0.866927	0.26	7.02
277.13330	-31.18887	2.51110	-9.21691	4.16	0.55	-2.04	15.697	15.116	0.506837	0.26	12.65
278.16715	-31.59649	2.53103	-10.18881	-1.16	0.32	-1.28	14.307	13.834	0.549556	0.33	7.26
277.86411	-31.42473	2.57408	-9.88148	-1.07	0.33	-1.26	14.114	13.859	0.549583	0.23	7.35
278.23293	-31.43692	2.70184	-10.17020	2.19	0.50	-1.89	14.951	14.731	0.516177	0.32	10.67
277.47514	-31.08821	2.73333	-9.43520	-1.51	0.32	-1.13	14.004	13.884	0.478565	0.34	6.90
277.70301	-31.16512	2.75001	-9.64424	-0.04	0.40	-1.41	14.310	14.274	0.491565	0.35	8.40
277.95775	-31.25982	2.76012	-9.88159	-1.08	0.35	-1.26	14.062	13.786	0.584505	0.30	7.34
277.64512	-31.06920	2.81545	-9.55766	0.26	0.42	-1.45	14.594	14.284	0.520313	0.28	8.70
277.87842	-31.15169	2.82884	-9.77336	2.80	0.55	-1.92	15.201	14.795	0.541460	0.34	11.28
277.93257	-31.15337	2.84782	-9.81580	-1.60	0.33	-1.16	13.893	13.567	0.614726	0.29	6.81
278.13484	-31.15673	2.92126	-9.97309	-1.52	0.35	-1.19	13.937	13.716	0.552746	0.31	6.90
277.60681	-30.93224	2.92563	-9.46807	0.01	0.42	-1.39	14.597	14.392	0.448175	0.26	8.44
278.24108	-31.16174	2.95677	-10.05715	-2.20	0.32	-1.08	13.433	13.193	0.714531	0.27	6.21
277.46495	-30.76097	3.02727	-9.28338	0.20	0.45	-1.39	14.366	14.135	0.583284	0.36	8.63
277.52344	-30.66246	3.13932	-9.28516	-0.76	0.41	-1.23	14.031	13.913	0.565723	0.35	7.66
278.27953	-30.95209	3.16309	-9.99582	0.78	0.50	-1.61	14.565	14.411	0.521722	0.24	9.24
278.44399	-30.92108	3.25360	-10.10949	0.42	0.50	-1.56	14.649	14.215	0.572666	0.27	8.87
278.19077	-30.80363	3.26522	-9.86268	-0.12	0.47	-1.42	14.207	14.003	0.610348	0.31	8.32
277.82166	-30.64498	3.26944	-9.50796	0.43	0.50	-1.47	14.697	14.250	0.555596	0.31	8.87
277.78645	-32.06089	1.96338	-10.09906	1.40	0.33	-1.73	14.441	14.230	0.688231	0.30	9.87
277.75206	-31.89534	2.10186	-10.00073	-1.44	0.25	-1.21	14.384	14.139	0.392082	0.34	6.98
277.27170	-31.44339	2.33244	-9.43527	1.12	0.38	-1.57	14.738	14.426	0.547876	0.37	9.56
278.14548	-31.33847	2.75905	-10.06024	-2.92	0.26	-0.95	13.651	13.403	0.472979	0.26	5.48
277.78811	-30.53387	3.35784	-9.43329	0.79	0.53	-1.52	14.971	14.632	0.429954	0.30	9.23
278.26080	-30.70249	3.38422	-9.87287	3.14	0.68	-2.01	14.988	14.887	0.529911	0.33	11.64
278.40257	-30.71738	3.42436	-9.98913	-0.64	0.46	-1.35	14.267	14.153	0.475934	0.27	7.80
277.82568	-30.43636	3.46107	-9.41961	7.87	0.98	-2.71	16.136	15.637	0.524742	0.29	16.43
278.46130	-30.61677	3.53866	-9.99099	0.57	0.55	-1.57	15.061	14.664	0.401218	0.35	9.03
278.12689	-30.46686	3.54847	-9.66645	0.44	0.54	-1.49	14.629	14.549	0.431090	0.31	8.89

Continued on next page...

Table A.1 – Continued

RA(J2000) deg	Dec(J2000) deg	ℓ deg	b deg	X kpc	Y kpc	Z kpc	J mag	K_s mag	P days	A_{K_s} mag	d kpc
277.93755	-30.37890	3.55629	-9.48115	-0.86	0.46	-1.24	14.019	13.832	0.593257	0.32	7.56
278.49425	-30.60374	3.56306	-10.01089	-1.59	0.42	-1.18	14.193	13.668	0.566739	0.32	6.83
278.38207	-29.85678	4.20290	-9.59879	0.29	0.63	-1.46	14.795	14.454	0.453579	0.30	8.74
278.68795	-29.96786	4.21844	-9.88584	-0.55	0.57	-1.35	14.335	14.184	0.474032	0.26	7.90
278.01828	-29.67986	4.22408	-9.23742	3.33	0.86	-1.91	15.240	15.031	0.481561	0.34	11.82
278.99041	-30.07640	4.23412	-10.16890	4.08	0.92	-2.24	15.014	14.852	0.633770	0.28	12.62
278.27209	-29.77374	4.23641	-9.47668	4.07	0.92	-2.09	15.244	15.095	0.511491	0.32	12.58
278.78987	-29.95956	4.26488	-9.96182	3.15	0.85	-2.03	15.098	14.890	0.530217	0.28	11.66
278.79781	-29.96160	4.26604	-9.96890	-0.83	0.56	-1.32	14.196	13.782	0.626833	0.30	7.61
278.28391	-29.72038	4.28961	-9.46259	2.15	0.78	-1.75	15.134	14.784	0.489764	0.32	10.63
278.21524	-29.64949	4.32777	-9.37793	0.43	0.66	-1.45	14.796	14.378	0.497673	0.35	8.87
278.69404	-29.73281	4.43567	-9.78857	1.33	0.75	-1.67	14.636	14.360	0.608543	0.21	9.81
278.58107	-29.59248	4.52057	-9.63914	-1.84	0.51	-1.10	13.739	13.354	0.692852	0.31	6.58
278.49107	-29.27672	4.77403	-9.43091	0.43	0.73	-1.46	14.682	14.544	0.431934	0.34	8.88
278.47605	-30.17439	3.94879	-9.81035	1.43	0.67	-1.69	14.739	14.315	0.643840	0.37	9.90
278.65401	-29.97670	4.19740	-9.86319	4.71	0.96	-2.28	15.503	14.967	0.627837	0.30	13.24
278.58748	-29.85125	4.28665	-9.75675	-0.44	0.59	-1.35	14.171	13.691	0.742975	0.30	8.00
278.41630	-29.28253	4.73984	-9.37478	0.94	0.77	-1.53	14.854	14.375	0.554813	0.26	9.40
279.24047	-29.56527	4.79767	-10.14421	-0.91	0.62	-1.33	14.574	14.155	0.446674	0.29	7.54
278.56280	-28.99021	5.06300	-9.36209	2.30	0.94	-1.76	15.295	14.832	0.482868	0.38	10.79
278.48906	-28.93296	5.08659	-9.27903	-2.43	0.52	-0.96	14.048	13.527	0.499555	0.29	5.98
278.84916	-29.07621	5.09519	-9.62491	-1.39	0.62	-1.17	14.223	13.803	0.532484	0.26	7.04
279.21820	-29.17918	5.14285	-9.96005	-0.87	0.67	-1.31	14.231	14.018	0.507056	0.31	7.58
279.01758	-28.98054	5.24750	-9.71599	-2.77	0.51	-0.94	14.050	13.509	0.454806	0.37	5.63
279.49533	-29.14318	5.28186	-10.16286	0.34	0.80	-1.56	14.850	14.271	0.539540	0.36	8.82
278.97300	-28.87403	5.32764	-9.63458	-2.83	0.51	-0.92	13.474	13.439	0.473979	0.25	5.58
278.68451	-28.62947	5.43905	-9.30036	-0.28	0.76	-1.32	14.628	14.194	0.500153	0.29	8.17
279.52379	-28.95993	5.46075	-10.10641	2.11	1.00	-1.87	15.279	14.879	0.451048	0.39	10.63
278.96702	-28.56528	5.60726	-9.49557	2.74	1.08	-1.87	14.844	14.608	0.633413	0.26	11.25
278.91773	-28.49651	5.65089	-9.42664	7.02	1.52	-2.58	16.033	15.527	0.524981	0.37	15.61
279.06378	-28.46376	5.73745	-9.52795	1.60	1.00	-1.68	15.016	14.541	0.548917	0.25	10.10
279.21070	-28.51491	5.74762	-9.66648	-2.00	0.63	-1.07	13.942	13.805	0.449168	0.35	6.43
279.20402	-28.50071	5.75802	-9.65503	0.83	0.92	-1.56	14.685	14.431	0.519486	0.24	9.31

Continued on next page...

Table A.1 – Continued

RA(J2000)	Dec(J2000)	ℓ	b	X	Y	Z	J	K_s	P	A_{K_s}	d
deg	deg	deg	deg	kpc	kpc	kpc	mag	mag	days	mag	kpc
279.51687	-28.57025	5.81512	-9.93289	1.60	1.01	-1.75	14.904	14.474	0.582992	0.29	10.11
279.66853	-28.41152	6.01890	-9.98466	0.71	0.95	-1.60	14.648	14.457	0.497555	0.31	9.21
278.96547	-28.09082	6.03948	-9.28753	-0.24	0.85	-1.32	14.476	14.130	0.534291	0.32	8.21
279.44237	-28.25850	6.07167	-9.73902	-4.27	0.43	-0.68	12.677	12.484	0.616724	0.30	4.12
280.02044	-28.44717	6.12138	-10.27939	-0.31	0.86	-1.46	14.442	14.219	0.490504	0.35	8.17
279.37047	-28.08864	6.19909	-9.60827	0.39	0.94	-1.48	14.681	14.287	0.538407	0.26	8.87
279.43320	-28.11036	6.20358	-9.66756	2.81	1.21	-1.91	14.827	14.726	0.580171	0.33	11.34
279.74065	-28.15668	6.28015	-9.93206	-1.12	0.79	-1.26	13.865	13.690	0.634317	0.35	7.34
279.35104	-29.33307	5.05267	-10.13101	-0.73	0.67	-1.36	14.128	13.979	0.543472	0.29	7.73
278.59248	-28.91503	5.14304	-9.35260	-0.18	0.73	-1.34	14.704	14.303	0.466057	0.26	8.27
279.26834	-28.03544	6.20800	-9.50399	3.62	1.30	-2.02	15.091	14.901	0.568253	0.29	12.17
279.13640	-27.82616	6.34753	-9.30794	2.20	1.17	-1.74	15.062	14.602	0.580659	0.25	10.71
279.73273	-28.07655	6.35047	-9.89119	6.18	1.61	-2.56	15.602	15.255	0.600842	0.31	14.79
279.52625	-27.90087	6.43119	-9.65081	-3.34	0.56	-0.84	13.444	12.921	0.619721	0.25	5.06
279.21575	-27.70482	6.48921	-9.31825	1.52	1.12	-1.63	14.818	14.623	0.504714	0.34	10.02
279.46390	-27.59960	6.68217	-9.47038	-1.48	0.80	-1.14	13.942	13.562	0.643878	0.23	6.97
279.49321	-27.41628	6.86100	-9.41413	-1.35	0.84	-1.16	14.240	13.706	0.588564	0.30	7.10
280.01403	-27.60567	6.89063	-9.91252	-0.22	0.98	-1.42	14.494	14.205	0.506937	0.32	8.27
280.09430	-27.59322	6.93314	-9.97136	5.15	1.64	-2.40	15.457	15.281	0.514104	0.25	13.76
279.61948	-27.29261	7.02331	-9.46142	0.35	1.07	-1.45	14.614	14.306	0.525845	0.30	8.84
279.41661	-27.15831	7.06635	-9.24056	-1.35	0.86	-1.13	14.076	13.834	0.526222	0.29	7.10
279.78212	-27.30039	7.07976	-9.59502	3.57	1.47	-2.03	15.324	14.875	0.578339	0.28	12.14
280.23316	-27.44042	7.12701	-10.01678	-0.01	1.04	-1.48	14.412	14.093	0.585964	0.26	8.49
279.65663	-27.15999	7.15896	-9.43358	1.58	1.24	-1.66	15.090	14.768	0.451853	0.33	10.10
280.24547	-27.35822	7.20714	-9.99129	3.04	1.43	-2.02	15.301	14.830	0.554069	0.36	11.61
279.90386	-27.05088	7.35541	-9.58458	-1.31	0.90	-1.19	14.343	13.840	0.531604	0.33	7.15
279.66196	-26.83176	7.46065	-9.29520	3.61	1.56	-1.98	15.382	14.801	0.620151	0.34	12.18
279.90478	-26.79940	7.58559	-9.47635	3.71	1.60	-2.04	15.356	15.110	0.483211	0.25	12.29
280.25898	-26.90352	7.62896	-9.80631	1.82	1.36	-1.77	15.224	14.674	0.513695	0.31	10.36
280.25364	-26.86243	7.66450	-9.78430	4.08	1.67	-2.17	15.302	14.938	0.594166	0.33	12.68
279.53996	-27.69085	6.62848	-9.57069	-4.01	0.50	-0.72	13.118	12.648	0.601971	0.31	4.39
280.00645	-26.93536	7.50116	-9.61698	-0.16	1.07	-1.39	14.362	14.148	0.539843	0.30	8.33
280.24446	-26.74438	7.76896	-9.72596	2.66	1.50	-1.91	15.027	14.684	0.590528	0.36	11.23

Continued on next page...

Table A.1 – Continued

RA(J2000) deg	Dec(J2000) deg	ℓ deg	b deg	X kpc	Y kpc	Z kpc	J mag	K_s mag	P days	A_{K_s} mag	d kpc
279.70489	-26.47509	7.80289	-9.17449	-0.23	1.11	-1.31	14.582	14.032	0.586342	0.26	8.25
279.94631	-26.42326	7.94543	-9.34658	7.77	2.24	-2.70	15.947	15.599	0.543449	0.35	16.45
280.69726	-26.71512	7.97245	-10.07841	3.07	1.59	-2.05	14.743	14.253	0.919261	0.20	11.66
279.79878	-26.31107	7.98956	-9.17877	2.61	1.53	-1.79	15.164	14.754	0.550097	0.25	11.16
279.79279	-26.24095	8.05113	-9.14340	-2.11	0.88	-1.00	13.693	13.333	0.658384	0.27	6.34
280.74098	-26.62462	8.07250	-10.07488	-1.83	0.92	-1.16	13.973	13.713	0.516710	0.32	6.64
280.25671	-26.39442	8.09392	-9.58463	7.90	2.30	-2.79	15.665	15.301	0.714771	0.25	16.60
280.74041	-26.58331	8.11018	-10.05670	10.51	2.68	-3.41	16.134	15.815	0.606612	0.31	19.31
281.01008	-26.58555	8.21305	-10.27558	-0.23	1.17	-1.48	14.479	14.227	0.500238	0.30	8.29
280.92833	-26.51564	8.24548	-10.17957	1.34	1.40	-1.75	14.992	14.771	0.434228	0.32	9.90
280.66185	-26.39291	8.25409	-9.91141	2.13	1.51	-1.85	15.052	14.775	0.499758	0.27	10.70
281.01015	-26.51369	8.27911	-10.24491	1.11	1.37	-1.72	15.024	14.569	0.494587	0.27	9.67
280.35729	-26.18900	8.32130	-9.57712	0.58	1.30	-1.52	14.633	14.278	0.568870	0.27	9.10
280.25735	-26.10856	8.35547	-9.46143	1.85	1.49	-1.72	14.728	14.489	0.607124	0.32	10.41
280.25719	-26.02665	8.43025	-9.42582	0.42	1.29	-1.47	14.435	14.028	0.682170	0.23	8.94
281.05157	-26.27511	8.51435	-10.17637	-1.22	1.06	-1.28	14.309	13.927	0.509583	0.33	7.28
280.77911	-26.07292	8.59326	-9.86874	-0.07	1.24	-1.45	14.246	13.777	0.763744	0.30	8.45
280.44954	-25.68025	8.82274	-9.43178	0.00	1.29	-1.40	14.218	13.910	0.691290	0.27	8.52
281.32525	-25.95869	8.91176	-10.26319	-1.82	1.02	-1.18	13.877	13.566	0.591930	0.29	6.67
281.16093	-25.67160	9.11100	-10.00661	3.84	1.95	-2.18	15.307	15.252	0.440556	0.37	12.49
280.92334	-25.55284	9.12639	-9.76212	-0.12	1.31	-1.43	14.103	13.716	0.797703	0.30	8.41
280.45584	-25.30528	9.16771	-9.27438	-0.68	1.23	-1.26	14.202	13.812	0.642426	0.25	7.82
281.34741	-25.65981	9.19495	-10.15343	0.95	1.50	-1.68	14.951	14.620	0.460344	0.30	9.52
280.58213	-25.29898	9.22362	-9.37454	-0.15	1.32	-1.36	14.464	14.076	0.579818	0.27	8.37
280.48246	-25.15633	9.31426	-9.23144	-2.15	1.01	-1.01	13.751	13.503	0.564953	0.32	6.32
281.27951	-25.49975	9.31523	-10.02954	-0.56	1.27	-1.39	14.777	14.390	0.403729	0.35	7.97
281.36970	-25.24320	9.58606	-9.99316	-1.53	1.14	-1.21	14.272	13.903	0.480314	0.37	6.97
280.98433	-25.04958	9.61117	-9.59496	-0.57	1.31	-1.32	14.401	14.132	0.502434	0.33	7.95
281.03393	-25.05627	9.62471	-9.63838	0.26	1.45	-1.48	14.533	14.245	0.551213	0.31	8.81
281.55899	-25.27196	9.63413	-10.16018	12.39	3.51	-3.80	16.087	15.908	0.673292	0.34	21.34
280.65953	-24.86124	9.65417	-9.24798	12.72	3.58	-3.51	16.605	16.130	0.569278	0.31	21.61
280.82484	-24.91265	9.67304	-9.40541	0.04	1.42	-1.40	14.192	13.907	0.702578	0.30	8.58
280.56238	-24.74134	9.72479	-9.11649	1.25	1.64	-1.56	14.474	14.284	0.651347	0.32	9.82

Continued on next page. . .

Table A.1 – Continued

RA(J2000) deg	Dec(J2000) deg	ℓ deg	b deg	X kpc	Y kpc	Z kpc	J mag	K_s mag	P days	A_{K_s} mag	d kpc
280.69788	-24.68945	9.82628	-9.20483	0.67	1.56	-1.48	14.508	14.181	0.634675	0.30	9.23
281.69914	-25.11785	9.83076	-10.20895	3.63	2.07	-2.19	15.115	14.806	0.630227	0.31	12.31
281.65392	-25.07677	9.85070	-10.15436	-1.41	1.20	-1.25	14.323	13.868	0.513152	0.31	7.11
280.93782	-24.73790	9.87770	-9.42227	-1.16	1.24	-1.20	14.006	13.743	0.607489	0.31	7.35
281.64226	-25.02727	9.89157	-10.12365	0.53	1.54	-1.60	14.671	14.463	0.485661	0.32	9.11
281.10781	-24.73211	9.95062	-9.55901	2.23	1.85	-1.81	14.993	14.707	0.543266	0.32	10.85
280.79991	-24.37341	10.15550	-9.15129	4.84	2.36	-2.17	15.388	15.097	0.583867	0.27	13.53
281.27702	-24.54813	10.18624	-9.61843	0.03	1.50	-1.43	14.896	14.450	0.440176	0.36	8.59
280.93900	-24.31609	10.26350	-9.24061	1.04	1.69	-1.55	14.660	14.302	0.617113	0.24	9.62
281.46034	-24.50255	10.30082	-9.74933	-1.71	1.20	-1.15	14.012	13.678	0.556034	0.28	6.80
281.60292	-24.40305	10.44861	-9.82374	0.24	1.58	-1.51	14.594	14.299	0.526457	0.23	8.82
281.67023	-24.28644	10.58221	-9.82903	-1.56	1.26	-1.18	14.269	13.674	0.583652	0.28	6.96
281.74912	-24.26440	10.63375	-9.88452	11.22	3.67	-3.50	16.292	16.035	0.543925	0.25	20.17
281.29604	-23.98802	10.70610	-9.39229	-5.25	0.58	-0.50	12.409	12.096	0.524332	0.30	3.15
268.74630	-41.52697	-9.90841	-8.03855	1.21	-1.66	-1.37	14.746	14.641	0.472833	0.30	9.76
269.36478	-41.72725	-9.85766	-8.53986	3.64	-2.08	-1.83	15.018	14.875	0.589605	0.33	12.26
269.58191	-41.77357	-9.81958	-8.70409	4.54	-2.22	-2.01	15.454	15.012	0.599208	0.38	13.19
270.10334	-41.97290	-9.80837	-9.14039	-0.13	-1.41	-1.33	14.474	14.087	0.578781	0.29	8.41
269.71593	-41.78803	-9.78376	-8.79865	1.95	-1.77	-1.62	14.940	14.473	0.628840	0.26	10.53
269.62530	-41.74500	-9.77848	-8.71869	1.72	-1.73	-1.56	14.730	14.348	0.671317	0.27	10.29
269.32730	-41.43981	-9.61716	-8.37611	-0.25	-1.36	-1.20	14.427	14.262	0.481343	0.35	8.26
269.39072	-41.40728	-9.56510	-8.40195	2.40	-1.80	-1.61	14.732	14.465	0.683723	0.23	10.97
269.72860	-41.48770	-9.51272	-8.66257	-0.24	-1.35	-1.25	14.570	14.283	0.474424	0.30	8.27
269.03954	-41.13132	-9.45112	-8.03712	-0.67	-1.27	-1.09	14.523	14.009	0.541568	0.37	7.82
269.71749	-41.35876	-9.40245	-8.59322	-0.86	-1.23	-1.14	14.082	13.769	0.637263	0.26	7.63
269.65597	-41.29780	-9.37093	-8.52338	0.71	-1.49	-1.37	14.323	14.134	0.662357	0.28	9.24
270.24180	-41.49129	-9.32971	-9.00183	3.41	-1.92	-1.89	15.395	15.033	0.495587	0.34	12.02
270.41215	-41.36916	-9.15942	-9.05610	-1.25	-1.14	-1.13	14.082	13.779	0.572194	0.27	7.24
270.17229	-41.27053	-9.15845	-8.85072	0.67	-1.45	-1.42	14.331	14.182	0.629759	0.36	9.20
270.22067	-41.27934	-9.14873	-8.88689	1.58	-1.59	-1.57	15.084	14.448	0.598466	0.31	10.13
270.16037	-41.12635	-9.03459	-8.77399	-0.98	-1.16	-1.14	14.459	14.036	0.489627	0.28	7.50
269.47617	-40.76722	-8.96777	-8.14815	1.90	-1.61	-1.49	15.005	14.476	0.617486	0.34	10.44
270.10643	-40.91001	-8.86206	-8.63479	1.57	-1.54	-1.52	14.910	14.633	0.508143	0.28	10.11

Continued on next page...

Table A.1 – Continued

RA(J2000) deg	Dec(J2000) deg	ℓ deg	b deg	X kpc	Y kpc	Z kpc	J mag	K_s mag	P days	A_{K_s} mag	d kpc
270.35879	-41.01206	-8.86074	-8.85096	1.34	-1.50	-1.52	14.749	14.418	0.585954	0.27	9.88
269.46786	-40.60325	-8.82601	-8.06313	0.53	-1.37	-1.27	14.715	14.261	0.569084	0.32	9.03
269.95183	-40.63820	-8.67769	-8.40168	2.07	-1.58	-1.56	15.569	15.035	0.392449	0.36	10.60
270.10748	-40.62769	-8.61106	-8.50027	1.81	-1.53	-1.53	14.978	14.594	0.548249	0.34	10.34
269.98112	-40.53540	-8.57576	-8.37178	1.63	-1.50	-1.48	14.785	14.506	0.571716	0.30	10.15
269.00651	-41.43027	-9.72692	-8.16133	0.12	-1.44	-1.23	14.293	13.998	0.656728	0.26	8.63
269.11833	-41.29606	-9.56721	-8.16919	-2.00	-1.06	-0.91	13.877	13.651	0.517874	0.32	6.46
270.74809	-40.74513	-8.48149	-8.98334	-0.18	-1.21	-1.30	14.716	14.299	0.472170	0.42	8.31
270.87139	-40.73419	-8.42703	-9.06050	-1.79	-0.97	-1.04	13.450	13.299	0.745234	0.32	6.67
270.24983	-40.30540	-8.27257	-8.44098	0.09	-1.22	-1.26	14.425	14.301	0.498925	0.33	8.57
269.84809	-40.08272	-8.22430	-8.06485	-1.66	-0.96	-0.95	14.022	13.831	0.484907	0.32	6.78
270.13225	-40.15370	-8.18149	-8.28949	1.17	-1.36	-1.40	14.734	14.412	0.567270	0.25	9.68
270.16467	-40.15066	-8.16678	-8.30977	-1.59	-0.96	-0.99	13.998	13.515	0.649705	0.31	6.85
271.06407	-40.36138	-8.02423	-9.01381	0.25	-1.21	-1.37	14.585	14.265	0.534248	0.37	8.75
270.51465	-40.07580	-7.97094	-8.50904	1.19	-1.33	-1.44	15.010	14.503	0.526078	0.23	9.69
270.53319	-40.08048	-7.96826	-8.52375	-0.06	-1.15	-1.25	14.310	14.109	0.569726	0.25	8.42
270.37107	-39.97157	-7.93142	-8.36267	1.69	-1.39	-1.49	14.663	14.493	0.583019	0.23	10.20
270.21254	-39.86262	-7.89362	-8.20376	-1.48	-0.95	-0.99	13.565	13.298	0.806959	0.24	6.96
270.41047	-39.87744	-7.83325	-8.34421	-0.72	-1.04	-1.12	14.157	14.184	0.456159	0.22	7.73
270.22292	-39.72979	-7.77203	-8.14701	0.22	-1.16	-1.23	14.382	14.244	0.538057	0.34	8.69
270.98383	-40.02240	-7.75097	-8.79983	2.02	-1.41	-1.62	14.824	14.646	0.543759	0.31	10.55
271.00173	-39.96205	-7.69060	-8.78340	-0.50	-1.05	-1.22	14.290	14.005	0.562756	0.30	7.97
270.89708	-39.89675	-7.67080	-8.68181	-1.48	-0.92	-1.05	14.075	13.765	0.539700	0.29	6.96
270.32152	-39.65638	-7.67019	-8.17838	-0.76	-1.02	-1.09	14.467	13.988	0.534302	0.34	7.69
270.18153	-39.55968	-7.63679	-8.03735	1.01	-1.25	-1.33	14.720	14.305	0.600413	0.34	9.49
270.42515	-39.54952	-7.53678	-8.19730	5.41	-1.82	-2.01	15.357	15.202	0.566707	0.27	13.98
270.67577	-39.60341	-7.49146	-8.39277	3.23	-1.52	-1.73	15.096	14.712	0.628354	0.31	11.76
271.16325	-39.76562	-7.45616	-8.79999	-0.04	-1.08	-1.29	14.536	14.150	0.551682	0.31	8.44
271.44631	-39.84839	-7.42663	-9.03083	1.86	-1.33	-1.64	15.225	14.787	0.467360	0.35	10.38
271.13365	-39.64450	-7.35897	-8.72278	6.48	-1.91	-2.31	15.738	15.659	0.439425	0.39	15.08
271.32476	-39.69344	-7.33253	-8.87560	-0.61	-0.99	-1.21	14.233	13.974	0.562658	0.26	7.85
271.14264	-39.60406	-7.31959	-8.70980	0.25	-1.10	-1.32	14.837	14.395	0.474892	0.31	8.72
271.48346	-39.73836	-7.31468	-9.00447	0.06	-1.07	-1.34	14.419	14.151	0.563990	0.33	8.54

Continued on next page. . .

Table A.1 – Continued

RA(J2000) deg	Dec(J2000) deg	ℓ deg	b deg	X kpc	Y kpc	Z kpc	J mag	K_s mag	P days	A_{K_s} mag	d kpc
270.92692	-39.43764	-7.25093	-8.48446	-1.62	-0.85	-1.00	14.584	14.093	0.390447	0.41	6.81
270.56208	-39.18314	-7.16059	-8.11504	-1.28	-0.88	-1.01	14.042	13.910	0.500065	0.27	7.15
271.65208	-39.59551	-7.12534	-9.05231	-4.14	-0.52	-0.66	12.945	12.712	0.537527	0.27	4.25
271.51319	-39.50408	-7.09430	-8.91488	1.32	-1.20	-1.53	14.736	14.488	0.545768	0.28	9.82
270.52704	-39.03100	-7.03878	-8.01840	0.81	-1.12	-1.30	14.267	14.054	0.713638	0.22	9.27
271.34213	-39.37093	-7.03816	-8.73571	-0.30	-0.99	-1.24	14.313	14.129	0.528594	0.26	8.16
270.96644	-39.16343	-6.99223	-8.38131	-1.24	-0.87	-1.04	14.364	13.844	0.534605	0.30	7.19
270.94553	-39.04225	-6.89221	-8.30951	0.22	-1.03	-1.25	14.753	14.304	0.508466	0.31	8.67
271.06746	-39.01156	-6.81950	-8.37834	-1.90	-0.77	-0.94	14.025	13.632	0.535857	0.25	6.52
270.83269	-38.76045	-6.68397	-8.09823	0.07	-0.98	-1.20	14.258	13.943	0.671998	0.29	8.52
270.82534	-38.71167	-6.64341	-8.06995	-0.89	-0.86	-1.06	14.431	14.053	0.487555	0.29	7.54
270.82656	-38.63280	-6.57293	-8.03319	-1.36	-0.80	-0.98	13.659	13.474	0.711698	0.27	7.06
271.34550	-38.76818	-6.49927	-8.45394	-0.50	-0.89	-1.17	14.539	14.095	0.517518	0.37	7.94
271.73419	-38.92160	-6.49231	-8.79325	-0.29	-0.91	-1.25	14.020	13.833	0.682757	0.24	8.16
271.11595	-38.62008	-6.45304	-8.22603	4.73	-1.47	-1.91	15.497	15.328	0.460588	0.26	13.26
271.05804	-38.55285	-6.41496	-8.15429	2.42	-1.21	-1.55	15.276	14.822	0.496739	0.37	10.91
272.09228	-38.91279	-6.35284	-9.03557	3.14	-1.27	-1.84	15.012	14.812	0.567469	0.33	11.66
271.13869	-38.48876	-6.32771	-8.17942	0.11	-0.93	-1.22	14.477	14.376	0.465643	0.34	8.55
271.24159	-38.52912	-6.32508	-8.26944	2.05	-1.15	-1.52	14.924	14.543	0.592550	0.33	10.53
271.10335	-38.42774	-6.28671	-8.12610	-1.81	-0.72	-0.93	14.369	13.892	0.437742	0.29	6.60
271.47110	-38.44022	-6.16012	-8.38580	0.92	-1.00	-1.37	14.390	14.364	0.557777	0.34	9.38
271.75595	-38.52642	-6.13106	-8.62313	1.43	-1.05	-1.49	14.876	14.557	0.522870	0.36	9.91
271.98379	-38.57481	-6.09002	-8.80325	0.03	-0.89	-1.30	14.368	14.206	0.530721	0.26	8.48
271.34054	-38.26450	-6.05245	-8.21257	2.10	-1.10	-1.52	14.939	14.580	0.577634	0.32	10.57
272.36509	-38.61026	-5.98151	-9.08358	-0.04	-0.87	-1.33	14.129	13.931	0.663033	0.28	8.41
271.81472	-38.36615	-5.96605	-8.58867	2.25	-1.10	-1.61	15.254	14.914	0.445800	0.23	10.74
272.33418	-38.56491	-5.95215	-9.04115	-2.47	-0.61	-0.92	13.619	13.288	0.606127	0.26	5.94
271.54261	-38.17097	-5.89339	-8.30836	-0.79	-0.78	-1.10	14.279	14.120	0.471076	0.20	7.64
272.11606	-38.37785	-5.86484	-8.80301	-0.25	-0.83	-1.25	14.623	14.199	0.501215	0.34	8.19
271.53697	-38.08049	-5.81487	-8.26179	-0.90	-0.75	-1.08	14.351	14.020	0.499059	0.24	7.52
271.80379	-38.14313	-5.77093	-8.47652	0.49	-0.89	-1.32	14.869	14.577	0.424558	0.26	8.94
271.61871	-37.96875	-5.68462	-8.26592	-0.18	-0.81	-1.19	14.592	14.204	0.505802	0.28	8.25
272.49341	-38.05214	-5.43352	-8.91420	0.77	-0.86	-1.43	14.608	14.403	0.523034	0.25	9.22

Continued on next page. . .

Table A.1 – Continued

RA(J2000) deg	Dec(J2000) deg	ℓ deg	b deg	X kpc	Y kpc	Z kpc	J mag	K_s mag	P days	A_{K_s} mag	d kpc
271.87075	-37.73135	-5.37831	-8.32991	1.14	-0.89	-1.39	14.567	14.306	0.611396	0.22	9.59
272.00165	-37.75412	-5.34959	-8.43202	-1.60	-0.63	-0.99	13.945	13.830	0.488926	0.34	6.81
272.29733	-37.64495	-5.14150	-8.58789	4.13	-1.12	-1.90	15.362	14.843	0.640246	0.33	12.63
272.01948	-37.36821	-4.99832	-8.26369	-1.71	-0.58	-0.96	14.194	13.697	0.530400	0.31	6.68
272.23364	-37.43764	-4.97989	-8.44653	-0.65	-0.67	-1.14	14.247	14.129	0.481726	0.25	7.76
272.78910	-37.64648	-4.96013	-8.93357	1.07	-0.81	-1.48	14.497	14.213	0.654138	0.27	9.52
272.63219	-37.57219	-4.95165	-8.78900	-0.98	-0.63	-1.13	14.315	13.864	0.559572	0.23	7.44
272.57881	-37.49616	-4.90334	-8.71626	1.28	-0.82	-1.48	15.020	14.632	0.474201	0.25	9.73
272.00671	-37.25296	-4.90029	-8.20067	-0.49	-0.67	-1.13	14.303	14.196	0.472306	0.35	7.92
272.24889	-37.28214	-4.83516	-8.38464	-1.62	-0.57	-0.98	14.050	13.781	0.505906	0.23	6.78
272.16854	-37.24389	-4.83120	-8.31022	6.52	-1.25	-2.19	15.713	15.509	0.497124	0.35	15.03
272.79973	-37.35707	-4.69641	-8.80735	-1.80	-0.53	-1.01	14.176	13.657	0.536671	0.30	6.60
271.99531	-37.01448	-4.69188	-8.08069	2.35	-0.87	-1.53	15.287	14.822	0.487522	0.25	10.80
272.57426	-37.20575	-4.64485	-8.57826	11.50	-1.61	-3.04	16.661	16.236	0.454275	0.45	20.10
273.28885	-37.41713	-4.56937	-9.18004	0.34	-0.69	-1.40	14.470	14.342	0.504370	0.31	8.79
272.87077	-37.22166	-4.54847	-8.79491	0.28	-0.68	-1.33	14.424	14.232	0.545712	0.25	8.71
272.77905	-37.13896	-4.50846	-8.69188	0.21	-0.67	-1.31	14.578	14.219	0.543658	0.32	8.64
272.64754	-37.06824	-4.49425	-8.56616	-0.46	-0.62	-1.18	14.245	14.210	0.470757	0.35	7.96
272.42571	-36.92352	-4.44806	-8.34200	2.65	-0.85	-1.62	15.181	14.791	0.527415	0.22	11.10
272.96444	-37.11621	-4.41894	-8.81244	-1.37	-0.54	-1.07	14.195	13.761	0.551910	0.26	7.04
272.35948	-36.85236	-4.40944	-8.26194	0.79	-0.70	-1.33	14.619	14.307	0.567260	0.28	9.21
273.17280	-37.14258	-4.36522	-8.97205	2.65	-0.84	-1.74	14.836	14.702	0.571893	0.27	11.13
272.45716	-36.81081	-4.33543	-8.31171	-2.00	-0.48	-0.92	13.895	13.589	0.535395	0.27	6.39
272.21462	-36.62578	-4.26200	-8.05335	6.21	-1.08	-2.08	15.612	15.464	0.495692	0.30	14.70
272.36322	-36.67682	-4.25120	-8.18259	0.20	-0.63	-1.23	14.693	14.374	0.472331	0.34	8.61
273.09390	-36.95723	-4.22796	-8.83087	0.38	-0.64	-1.35	14.725	14.260	0.543886	0.31	8.81
272.59759	-36.72644	-4.20702	-8.37196	0.79	-0.67	-1.35	14.674	14.146	0.652835	0.25	9.22
273.09090	-36.87135	-4.15195	-8.78918	-0.11	-0.60	-1.27	14.433	13.948	0.639795	0.20	8.32
272.60813	-37.91412	-5.26731	-8.93043	2.87	-1.03	-1.77	15.096	14.962	0.474816	0.36	11.36
272.83455	-37.51674	-4.82681	-8.90563	0.44	-0.74	-1.38	14.324	14.070	0.650893	0.21	8.89
272.96063	-37.51318	-4.77693	-8.99272	-1.58	-0.56	-1.06	13.617	13.320	0.764924	0.21	6.83
272.99201	-37.48867	-4.74330	-9.00354	1.84	-0.84	-1.62	14.344	14.085	0.845780	0.22	10.31
273.28773	-36.78340	-3.99956	-8.88859	6.83	-1.06	-2.40	15.591	15.360	0.588263	0.23	15.36

Continued on next page...

Table A.1 – Continued

RA(J2000) deg	Dec(J2000) deg	ℓ deg	b deg	X kpc	Y kpc	Z kpc	J mag	K_s mag	P days	A_{K_s} mag	d kpc
273.16913	-36.72506	-3.99137	-8.77739	0.78	-0.63	-1.41	14.552	14.586	0.445500	0.29	9.21
273.02053	-36.52499	-3.86745	-8.57929	4.65	-0.88	-1.97	15.494	15.061	0.570047	0.24	13.13
272.46851	-36.27389	-3.85139	-8.06917	0.32	-0.58	-1.23	14.471	14.147	0.588984	0.32	8.73
273.49607	-36.64614	-3.79856	-8.97406	-1.85	-0.43	-1.02	13.888	13.793	0.470396	0.36	6.55
272.81554	-36.35286	-3.79043	-8.35341	-0.15	-0.54	-1.20	14.013	13.705	0.778931	0.28	8.26
273.51019	-36.60692	-3.75801	-8.96617	-0.29	-0.53	-1.27	14.318	14.009	0.582086	0.27	8.13
272.76491	-36.23237	-3.70175	-8.26130	-0.17	-0.53	-1.18	14.479	13.977	0.612775	0.19	8.24
273.25030	-36.36375	-3.63651	-8.66890	-0.28	-0.51	-1.22	14.473	14.132	0.523733	0.32	8.13
273.39140	-36.41009	-3.62529	-8.79107	-0.92	-0.47	-1.14	13.899	13.767	0.615684	0.46	7.49
273.67602	-36.51232	-3.61116	-9.04138	1.69	-0.63	-1.60	15.197	14.689	0.487439	0.30	10.14
273.69153	-36.45162	-3.55071	-9.02476	0.22	-0.53	-1.36	14.663	14.378	0.474532	0.35	8.65
273.04880	-36.06179	-3.44156	-8.38527	1.71	-0.60	-1.48	14.847	14.373	0.640176	0.24	10.14
273.09348	-36.02631	-3.39287	-8.40089	0.89	-0.55	-1.36	14.539	14.393	0.537138	0.28	9.31
273.57047	-36.11241	-3.29062	-8.78277	0.01	-0.48	-1.29	14.382	14.110	0.570363	0.25	8.43
272.87609	-35.73778	-3.21708	-8.11104	-0.81	-0.42	-1.07	14.030	13.771	0.627778	0.31	7.58
273.88253	-36.14118	-3.19990	-9.02011	1.25	-0.53	-1.52	14.664	14.499	0.527757	0.31	9.69
273.87168	-36.09407	-3.16149	-8.99083	-0.80	-0.41	-1.19	14.252	13.800	0.617086	0.33	7.61
273.06611	-35.74363	-3.15001	-8.25037	1.04	-0.51	-1.36	14.884	14.420	0.539561	0.24	9.45
273.64024	-35.91527	-3.08716	-8.74257	-0.17	-0.44	-1.25	14.681	14.194	0.508839	0.25	8.24
273.37759	-35.78741	-3.07123	-8.49475	-0.24	-0.43	-1.21	13.967	13.615	0.825110	0.30	8.17
273.51628	-35.80930	-3.03855	-8.60470	2.36	-0.57	-1.62	15.126	14.767	0.511535	0.33	10.80
272.93465	-35.54562	-3.02289	-8.06385	-0.73	-0.40	-1.07	14.165	13.740	0.657800	0.32	7.66
273.25348	-35.65688	-3.00114	-8.34513	7.21	-0.81	-2.30	15.469	15.313	0.638574	0.26	15.71
274.09310	-36.00479	-2.99848	-9.10960	1.38	-0.51	-1.56	14.629	14.368	0.605301	0.21	9.82
273.84303	-35.79023	-2.89855	-8.83152	0.83	-0.46	-1.42	14.715	14.273	0.589477	0.25	9.26
273.53032	-35.57049	-2.81878	-8.50504	0.20	-0.42	-1.27	14.359	14.124	0.585514	0.29	8.61
273.19259	-35.41584	-2.80834	-8.18973	-4.79	-0.17	-0.49	12.936	12.353	0.524444	0.32	3.55
273.89425	-35.69066	-2.78970	-8.82302	-1.48	-0.33	-1.06	13.982	13.744	0.542023	0.26	6.91
273.12686	-35.35252	-2.77673	-8.11291	-1.54	-0.33	-0.96	14.423	13.850	0.485030	0.34	6.84
274.17028	-35.77056	-2.75839	-9.05890	0.09	-0.40	-1.34	14.469	13.964	0.657761	0.31	8.51
274.08198	-35.63438	-2.66861	-8.93311	-3.22	-0.24	-0.79	13.454	13.268	0.474672	0.30	5.15
273.57901	-35.37856	-2.62802	-8.45198	-1.66	-0.30	-0.98	14.433	14.046	0.396421	0.21	6.72
272.61630	-36.46865	-3.96936	-8.26527	-2.14	-0.43	-0.89	13.569	13.054	0.814930	0.29	6.25

Continued on next page...

Table A.1 – Continued

RA(J2000) deg	Dec(J2000) deg	ℓ deg	b deg	X kpc	Y kpc	Z kpc	J mag	K_s mag	P days	A_{K_s} mag	d kpc
273.46927	-36.24191	-3.44496	-8.76959	-1.65	-0.40	-1.02	13.975	13.919	0.444735	0.34	6.74
273.54809	-35.77034	-2.99156	-8.60971	0.12	-0.44	-1.28	14.159	13.983	0.651279	0.31	8.54
273.62743	-35.39335	-2.62297	-8.49384	0.51	-0.40	-1.32	14.652	14.279	0.547151	0.32	8.92
273.69462	-35.41566	-2.61757	-8.55274	-0.44	-0.36	-1.18	14.388	14.037	0.546305	0.25	7.96
273.48886	-35.31526	-2.60544	-8.35757	2.34	-0.48	-1.57	14.633	14.311	0.754245	0.27	10.77
273.15619	-35.13261	-2.56872	-8.03216	-2.07	-0.28	-0.87	14.036	13.692	0.477544	0.35	6.30
273.69093	-35.34323	-2.55390	-8.51682	-1.25	-0.31	-1.05	14.074	13.676	0.609567	0.35	7.14
273.99504	-35.46522	-2.54886	-8.79304	2.50	-0.48	-1.68	14.966	14.750	0.532122	0.29	10.94
273.61069	-35.24709	-2.49799	-8.41448	0.35	-0.38	-1.28	14.883	14.454	0.455158	0.35	8.76
274.12298	-35.41875	-2.45891	-8.86464	-2.46	-0.25	-0.90	13.811	13.475	0.512702	0.32	5.92
273.74338	-35.22355	-2.42652	-8.49994	0.72	-0.38	-1.35	14.760	14.389	0.520159	0.30	9.14
274.20697	-35.33827	-2.35484	-8.88899	-1.03	-0.30	-1.14	14.345	13.979	0.497953	0.34	7.37
274.12093	-35.27487	-2.33007	-8.79760	-0.59	-0.31	-1.19	14.073	13.740	0.681566	0.30	7.81
273.56321	-34.95407	-2.25316	-8.24510	-1.32	-0.27	-1.01	13.976	13.738	0.567183	0.29	7.06
273.64455	-34.98508	-2.24997	-8.31854	1.73	-0.39	-1.47	15.012	14.686	0.489179	0.24	10.15
273.78161	-35.02185	-2.23083	-8.43515	2.20	-0.41	-1.57	14.849	14.615	0.566248	0.31	10.63
273.77705	-34.90318	-2.12599	-8.37735	5.04	-0.50	-1.98	15.762	15.189	0.536993	0.30	13.50
274.54829	-35.10922	-2.02012	-9.03352	1.64	-0.35	-1.59	14.948	14.707	0.473711	0.34	10.07
273.84144	-34.70035	-1.91934	-8.33118	-0.43	-0.26	-1.15	14.554	14.032	0.549354	0.28	7.97
273.99531	-34.74914	-1.90456	-8.46594	-2.14	-0.21	-0.91	13.718	13.500	0.553085	0.29	6.24
274.35280	-34.89794	-1.90306	-8.79497	-0.06	-0.27	-1.28	14.593	14.332	0.462888	0.29	8.35
273.89605	-34.70067	-1.89880	-8.37121	-0.77	-0.25	-1.11	14.542	14.085	0.483075	0.37	7.62
274.28965	-34.79178	-1.83128	-8.70052	1.39	-0.31	-1.49	14.814	14.595	0.497045	0.25	9.81
274.42597	-34.81017	-1.79634	-8.80857	-4.14	-0.13	-0.63	12.976	12.531	0.619138	0.35	4.22
274.45808	-34.68777	-1.67387	-8.77647	-0.07	-0.24	-1.27	14.516	14.168	0.531098	0.24	8.33
274.22782	-34.52119	-1.61115	-8.53189	3.95	-0.34	-1.85	15.526	15.224	0.445230	0.41	12.40
274.71887	-34.68535	-1.57331	-8.96653	-0.52	-0.21	-1.23	14.397	13.954	0.576515	0.27	7.88
274.04391	-34.37593	-1.55067	-8.33058	0.38	-0.24	-1.27	14.513	14.042	0.651988	0.28	8.78
274.20864	-34.42130	-1.52860	-8.47220	1.49	-0.26	-1.46	15.023	14.601	0.503398	0.29	9.91
274.24173	-34.42668	-1.52083	-8.49894	0.95	-0.25	-1.39	14.557	14.354	0.560834	0.27	9.36
273.82949	-34.24352	-1.51399	-8.11245	1.53	-0.26	-1.41	15.127	14.675	0.475048	0.31	9.94
273.98620	-34.30637	-1.51028	-8.25634	6.35	-0.39	-2.15	15.555	15.353	0.553934	0.29	14.82
274.44857	-34.41799	-1.43437	-8.64686	0.73	-0.23	-1.38	14.368	14.181	0.623088	0.31	9.14

Continued on next page...

Table A.1 – Continued

RA(J2000) deg	Dec(J2000) deg	ℓ deg	b deg	X kpc	Y kpc	Z kpc	J mag	K_s mag	P days	A_{K_s} mag	d kpc
274.25208	-34.29108	-1.39491	-8.44463	1.17	-0.23	-1.41	14.913	14.650	0.453256	0.36	9.58
274.10190	-34.22018	-1.38857	-8.30181	4.24	-0.30	-1.85	15.396	15.166	0.488091	0.35	12.68
274.27784	-34.27051	-1.36658	-8.45417	0.11	-0.20	-1.25	14.304	13.919	0.684266	0.26	8.51
274.53499	-34.31229	-1.30633	-8.66234	-2.99	-0.12	-0.80	13.489	13.006	0.643832	0.33	5.38
274.62995	-34.29129	-1.25137	-8.72269	-0.90	-0.16	-1.13	14.268	13.866	0.565563	0.25	7.49
274.18024	-34.02286	-1.18129	-8.26911	1.53	-0.20	-1.43	14.660	14.394	0.605631	0.35	9.94
274.13012	-35.29077	-2.34093	-8.81153	-1.40	-0.28	-1.07	14.284	13.904	0.481900	0.32	6.99
274.18991	-33.86398	-1.03487	-8.20348	1.41	-0.18	-1.41	14.690	14.517	0.532439	0.32	9.82
274.36374	-33.92559	-1.02356	-8.35997	-1.06	-0.13	-1.06	13.968	13.612	0.675320	0.20	7.32
274.44444	-33.94848	-1.01327	-8.42999	-0.94	-0.13	-1.09	14.192	13.849	0.567769	0.27	7.44
274.62482	-33.93660	-0.93369	-8.55782	-0.04	-0.13	-1.24	14.206	14.001	0.616835	0.27	8.36
274.13404	-33.72218	-0.92906	-8.09721	0.68	-0.15	-1.28	14.717	14.315	0.547981	0.32	9.08
274.68261	-33.94204	-0.91656	-8.60300	-2.10	-0.10	-0.93	13.719	13.477	0.570402	0.28	6.27
274.13456	-33.69497	-0.90444	-8.08511	-0.87	-0.12	-1.05	14.453	14.015	0.499880	0.32	7.51
274.78724	-33.89837	-0.83736	-8.66057	0.98	-0.14	-1.42	15.094	14.543	0.479322	0.32	9.39
274.18982	-33.56654	-0.76787	-8.06708	-0.02	-0.11	-1.17	14.826	14.310	0.473458	0.32	8.37
275.15621	-33.91612	-0.71335	-8.94176	-1.45	-0.09	-1.07	14.180	14.004	0.435692	0.36	6.94
275.23253	-33.92773	-0.69499	-9.00354	-0.71	-0.09	-1.20	14.397	14.122	0.476669	0.35	7.69
275.28264	-33.94615	-0.69272	-9.04896	-2.84	-0.07	-0.86	13.986	13.517	0.437311	0.37	5.54
274.63456	-33.63255	-0.65618	-8.42675	0.25	-0.10	-1.27	14.336	14.107	0.599797	0.27	8.65
274.44042	-33.53729	-0.64502	-8.23937	2.26	-0.12	-1.54	15.266	14.915	0.440511	0.24	10.67
274.43799	-33.50701	-0.61874	-8.22374	3.26	-0.12	-1.68	15.165	14.951	0.505283	0.30	11.69
275.24884	-33.76533	-0.54198	-8.94257	1.64	-0.09	-1.57	14.806	14.385	0.624859	0.32	10.07
274.27284	-33.32804	-0.52173	-8.01927	-1.86	-0.06	-0.90	13.950	13.591	0.553302	0.32	6.51
275.42603	-33.66811	-0.38699	-9.03053	0.27	-0.06	-1.36	14.505	14.143	0.585484	0.31	8.68
275.24276	-33.58932	-0.38522	-8.85880	2.96	-0.08	-1.77	14.945	14.811	0.544324	0.26	11.40
274.95965	-33.41242	-0.33345	-8.56827	0.84	-0.05	-1.38	14.359	13.941	0.783883	0.21	9.25
275.31567	-33.44956	-0.23123	-8.85013	3.04	-0.05	-1.78	15.174	14.677	0.619333	0.29	11.48
274.82099	-33.23096	-0.22312	-8.38268	1.48	-0.04	-1.45	14.955	14.682	0.468064	0.36	9.89
275.66048	-33.51822	-0.16267	-9.13793	0.50	-0.02	-1.42	14.556	14.337	0.520172	0.23	8.92
274.71397	-33.10404	-0.15009	-8.24515	-2.99	-0.01	-0.76	13.579	13.260	0.516041	0.28	5.37
274.52230	-32.97828	-0.11114	-8.04480	2.03	-0.02	-1.47	14.898	14.522	0.593349	0.41	10.44
274.79550	-33.07267	-0.09045	-8.29169	-1.47	-0.01	-0.99	14.007	13.811	0.510326	0.31	6.90

Continued on next page...

Table A.1 – Continued

RA(J2000) deg	Dec(J2000) deg	ℓ deg	b deg	X kpc	Y kpc	Z kpc	J mag	K_s mag	P days	A_{K_s} mag	d kpc
274.56048	-32.94595	-0.06731	-8.05851	-0.42	-0.01	-1.11	14.612	14.226	0.464313	0.28	7.96
274.73926	-33.00944	-0.05525	-8.22093	-0.53	-0.01	-1.12	14.596	14.048	0.528505	0.29	7.86
275.09426	-33.10220	-0.00221	-8.52814	0.39	-0.00	-1.31	14.956	14.429	0.468187	0.33	8.79
274.92692	-33.02740	0.00091	-8.36923	2.80	0.00	-1.64	15.210	14.765	0.550170	0.32	11.22
275.41025	-33.15286	0.07289	-8.78715	-0.34	0.01	-1.23	14.556	14.273	0.456171	0.30	8.06
275.25206	-33.07148	0.08594	-8.63219	1.57	0.01	-1.50	14.660	14.370	0.623873	0.23	9.99
274.97674	-32.79682	0.22774	-8.30178	-0.34	0.03	-1.16	14.233	14.032	0.559394	0.24	8.04
275.24902	-33.56405	-0.36001	-8.85207	-1.46	-0.04	-1.06	13.937	13.533	0.652857	0.25	6.93
275.79051	-32.97007	0.38301	-8.98987	0.06	0.06	-1.32	14.773	14.331	0.475552	0.16	8.47
275.82217	-32.90783	0.45140	-8.98577	2.27	0.08	-1.68	15.100	14.729	0.520657	0.30	10.71
275.30210	-32.59177	0.53791	-8.45295	4.49	0.12	-1.92	15.503	15.129	0.522630	0.22	12.94
275.91646	-32.78210	0.60112	-9.00038	-2.01	0.07	-0.99	13.854	13.437	0.608010	0.26	6.37
275.69159	-32.51173	0.75983	-8.70993	1.63	0.13	-1.53	15.148	14.705	0.472932	0.24	10.06
275.98276	-32.62547	0.76823	-8.98026	-2.88	0.07	-0.85	13.515	13.084	0.625512	0.25	5.49
276.09896	-32.65334	0.78722	-9.08025	-0.16	0.11	-1.30	14.537	14.068	0.568544	0.21	8.25
275.50146	-32.36087	0.82299	-8.49872	4.13	0.18	-1.87	15.334	15.004	0.552370	0.35	12.57
276.25684	-32.62023	0.87722	-9.18454	0.22	0.13	-1.38	14.448	14.089	0.607161	0.18	8.63
275.70836	-32.38968	0.87656	-8.66771	-1.33	0.11	-1.06	14.019	13.426	0.740543	0.35	7.06
275.58289	-32.32687	0.88504	-8.54480	-0.59	0.12	-1.16	14.339	14.250	0.437738	0.27	7.80
275.54079	-32.27315	0.91730	-8.48881	-0.28	0.13	-1.20	14.385	14.036	0.566502	0.32	8.11
275.37477	-32.19763	0.92129	-8.32941	-1.17	0.11	-1.04	14.387	13.805	0.556502	0.32	7.21
275.27706	-31.83133	1.21327	-8.08958	-0.09	0.17	-1.17	14.497	14.074	0.571569	0.29	8.30
275.98443	-32.12331	1.22337	-8.75680	-2.01	0.13	-0.96	14.155	13.732	0.470526	0.35	6.37
275.76618	-32.01945	1.23325	-8.54492	2.84	0.24	-1.68	15.073	14.902	0.492776	0.31	11.27
275.37144	-31.83741	1.24454	-8.16380	0.94	0.20	-1.33	14.867	14.570	0.463979	0.40	9.34
275.62371	-31.89767	1.28812	-8.38214	1.36	0.22	-1.43	14.803	14.587	0.496165	0.32	9.77
275.29756	-31.72974	1.31269	-8.05900	2.30	0.24	-1.51	14.887	14.636	0.564503	0.30	10.71
276.00216	-31.99174	1.34918	-8.71127	6.23	0.34	-2.25	15.819	15.387	0.530904	0.33	14.71
276.19135	-32.04962	1.36943	-8.88062	0.43	0.21	-1.37	14.856	14.338	0.511776	0.30	8.84
275.70449	-31.83406	1.37678	-8.41469	-0.04	0.20	-1.22	14.385	14.116	0.558329	0.29	8.36
275.94094	-31.87068	1.43505	-8.61054	-0.60	0.19	-1.16	14.545	14.015	0.535097	0.33	7.79
275.81330	-31.79593	1.45330	-8.48007	2.86	0.28	-1.67	15.244	14.808	0.536406	0.27	11.29
276.11542	-31.88125	1.49269	-8.74773	1.97	0.27	-1.59	14.852	14.588	0.557001	0.32	10.40

Continued on next page...

Table A.1 – Continued

RA(J2000) deg	Dec(J2000) deg	ℓ deg	b deg	X kpc	Y kpc	Z kpc	J mag	K_s mag	P days	A_{K_s} mag	d kpc
275.46230	-31.60398	1.49013	-8.12694	-3.85	0.12	-0.62	13.053	12.989	0.470252	0.32	4.50
275.38624	-31.49833	1.55557	-8.02127	-0.27	0.22	-1.13	14.747	14.282	0.458739	0.33	8.12
276.08834	-31.76038	1.59160	-8.67302	4.68	0.36	-2.00	15.678	15.230	0.493408	0.33	13.14
275.71584	-31.56999	1.61941	-8.30422	-2.05	0.18	-0.91	14.091	13.564	0.537086	0.26	6.32
275.64344	-31.49384	1.65991	-8.21478	-0.50	0.23	-1.13	14.561	14.107	0.505738	0.30	7.89
276.42083	-31.81068	1.67384	-8.94834	-2.41	0.17	-0.92	13.878	13.429	0.542820	0.30	5.97
276.02193	-31.59664	1.71398	-8.54907	-0.20	0.24	-1.22	14.666	14.168	0.515063	0.31	8.20
276.31606	-31.71865	1.71700	-8.82757	1.52	0.29	-1.53	14.857	14.360	0.624496	0.33	9.95
275.62952	-31.37707	1.75971	-8.15141	0.15	0.26	-1.21	14.659	14.159	0.560636	0.27	8.54
275.14730	-32.44233	0.61283	-8.26890	0.77	0.10	-1.32	14.693	14.489	0.480705	0.35	9.17
275.92541	-32.07316	1.24605	-8.68963	-2.28	0.13	-0.91	13.583	13.411	0.572702	0.30	6.10
276.45127	-31.66327	1.81910	-8.90584	-1.90	0.20	-1.00	14.032	13.545	0.571442	0.36	6.48
276.63460	-31.70629	1.85037	-9.06469	0.19	0.27	-1.36	14.514	14.233	0.533296	0.26	8.61
276.14382	-31.49510	1.85288	-8.59637	-1.51	0.22	-1.02	14.279	13.872	0.480206	0.30	6.87
275.66298	-31.20737	1.92567	-8.10016	-1.31	0.24	-0.99	14.420	13.973	0.463222	0.37	7.07
275.60442	-31.13163	1.97098	-8.02120	-1.74	0.23	-0.92	14.359	13.919	0.431326	0.38	6.63
275.89835	-31.01799	2.18829	-8.19443	6.41	0.56	-2.14	15.497	15.248	0.610728	0.30	14.88
276.41141	-31.14347	2.27440	-8.64339	2.08	0.41	-1.59	14.498	14.359	0.692789	0.30	10.52
275.86059	-30.90167	2.27840	-8.11304	0.51	0.35	-1.26	14.672	14.343	0.516919	0.27	8.91
276.28529	-31.08091	2.28211	-8.51883	0.31	0.34	-1.29	14.462	14.271	0.528510	0.31	8.72
275.95906	-30.88241	2.33427	-8.17976	0.87	0.37	-1.32	14.590	14.416	0.522974	0.31	9.28
276.70890	-31.16519	2.36960	-8.88094	-0.42	0.33	-1.23	14.455	13.974	0.580077	0.29	7.98
276.85358	-31.17517	2.41623	-8.99628	-0.46	0.33	-1.24	14.293	14.142	0.498030	0.33	7.95
276.35232	-30.94231	2.43342	-8.50810	1.65	0.42	-1.50	14.673	14.353	0.643124	0.33	10.07
276.38682	-30.84908	2.53111	-8.49281	0.75	0.40	-1.36	14.774	14.302	0.564149	0.22	9.17
276.38003	-30.84184	2.53501	-8.48436	1.13	0.42	-1.41	14.653	14.411	0.554115	0.25	9.55
276.52624	-30.90340	2.53610	-8.62414	0.23	0.38	-1.30	14.649	14.284	0.513302	0.27	8.64
276.12318	-30.69801	2.56477	-8.22258	1.40	0.43	-1.41	14.925	14.539	0.521436	0.34	9.81
276.61579	-30.76630	2.69491	-8.63172	-1.62	0.31	-1.01	14.142	13.930	0.443626	0.38	6.77
276.04888	-30.45225	2.75729	-8.05476	1.26	0.46	-1.36	14.772	14.620	0.473788	0.36	9.67
276.49343	-30.59860	2.79904	-8.46262	2.81	0.54	-1.66	15.298	14.939	0.475527	0.28	11.25
277.10493	-30.81657	2.83839	-9.03044	3.49	0.58	-1.89	15.337	15.109	0.459897	0.28	11.96
276.97718	-30.75361	2.84627	-8.90416	-0.02	0.41	-1.30	14.596	14.233	0.508730	0.20	8.39

Continued on next page. . .

Table A.1 – Continued

RA(J2000) deg	Dec(J2000) deg	ℓ deg	b deg	X kpc	Y kpc	Z kpc	J mag	K_s mag	P days	A_{K_s} mag	d kpc
276.53686	-30.56282	2.84831	-8.48005	-1.75	0.33	-0.97	14.159	13.765	0.493715	0.24	6.64
277.11164	-30.77177	2.88165	-9.01577	0.86	0.46	-1.46	14.874	14.520	0.479108	0.38	9.29
276.55643	-30.51701	2.89736	-8.47463	0.54	0.45	-1.32	14.437	14.107	0.639313	0.28	8.95
276.54050	-30.47083	2.93290	-8.44169	-0.51	0.40	-1.16	14.469	13.827	0.643770	0.37	7.89
277.02432	-30.65462	2.95427	-8.89655	-1.13	0.37	-1.12	14.132	13.904	0.518065	0.30	7.27
276.40512	-30.33313	3.00443	-8.27560	-1.96	0.33	-0.92	13.850	13.491	0.588256	0.28	6.42
277.12354	-30.58193	3.05854	-8.94084	1.71	0.54	-1.58	14.693	14.385	0.635021	0.26	10.16
276.15664	-30.15640	3.06635	-8.00439	3.61	0.64	-1.69	15.288	14.957	0.531333	0.37	12.04
277.27338	-30.54869	3.14655	-9.04181	-0.49	0.43	-1.24	14.311	13.964	0.577297	0.30	7.93
276.56392	-31.23277	2.25248	-8.79999	0.36	0.34	-1.34	14.590	14.382	0.485307	0.34	8.77
276.40984	-29.98866	3.31724	-8.12455	-0.10	0.48	-1.17	14.374	14.146	0.536907	0.30	8.30
276.63053	-30.03615	3.36098	-8.31664	2.46	0.63	-1.59	15.128	14.744	0.531141	0.23	10.90
277.34338	-30.32759	3.37436	-8.99817	-0.58	0.46	-1.22	14.451	14.179	0.469728	0.35	7.84
276.73223	-29.99890	3.43447	-8.37873	0.53	0.53	-1.31	14.470	14.149	0.616101	0.34	8.95
276.44948	-29.82509	3.48043	-8.08173	0.32	0.52	-1.23	14.650	14.273	0.528164	0.30	8.73
276.81365	-29.94839	3.51201	-8.41924	4.20	0.77	-1.87	15.117	14.824	0.653992	0.25	12.67
277.38398	-30.16577	3.53700	-8.95806	-2.60	0.35	-0.89	13.603	13.572	0.452104	0.35	5.78
276.77521	-29.86371	3.57353	-8.35159	1.79	0.63	-1.49	15.164	14.702	0.488993	0.21	10.22
277.12127	-29.97673	3.60645	-8.67045	1.90	0.64	-1.56	14.852	14.601	0.544609	0.32	10.34
277.07612	-29.89718	3.66091	-8.60003	2.94	0.72	-1.71	15.110	14.796	0.550982	0.28	11.39
277.21671	-29.95429	3.66395	-8.73457	0.84	0.59	-1.41	14.795	14.753	0.390274	0.40	9.27
276.83298	-29.55142	3.87848	-8.25679	-3.60	0.32	-0.67	13.027	12.782	0.624945	0.33	4.77
276.79688	-29.53069	3.88301	-8.21943	1.82	0.69	-1.47	14.964	14.604	0.534614	0.31	10.25
276.89784	-29.52560	3.92732	-8.29572	-0.27	0.55	-1.17	14.251	14.007	0.584505	0.30	8.14
277.58894	-29.80764	3.94165	-8.95901	3.23	0.79	-1.83	15.363	15.053	0.463678	0.26	11.70
277.07383	-29.57203	3.95439	-8.45344	2.61	0.75	-1.63	15.159	14.694	0.569684	0.22	11.06
277.62856	-29.80659	3.95797	-8.98939	2.08	0.72	-1.65	15.041	14.846	0.456486	0.31	10.54
277.47640	-29.65098	4.04011	-8.80208	-0.25	0.57	-1.25	14.481	14.052	0.565368	0.29	8.17
276.95858	-29.29650	4.15830	-8.24064	-0.23	0.59	-1.17	14.357	14.255	0.475663	0.32	8.18
277.10228	-29.22452	4.27997	-8.32065	-3.19	0.38	-0.74	13.372	13.091	0.559538	0.28	5.19
277.39786	-29.25909	4.36475	-8.56698	-0.59	0.59	-1.16	14.177	14.036	0.529532	0.24	7.82
276.93040	-29.03919	4.37966	-8.10350	0.26	0.66	-1.22	14.745	14.239	0.537845	0.29	8.67
276.82676	-28.99360	4.37980	-8.00206	0.15	0.65	-1.19	14.233	13.918	0.693611	0.33	8.57

Continued on next page…

Table A.1 – Continued

RA(J2000) deg	Dec(J2000) deg	ℓ deg	b deg	X kpc	Y kpc	Z kpc	J mag	K_s mag	P days	A_{K_s} mag	d kpc
277.55737	-29.28830	4.40071	-8.70464	1.66	0.77	-1.54	15.049	14.778	0.448593	0.40	10.11
277.02465	-29.05776	4.40012	-8.18550	1.87	0.78	-1.47	15.166	14.844	0.439228	0.34	10.31
277.66012	-29.30318	4.42734	-8.79158	-0.58	0.60	-1.20	14.385	14.197	0.462299	0.31	7.84
277.19983	-29.09254	4.43775	-8.33803	-0.41	0.61	-1.16	14.291	14.001	0.569376	0.30	8.00
278.04845	-29.32693	4.55692	-9.10595	0.54	0.70	-1.42	14.707	14.324	0.533732	0.30	8.99
277.12331	-28.90857	4.57393	-8.19603	-0.88	0.59	-1.07	14.415	14.077	0.475703	0.24	7.53
277.91575	-29.22778	4.59546	-8.95838	-0.44	0.63	-1.24	14.606	14.330	0.427241	0.35	7.99
277.54636	-29.06946	4.59481	-8.59902	0.61	0.72	-1.35	14.839	14.244	0.578700	0.25	9.04
277.53927	-29.05172	4.60811	-8.58560	0.76	0.73	-1.38	14.839	14.316	0.560808	0.37	9.20
277.20210	-28.87700	4.63360	-8.24366	-2.17	0.50	-0.88	14.242	13.600	0.503692	0.35	6.21
277.64203	-28.94881	4.74171	-8.62051	4.65	1.07	-1.99	15.571	15.136	0.535667	0.24	13.15
277.00356	-29.74071	3.77421	-8.47398	2.39	0.71	-1.60	14.886	14.601	0.594099	0.25	10.84
277.20786	-29.31347	4.24099	-8.44275	-1.12	0.53	-1.07	13.945	13.637	0.655261	0.36	7.29
277.72810	-29.37434	4.38925	-8.87619	0.06	0.64	-1.31	14.685	14.108	0.578777	0.30	8.49
277.26553	-28.96943	4.57501	-8.33457	0.92	0.74	-1.36	14.989	14.618	0.445788	0.37	9.35
277.13970	-28.72283	4.74828	-8.12588	6.53	1.23	-2.15	15.474	15.018	0.759659	0.21	15.03
278.23546	-29.18255	4.76088	-9.18913	1.71	0.83	-1.63	14.818	14.508	0.573763	0.30	10.18
277.74607	-28.89185	4.83416	-8.67693	0.29	0.73	-1.32	14.589	14.322	0.506598	0.30	8.73
277.72918	-28.87560	4.84227	-8.65648	3.60	1.01	-1.83	15.125	14.646	0.698880	0.28	12.08
277.36137	-28.69001	4.86563	-8.28522	0.48	0.75	-1.29	14.939	14.417	0.485154	0.29	8.91
277.12985	-28.56629	4.88580	-8.04815	1.10	0.80	-1.34	14.698	14.523	0.501339	0.35	9.53
277.51594	-28.72168	4.89793	-8.42072	1.96	0.88	-1.53	14.607	14.403	0.654420	0.28	10.41
277.56908	-28.67981	4.95679	-8.44388	3.20	1.00	-1.72	15.164	14.917	0.518850	0.27	11.67
277.56938	-28.58736	5.04064	-8.40303	-1.91	0.56	-0.94	13.966	13.489	0.599934	0.33	6.48
277.61758	-28.58854	5.05858	-8.44148	-0.74	0.67	-1.12	14.371	14.124	0.473981	0.36	7.68
277.21716	-28.36680	5.10066	-8.02757	-0.49	0.70	-1.11	14.446	14.173	0.481837	0.36	7.92
277.89691	-28.47931	5.26759	-8.61302	6.22	1.34	-2.23	15.700	15.516	0.477546	0.34	14.76
278.32305	-28.59550	5.32912	-9.00026	2.82	1.04	-1.78	15.056	14.733	0.574082	0.27	11.31
277.43131	-28.15877	5.37374	-8.10340	0.75	0.85	-1.30	14.833	14.417	0.512792	0.29	9.18
277.61040	-28.17131	5.43347	-8.25033	1.82	0.96	-1.48	15.099	14.582	0.547339	0.31	10.27
278.07432	-28.27871	5.51939	-8.66433	-1.03	0.70	-1.11	14.212	13.862	0.553983	0.21	7.39
277.99714	-28.23394	5.52960	-8.58356	0.89	0.89	-1.40	14.998	14.507	0.489275	0.34	9.34
278.08880	-28.25411	5.54741	-8.66491	-0.82	0.73	-1.14	14.560	14.123	0.465731	0.32	7.60

Continued on next page...

Table A.1 – Continued

RA(J2000) deg	Dec(J2000) deg	ℓ deg	b deg	X kpc	Y kpc	Z kpc	J mag	K_s mag	P days	A_{K_s} mag	d kpc
277.98230	-28.00882	5.72787	-8.47217	5.86	1.42	-2.14	15.945	15.372	0.516097	0.34	14.39
278.57578	-28.12702	5.85414	-8.99432	-0.33	0.82	-1.27	14.361	13.990	0.589057	0.24	8.11
277.75797	-27.77051	5.85474	-8.18871	-1.40	0.71	-0.99	13.994	13.549	0.658814	0.30	7.01
278.23180	-27.79329	6.02196	-8.57458	0.43	0.92	-1.33	14.889	14.277	0.543889	0.26	8.88
278.52676	-27.91922	6.02386	-8.86416	-1.13	0.76	-1.12	14.305	13.652	0.648433	0.27	7.30
278.66540	-27.93671	6.06241	-8.98190	1.78	1.07	-1.61	15.121	14.810	0.448815	0.21	10.27
277.80473	-27.49116	6.12608	-8.10150	-0.52	0.84	-1.11	14.847	14.179	0.477213	0.34	7.91
277.95839	-27.48643	6.19158	-8.22150	1.07	1.02	-1.37	14.710	14.310	0.601417	0.34	9.52
278.52850	-28.35315	5.62989	-9.05610	1.04	0.92	-1.50	14.706	14.201	0.659387	0.29	9.51
277.80973	-27.87299	5.78254	-8.27528	-0.13	0.83	-1.20	14.443	13.870	0.682715	0.31	8.31
278.45793	-27.64692	6.24415	-8.68963	-0.49	0.85	-1.20	14.460	14.007	0.559425	0.29	7.95
278.79070	-27.78398	6.25057	-9.01449	0.58	0.97	-1.42	14.461	14.259	0.571719	0.34	9.05
278.79669	-27.73401	6.29840	-8.99735	1.22	1.05	-1.52	14.918	14.724	0.435724	0.37	9.71
278.62582	-27.62098	6.33395	-8.81177	-2.17	0.68	-0.95	13.562	13.290	0.664531	0.28	6.24
278.81282	-27.69756	6.33790	-8.99420	5.75	1.56	-2.26	15.616	15.382	0.507344	0.34	14.32
278.47445	-27.51127	6.37384	-8.64298	-1.20	0.79	-1.08	14.442	14.047	0.452798	0.18	7.23
278.83887	-27.58460	6.45093	-8.96543	0.67	1.01	-1.43	14.441	14.055	0.694758	0.27	9.14
277.92561	-27.17063	6.46425	-8.05501	0.41	0.99	-1.24	14.276	14.012	0.680851	0.31	8.86
278.75942	-27.43826	6.55274	-8.83789	8.40	1.92	-2.64	15.807	15.524	0.617577	0.32	17.02
278.41300	-27.27203	6.56660	-8.48844	0.38	1.00	-1.31	14.771	14.494	0.446630	0.37	8.83
278.24928	-27.08359	6.67227	-8.27446	0.65	1.05	-1.31	14.681	14.313	0.552364	0.33	9.11
278.25286	-27.08359	6.67371	-8.27731	1.06	1.10	-1.38	14.631	14.283	0.616333	0.23	9.53
278.90247	-27.28807	6.74575	-8.88612	-1.42	0.81	-1.08	14.250	13.882	0.494130	0.33	7.01
278.88377	-27.15915	6.85561	-8.81460	0.34	1.04	-1.35	14.592	14.331	0.511091	0.24	8.81
278.37274	-26.93228	6.85860	-8.30605	1.05	1.12	-1.38	14.784	14.577	0.477158	0.32	9.52
278.83090	-27.02782	6.95405	-8.71462	1.00	1.14	-1.44	15.074	14.552	0.484611	0.27	9.49
279.19697	-27.17313	6.96646	-9.07121	-0.22	0.99	-1.30	14.108	13.861	0.679750	0.32	8.25
278.91172	-27.00745	7.00457	-8.77033	0.00	1.02	-1.29	14.469	14.268	0.501819	0.33	8.47
278.34649	-26.71531	7.04467	-8.18893	-0.90	0.92	-1.07	14.337	13.898	0.556929	0.25	7.54
278.95659	-26.88623	7.13254	-8.75304	-0.83	0.94	-1.16	14.428	13.977	0.531082	0.29	7.62
279.27535	-27.00708	7.14858	-9.06141	-1.06	0.91	-1.16	14.459	13.844	0.563276	0.31	7.40
278.88470	-26.81489	7.16885	-8.66407	2.40	1.35	-1.65	15.217	14.838	0.490952	0.42	10.92
278.83741	-26.73436	7.22320	-8.59072	-3.87	0.56	-0.66	13.166	12.774	0.570321	0.28	4.52

Continued on next page...

Table A.1 – Continued

RA(J2000) deg	Dec(J2000) deg	ℓ deg	b deg	X kpc	Y kpc	Z kpc	J mag	K_s mag	P days	A_{K_s} mag	d kpc
278.41985	-26.43928	7.32399	-8.12536	-1.12	0.92	-1.03	13.878	13.632	0.663064	0.30	7.32
278.98013	-26.66694	7.34116	-8.67556	-1.05	0.94	-1.11	14.248	13.850	0.561337	0.31	7.40
279.16406	-26.64182	7.43702	-8.81223	4.38	1.66	-2.00	15.388	14.940	0.616314	0.32	12.95
279.48796	-26.78087	7.43852	-9.13324	5.84	1.85	-2.31	15.742	15.318	0.544695	0.25	14.45
278.63673	-26.39151	7.45417	-8.27837	-0.71	0.99	-1.11	14.418	13.993	0.539095	0.22	7.74
279.39535	-26.70214	7.47369	-9.02446	0.04	1.09	-1.34	14.544	14.197	0.539779	0.25	8.52
279.21958	-26.57746	7.51757	-8.82863	0.86	1.21	-1.44	14.594	14.228	0.625168	0.18	9.36
278.51432	-26.17542	7.60082	-8.08427	-0.70	1.01	-1.09	14.639	14.187	0.456886	0.34	7.75
279.52028	-26.61053	7.60651	-9.08490	-1.15	0.95	-1.15	14.367	13.827	0.558887	0.27	7.31
278.51395	-27.26756	6.61071	-8.56699	-0.09	0.95	-1.25	14.600	14.199	0.520592	0.39	8.36
278.64422	-26.60680	7.26198	-8.37952	0.80	1.16	-1.35	14.740	14.324	0.566049	0.24	9.28
278.58930	-26.48407	7.35130	-8.28120	0.42	1.13	-1.28	14.710	14.221	0.571759	0.25	8.89
279.41392	-26.63591	7.54135	-9.01045	1.48	1.29	-1.57	14.989	14.421	0.597001	0.27	9.99
279.13883	-26.30350	7.73454	-8.64345	-1.47	0.93	-1.04	14.398	13.744	0.551794	0.29	6.98
279.15747	-26.22398	7.81422	-8.62352	0.03	1.14	-1.28	14.647	13.975	0.652197	0.33	8.51
279.34159	-26.25218	7.86191	-8.78429	0.29	1.19	-1.34	14.817	14.358	0.495955	0.33	8.77
279.12579	-26.07135	7.94022	-8.53087	2.42	1.50	-1.63	15.097	14.545	0.635538	0.33	10.95
278.84288	-25.94127	7.94491	-8.24530	0.27	1.20	-1.25	15.171	14.505	0.433903	0.34	8.74
278.99788	-25.86923	8.07244	-8.33859	1.30	1.36	-1.43	15.171	14.498	0.539820	0.34	9.81
279.09527	-25.90529	8.07876	-8.43314	0.70	1.28	-1.35	14.441	14.176	0.632495	0.33	9.19
279.03305	-25.74567	8.19863	-8.31251	0.62	1.29	-1.32	14.683	14.215	0.601728	0.31	9.11
279.53472	-25.85144	8.30332	-8.76469	-0.41	1.15	-1.23	14.746	14.117	0.523390	0.25	8.07
279.54790	-25.79723	8.35789	-8.75162	-1.00	1.07	-1.13	14.245	14.071	0.471930	0.34	7.47
279.01400	-25.21663	8.67046	-8.06338	4.03	1.88	-1.78	14.941	14.639	0.760104	0.25	12.60
279.53543	-25.31126	8.79465	-8.52837	1.34	1.49	-1.47	14.894	14.690	0.463188	0.33	9.87
279.53321	-25.29243	8.81086	-8.51830	-2.50	0.90	-0.87	13.895	13.542	0.487524	0.32	5.94
279.79705	-25.12128	9.07231	-8.65776	-3.19	0.82	-0.78	13.534	13.083	0.573984	0.30	5.24
279.97713	-25.17471	9.09584	-8.82772	0.75	1.45	-1.43	14.298	13.933	0.794553	0.22	9.28
279.76146	-25.02424	9.14624	-8.58626	1.11	1.52	-1.44	14.627	14.383	0.577711	0.33	9.64
279.38003	-24.84290	9.15713	-8.19588	0.91	1.48	-1.35	14.760	14.445	0.525100	0.31	9.42
279.55441	-26.03058	8.14817	-8.85903	2.11	1.49	-1.65	15.365	14.628	0.562107	0.31	10.65
279.92016	-25.08894	9.15108	-8.74384	0.43	1.41	-1.36	14.345	13.968	0.720088	0.31	8.95
279.33392	-24.68407	9.28245	-8.08822	0.03	1.36	-1.20	14.853	14.421	0.445665	0.40	8.53

Continued on next page...

Table A.1 – Continued

RA(J2000) deg	Dec(J2000) deg	ℓ deg	b deg	X kpc	Y kpc	Z kpc	J mag	K_s mag	P days	A_{K_s} mag	d kpc
279.34011	-24.67526	9.29294	-8.08938	0.61	1.46	-1.29	14.593	14.494	0.474280	0.34	9.13
280.25277	-24.94464	9.41565	-8.95200	3.54	1.97	-1.90	15.309	14.853	0.591642	0.22	12.16
279.46780	-24.47882	9.52276	-8.10686	9.19	2.94	-2.56	16.065	15.747	0.560620	0.36	17.93
279.89335	-24.65358	9.53619	-8.53132	10.40	3.14	-2.88	16.450	15.989	0.515841	0.34	19.19
279.98248	-24.66636	9.56047	-8.60972	-2.91	0.91	-0.82	13.479	13.104	0.624103	0.36	5.53
280.42747	-24.80842	9.60968	-9.03534	1.08	1.59	-1.52	14.745	14.385	0.576399	0.26	9.64
279.93809	-24.57720	9.62364	-8.53438	-0.18	1.38	-1.24	14.327	14.071	0.577207	0.28	8.33
279.51775	-24.34379	9.66542	-8.08810	-0.89	1.26	-1.07	14.086	13.855	0.585929	0.30	7.59
279.73040	-24.42207	9.68063	-8.29646	1.61	1.69	-1.47	14.982	14.526	0.563523	0.24	10.17
279.73029	-24.36220	9.73492	-8.27003	6.16	2.48	-2.15	16.104	15.509	0.484700	0.40	14.83
280.25056	-24.40772	9.90365	-8.71587	0.34	1.51	-1.35	14.757	14.259	0.552175	0.31	8.88
280.64181	-24.51315	9.96470	-9.08234	1.57	1.74	-1.61	15.076	14.599	0.528111	0.32	10.16
279.74207	-24.08248	9.99345	-8.15653	-0.92	1.30	-1.07	14.197	13.992	0.518285	0.32	7.58
280.79277	-24.42022	10.10993	-9.16575	-2.01	1.12	-1.03	13.900	13.534	0.575848	0.28	6.48
279.97160	-24.05384	10.11260	-8.33215	4.90	2.36	-1.98	15.515	15.142	0.563688	0.32	13.56
280.15062	-24.08382	10.15787	-8.49218	-0.65	1.37	-1.16	14.293	13.936	0.582632	0.25	7.86
280.65259	-24.27525	10.18594	-8.98774	-1.10	1.29	-1.15	14.487	13.948	0.516198	0.24	7.41
280.12937	-23.59086	10.59698	-8.25838	0.27	1.60	-1.27	14.455	14.143	0.601927	0.20	8.81
270.85027	-40.88353	-8.56800	-9.11689	-1.40	-1.04	-1.12	13.993	13.568	0.657026	0.29	7.07
271.31020	-40.99629	-8.50353	-9.47658	0.27	-1.28	-1.45	14.542	14.254	0.543839	0.34	8.79
272.17791	-38.93273	-6.33938	-9.10383	-3.35	-0.55	-0.79	13.635	13.293	0.447351	0.34	5.05
272.27550	-38.89191	-6.26708	-9.15217	-0.55	-0.85	-1.25	14.709	14.263	0.443135	0.34	7.90
274.36480	-35.73419	-2.65306	-9.18310	1.02	-0.43	-1.51	14.474	14.252	0.623970	0.30	9.46
274.65971	-35.23092	-2.08837	-9.16978	1.92	-0.37	-1.66	14.500	14.339	0.686243	0.32	10.37
274.39153	-35.51941	-2.44914	-9.10521	0.20	-0.36	-1.36	14.272	14.094	0.602439	0.33	8.62
275.16168	-34.25712	-1.01961	-9.09927	0.63	-0.16	-1.43	14.446	14.194	0.605451	0.26	9.05
275.85161	-33.21501	0.18433	-9.14518	0.75	0.03	-1.46	14.970	14.382	0.527412	0.31	9.17
276.44465	-33.27731	0.35112	-9.61719	-1.39	0.04	-1.17	14.360	13.846	0.509204	0.33	7.01
276.95395	-33.47388	0.36179	-10.08560	0.17	0.05	-1.51	14.687	14.217	0.540570	0.34	8.61
276.23051	-33.17875	0.36026	-9.41294	0.37	0.05	-1.44	14.518	14.166	0.587058	0.26	8.79
276.27971	-32.50709	0.98855	-9.15146	-0.54	0.13	-1.25	14.476	14.096	0.507882	0.34	7.87
276.28983	-32.48110	1.01597	-9.14754	-0.40	0.14	-1.27	14.031	13.758	0.702716	0.27	8.01
276.48371	-32.21388	1.33218	-9.17545	3.25	0.27	-1.88	15.022	14.883	0.537141	0.23	11.70

Continued on next page...

Table A.1 – Continued

RA(J2000)	Dec(J2000)	ℓ	b	X	Y	Z	J	K_s	P	A_{K_s}	d
deg	deg	deg	deg	kpc	kpc	kpc	mag	mag	days	mag	kpc
276.48484	-32.15745	1.38382	-9.15124	-0.89	0.18	-1.19	14.093	13.727	0.640578	0.32	7.51
276.68920	-31.81078	1.77641	-9.15266	-0.19	0.25	-1.31	14.339	14.247	0.483908	0.33	8.22
277.34934	-30.65940	3.07522	-9.14938	-0.48	0.42	-1.26	14.367	14.175	0.482551	0.31	7.94
278.62448	-28.46489	5.56563	-9.18096	-2.16	0.60	-0.99	14.304	13.726	0.456608	0.33	6.25
278.29553	-28.92717	5.01666	-9.12425	1.04	0.82	-1.51	14.631	14.227	0.643360	0.28	9.50
279.01308	-27.71143	6.40386	-9.15969	0.43	0.98	-1.42	14.704	14.468	0.463633	0.34	8.91
279.73929	-28.15098	6.28485	-9.92852	1.35	1.06	-1.70	14.490	14.339	0.625821	0.34	9.86
279.09664	-27.62426	6.51603	-9.18819	-0.28	0.92	-1.31	14.426	14.202	0.498331	0.25	8.18
279.78643	-26.20477	8.08159	-9.12250	1.49	1.39	-1.59	14.819	14.584	0.521360	0.31	10.02
279.85685	-26.59418	7.75416	-9.34871	-1.27	0.96	-1.16	13.919	13.627	0.645332	0.31	7.19
271.54456	-39.46189	-7.04509	-8.91649	-0.20	-1.00	-1.28	14.634	14.252	0.486107	0.31	8.26
272.78738	-38.19457	-5.45326	-9.18510	2.69	-1.05	-1.79	14.711	14.577	0.643468	0.30	11.19
274.84609	-32.62222	0.33433	-8.12447	0.29	0.05	-1.23	14.808	14.246	0.535957	0.30	8.68
276.30356	-31.62049	1.80106	-8.77420	2.72	0.35	-1.71	14.985	14.880	0.493223	0.34	11.16
276.39288	-31.65516	1.80402	-8.85773	1.82	0.32	-1.58	15.230	14.723	0.482623	0.28	10.25
276.38339	-30.01865	3.27978	-8.11756	-2.74	0.32	-0.79	13.511	13.283	0.551809	0.32	5.63
277.93301	-29.06705	4.74823	-8.90105	-1.06	0.60	-1.14	14.344	14.073	0.457924	0.33	7.36

Bibliography

Alard, C. 1996, ApJ, 458, L17

Alcock, C., Allsman, R. A., Alves, D. R., et al. 1997, ApJ, 474, 217

Alcock, C., Allsman, R. A., Axelrod, T. S., et al. 1996, AJ, 111, 1146

Alonso-García, J., Dékány, I., Catelan, M., et al. 2015, AJ, 149, 99

Alves, D. R. 2000, ApJ, 539, 732

Alves, D. R., Rejkuba, M., Minniti, D., & Cook, K. H. 2002, ApJ, 573, L51

Angeloni, R., Contreras Ramos, R., Catelan, M., et al. 2014, A&A, 567, A100

Aubourg, E., Bareyre, P., Brehin, S., et al. 1993, The Messenger, 72, 20

Bailey, S. I. 1902, Annals of Harvard College Observatory, 38, 1

Benjamin, R. A., Churchwell, E., Babler, B. L., et al. 2005, ApJ, 630, L149

Borissova, J., Rejkuba, M., Minniti, D., Catelan, M., & Ivanov, V. D. 2009, A&A, 502, 505

Cardelli, J. A., Clayton, G. C., & Mathis, J. S. 1989, ApJ, 345, 245

Carney, B. W., Fulbright, J. P., Terndrup, D. M., Suntzeff, N. B., & Walker, A. R. 1995, AJ, 110, 1674

Carpenter, J. M., Hillenbrand, L. A., & Skrutskie, M. F. 2001, AJ, 121, 3160

Catelan, M., Angeloni, R., Dékány, I., et al. 2011a, in Revista Mexicana de Astronomia y Astrofisica, vol. 27, Vol. 40, Revista Mexicana de Astronomia y Astrofisica Conference Series, 269–269

Catelan, M., Dekany, I., Hempel, M., & Minniti, D. 2013a, Boletin de la Asociacion Argentina de Astronomia La Plata Argentina, 56, 153

Catelan, M., Minniti, D., Lucas, P. W., et al. 2011b, in RR Lyrae Stars, Metal-Poor Stars, and the Galaxy, ed. A. McWilliam, 145

Catelan, M., Minniti, D., Lucas, P. W., et al. 2013b, ArXiv e-prints

Catelan, M., Pritzl, B. J., & Smith, H. A. 2004, ApJS, 154, 633

Catelan, M. & Smith, H. A. 2015, Pulsating Stars (Wiley-VCH)

Clement, C. M., Muzzin, A., Dufton, Q., et al. 2001, AJ, 122, 2587

Cohen, R. E. & Sarajedini, A. 2012, MNRAS, 419, 342

Coppola, G., Dall'Ora, M., Ripepi, V., et al. 2011, MNRAS, 416, 1056

Cutri, R. M., Skrutskie, M. F., van Dyk, S., et al. 2003, VizieR Online Data Catalog, 2246, 0

Dall'Ora, M., Storm, J., Bono, G., et al. 2004, ApJ, 610, 269

Dalton, G. B., Caldwell, M., Ward, A. K., et al. 2006, in Society of Photo-Optical Instrumentation Engineers (SPIE) Conference Series, Vol. 6269, Society of Photo-Optical Instrumentation Engineers (SPIE) Conference Series

Dékány, I., Minniti, D., Catelan, M., et al. 2013, ApJ, 776, L19

Dékány, I., Minniti, D., Hajdu, G., et al. 2015, ApJ, 799, L11

Del Principe, M., Piersimoni, A. M., Bono, G., et al. 2005, AJ, 129, 2714

Del Principe, M., Piersimoni, A. M., Storm, J., et al. 2006, ApJ, 652, 362

Emerson, J. P. & Sutherland, W. J. 2010, in Society of Photo-Optical Instrumentation Engineers (SPIE) Conference Series, Vol. 7733, Society of Photo-Optical Instrumentation Engineers (SPIE) Conference Series

Feast, M. W., Laney, C. D., Kinman, T. D., van Leeuwen, F., & Whitelock, P. A. 2008, MNRAS, 386, 2115

Fiorentino, G., Bono, G., Monelli, M., et al. 2015, ApJ, 798, L12

Francis, C. & Anderson, E. 2014, MNRAS, 441, 1105

Freudenreich, H. T. 1996, ApJ, 468, 663

Gavrilchenko, T., Klein, C. R., Bloom, J. S., & Richards, J. W. 2014, MNRAS, 441, 715

Gonzalez, O. A., Rejkuba, M., Zoccali, M., et al. 2013, A&A, 552, A110

Gonzalez, O. A., Rejkuba, M., Zoccali, M., Valenti, E., & Minniti, D. 2011, A&A, 534, A3

Gonzalez, O. A., Rejkuba, M., Zoccali, M., et al. 2012, A&A, 543, A13

Gran, F., Minniti, D., Saito, R. K., et al. 2015, A&A, 575, A114

Gratton, R. & Carretta, E. 1996, in Astronomical Society of the Pacific Conference Series, Vol. 92, Formation of the Galactic Halo...Inside and Out, ed. H. L. Morrison & A. Sarajedini, 371

Groenewegen, M. A. T., Udalski, A., & Bono, G. 2008, A&A, 481, 441

Harris, W. E. 1996, AJ, 112, 1487

Hempel, M., Minniti, D., Dékány, I., et al. 2014, The Messenger, 155, 29

Jurcsik, J. & Kovacs, G. 1996, A&A, 312, 111

Kooreman, C. J. 1966, Annalen van de Sterrewacht te Leiden, 22, 159

Kovács, G. & Kupi, G. 2007, A&A, 462, 1007

Kunder, A. & Chaboyer, B. 2009a, AJ, 138, 1284

Kunder, A. & Chaboyer, B. 2009b, AJ, 137, 4478

Kunder, A., Popowski, P., Cook, K. H., & Chaboyer, B. 2008, AJ, 135, 631

Longmore, A. J., Dixon, R., Skillen, I., Jameson, R. F., & Fernley, J. A. 1990, MNRAS, 247, 684

Lucas, P. W., Hoare, M. G., Longmore, A., et al. 2008, MNRAS, 391, 136

McWilliam, A. & Zoccali, M. 2010, ApJ, 724, 1491

Minniti, D., Lucas, P. W., Emerson, J. P., et al. 2010, New A, 15, 433

Minniti, D., Saito, R. K., Alonso-García, J., Lucas, P. W., & Hempel, M. 2011, ApJ, 733, L43

Navarrete, C., Contreras Ramos, R., Catelan, M., et al. 2015, A&A, 577, A99

Nishiyama, S., Tamura, M., Hatano, H., et al. 2009, ApJ, 696, 1407

Pietrukowicz, P., Udalski, A., Soszyński, I., et al. 2012, ApJ, 750, 169

Pietrzyński, G., Gieren, W., Szewczyk, O., et al. 2008, AJ, 135, 1993

Ponsen, J. 1954, Annalen van de Sterrewacht te Leiden, 20, 369

Rattenbury, N. J., Mao, S., Sumi, T., & Smith, M. C. 2007, MNRAS, 378, 1064

Saito, R. K., Hempel, M., Minniti, D., et al. 2012a, A&A, 537, A107

Saito, R. K., Minniti, D., Dias, B., et al. 2012b, A&A, 544, A147

Saito, R. K., Zoccali, M., McWilliam, A., et al. 2011, AJ, 142, 76

Samus, N. N., Durlevich, O. V., & et al. 2009, VizieR Online Data Catalog, 1, 2025

Scargle, J. D., Norris, J. P., Jackson, B., & Chiang, J. 2013, ApJ, 764, 167

Schultheis, M., Chen, B. Q., Jiang, B. W., et al. 2014, A&A, 566, A120

Schwarzenberg-Czerny, A. 1989, MNRAS, 241, 153

Sesar, B., Grillmair, C. J., Cohen, J. G., et al. 2013, ApJ, 776, 26

Skrutskie, M. F., Cutri, R. M., Stiening, R., et al. 2006, AJ, 131, 1163

Smith, H. A. 2004, RR Lyrae Stars (Cambridge University Press)

Smolec, R. 2005, Acta Astron., 55, 59

Sollima, A., Cacciari, C., & Valenti, E. 2006, MNRAS, 372, 1675

Soszyński, I., Dziembowski, W. A., Udalski, A., et al. 2011, Acta Astron., 61, 1

Soszyński, I., Udalski, A., Szymański, M. K., et al. 2014, Acta Astron., 64, 177

Swope, H. H. 1942, Annals of Harvard College Observatory, 109, 41

Udalski, A., Szymański, M. K., & Szymański, G. 2015, Acta Astron., 65, 1

Valenti, E., Ferraro, F. R., & Origlia, L. 2004, MNRAS, 351, 1204

Valenti, E., Origlia, L., & Ferraro, F. R. 2005, MNRAS, 361, 272

Vanderplas, J., Connolly, A., Ivezić, Ž., & Gray, A. 2012, in Conference on Intelligent Data Understanding (CIDU), 47

Walker, A. R. & Terndrup, D. M. 1991, ApJ, 378, 119

Wegg, C. & Gerhard, O. 2013, MNRAS, 435, 1874

Wright, E. L., Eisenhardt, P. R. M., Mainzer, A. K., et al. 2010, AJ, 140, 1868